BNWL-1056 A
UC-25

IRRADIATION OF GRAPHITE AT TEMPERATURES OF 300 TO 1200 °C

June 1969

AEC RESEARCH & DEVELOPMENT REPORT

BNWL-1056 A

BATTELLE NORTHWEST
BATTELLE MEMORIAL INSTITUTE PACIFIC NORTHWEST LABORATORY
BATTELLE BOULEVARD, P. O. BOX 999, RICHLAND, WASHINGTON 99352

PACIFIC NORTHWEST LABORATORY
RICHLAND, WASHINGTON
operated by
BATTELLE MEMORIAL INSTITUTE
for the
UNITED STATES ATOMIC ENERGY COMMISSION UNDER CONTRACT AT(45-1)-1830

AEC-RL RICHLAND, WASH.

BNWL-1056A

UC-25, Metals, Ceramics,
and Materials

IRRADIATION OF GRAPHITE AT TEMPERATURES OF 300 TO 1200 °C

By

J. W. Helm*

Metallurgy and Ceramics Department
Chemistry and Metallurgy Division

June 1969

* Presently with FFTF Division

BATTELLE MEMORIAL INSTITUTE
PACIFIC NORTHWEST LABORATORY
RICHLAND, WASHINGTON 99352

Printed in the United States of America
Available from
Clearinghouse for Federal Scientific and Technical Information
National Bureau of Standards, U.S. Department of Commerce
Springfield, Virginia 22151
Price: Printed Copy $3.00; Microfiche $0.65

IRRADIATION OF GRAPHITE AT TEMPERATURES OF 300 TO 1200 °C

J. W. Helm

ABSTRACT

Irradiations of a large variety of graphites have been conducted at temperatures from 300 to 1200 °C to maximum neutron fluences of 2.7×10^{22} nvt (E > 0.18 MeV). As temperatures and neutron fluences increase, bulk expansion of the graphite becomes the controlling behavior in all orientations. Materials which are well graphitized, highly crystalline, isotropic, and have a high CTE show the lowest contraction at moderate fluences.

The dimensional-change data for all graphite types may be separated into two bands. The first band represents data for samples irradiated in the temperature range 300 to 800 °C. The second band, showing a highly accelerated damage rate, represents data for samples irradiated at 900 to 1200 °C. Thus, the transition from the lower damage rate to the higher one takes place over narrow temperature range (∿800 to 900 °C). The data are grouped closely within each band.

These observations are based on relatively small samples, generally less than 1/2 in. diameter by less than 4 in. long. While the behavior of these small samples may not exactly represent the behavior of larger pieces, it is felt that expansion will ultimately be the controlling behavior in the larger sizes also.

CONTENTS

FIGURES

IRRADIATION OF GRAPHITE AT TEMPERATURES OF 300 TO 1200 °C

J. W. Helm

INTRODUCTION

Experimental programs are underway to determine the behavior of a large variety of graphites under neutron irradiation in the temperature range of 300 to 1200 °C. The studies are being conducted to provide engineering data on graphites used or considered for use in nuclear reactors and to provide information on newer types of graphites considered potentially capable of more stable behavior. The long-term goal of these programs is the gathering of information useful to the development of a graphite more resistant under neutron irradiation to dimensional changes, particularly at temperatures of 800 to 1200 °C which are of primary interest for gas-cooled, graphite-moderated reactors.

This document, combining all irradiation data obtained as of September 1967 on 58 different graphites produced from a variety of cokes and binders under various processing conditions, is issued in two separate parts. The appendices to this report, presenting the experimental procedures, the results, and supplemental figures, are issued as BNWL-1056B.

Current neutron spectra and monitor activation cross sections have been used in correcting previously reported neutron fluence* data on CSF and NC8 graphites (H-3-X irradiation experiments),[1,2] on N-Reactor graphites (H-4, -5, -6 irradiation experiments),[3] and on N-Reactor prototype graphites.[4] Additional data on isotropic graphites

* *All neutron fluences reported herein are based on neutrons having energies greater than 0.18 MeV.*

(GEH-13-10)[5] and data on several newer graphite types (H-3-2X and GEH-13-1X experiments) have also been obtained and are reported herein.

The primary data obtained on all these graphites concern changes in physical dimension under neutron irradiation. Thus, the changes in length and volume are of major interest. These length change data have been summarized previously.[6] The secondary objective is determining, in materials subjected to irradiation, the extent of change in such properties as coefficient of thermal expansion, thermal conductivity, electrical resistivity, Young's modulus, and crystallite parameters.

MATERIAL DESCRIPTION AND SAMPLE SELECTION

The materials being irradiated are described in Table 1. All property measurements were made by Battelle-Northwest. Irradiation data are not reported for all materials since some are still under irradiation. The sampling schemes used are given in BNWL-1056B as Figures A1 through A5 in Appendix A. The appropriate figure number is listed in Table 1 for each material. After machining, individual samples were annealed at 1600 to 1800 °C for 1 hr in a vacuum of 3×10^{-4} Torr.[1,7]

Details on the individual capsules are presented in BNWL-1056B, Appendix B.

EXPERIMENTAL RESULTS

Data on the irradiation behavior over the temperature range of 300 to 1200 °C of a wide variety of graphites have been obtained to neutron fluences of 2.1×10^{22} nvt. The complete irradiation results for all the samples are presented by capsule number in BNWL-1056B, Appendix C. Correction of neutron fluences are all based on the current calculated activation cross sections of the nickel and iron flux monitors.[5]

TABLE 1. Graphite Description

Type	Block Numbers	Block Size, in.	Sample Scheme Figure Number	Manufacturer	Coke Source	Coke Type	Coke Shape	Binder	Additive	Impregnations Number	Impregnations Type	Forming Method	Graphitization Temperature, °C	Description	Density, g/cm³	CTE (25-425C), in./in./°C × 10^6 Transverse	CTE Parallel	Resistivity, ohm-cm × 10^-4 Transverse	Resistivity Parallel	Young's Modulus, psi × 10^-6 Transverse	Young's Modulus Parallel	X-Ray Parameters, Å c	Lc	a	La
CSF	122,136,141,142, 222,233,238	4 × 4 × 50	1	UCC	Cleves	Petroleum	Conventional	Coal tar pitch	None	1	Coal tar pitch	Extruded	2800	Reactor grade, normal bake, F-purified.	1.66	3.79	1.78	13.3	7.7	0.70	1.58	6.731	513	2.4638	764
TSX	158,160,167,185, 234	6 × 6 × 48	2	UCC	Continental-Lake Charles	Petroleum	Needle	Coal tar pitch	None	1	Coal tar pitch	Extruded	3000	Reactor grade, N-Reactor graphite, normal bake, halogen purified, anisotropic.	1.71	3.99	1.01	12.6	6.0	0.89	2.01	6.734	544	2.4639	847
NC7	NC7	16 3/8 × 16 3/8 × 240	3	UCC	Continental-Lake Charles	Petroleum	Needle	Coal tar pitch	None	1	Coal tar pitch	Extruded	~2700	Electrode stock, similar to NC8 except larger grain size.	1.70							6.726	642	2.4610	400
NC8	NC8	17 1/2 × 17 1/2 × 240	3	UCC	Continental-Lake Charles	Petroleum	Needle	Coal tar pitch	None	1	Coal tar pitch	Extruded	2800	Reactor grade, EGCR graphite, normal bake.	1.72	3.34	1.66	11.0	6.7	0.83	1.50	6.729	516	2.4638	1016
TSGBF	125,225	3 3/4 × 3 3/4 × 48	1	UCC	Texas-Lockport	Petroleum	Conventional	Coal tar pitch	None			Extruded	2450	Reactor grade, graphitized and F-purified in one step.	1.65	3.80	2.59	19.9	13.8	0.86	1.58	6.762	340	2.4616	542
KC	187	3 3/4 × 3 3/4 × 48	1	UCC	Kendall	Petroleum	Needle	Coal tar pitch	None	1	Coal tar pitch	Extruded	2800	Reactor grade, AGOT, thermally purified, normal bake.	1.73	4.70	1.10	12.4	6.2	0.85	1.39	6.734	515	2.4626	1672
RHM(JOZ)	GL-9	1 × 2 × 6	1 (6)	GLCC	Texas	Petroleum	Raw		None	>1		Molded		Experimental raw coke graphite.	1.75	6.11	5.32	9.8				6.731	468	2.4630	568
HPJ	GL-10	4 3/16 × 4 3/16 × 24	1	GLCC	Sunray-Tulsa	Petroleum	Needle	Coal tar pitch	None	None		Extruded	2800	Reactor grade, prototype graphite for N-Reactor, regular particle size mix, thermally purified.	1.60	3.80	1.22	14.4	7.4			6.719	700		700
HPDA	GL-11	4 3/16 × 4 3/16 × 24	1	GLCC	Continental-Ponca City	Petroleum	Needle	Coal tar pitch	None	None		Extruded	2800	Reactor grade, prototype graphite for N-Reactor, regular particle size mix, thermally purified.	1.59	3.45	1.15	14.7	7.8			6.712	558		555
VC	VC	4 3/8 × 4 3/8 × 12	1	UCC	Continental	Petroleum	Needle	Coal tar pitch	None	1	Coal tar pitch	Extruded	2800	Reactor grade, prototype graphite for N-Reactor, AGOT processed, regular particle size mix.	1.70	3.49	1.10					6.702	740		530
RC	RC	2 (diam) × 8	4	UCC	Continental	Petroleum	Needle	Coal tar pitch	None	1	Coal tar pitch	Extruded	2800	AGOT processed, regular particle size mix.	1,59		1.21					6.698	550	2.462	1310
RX-1	RX-1	2 (diam) × 18	4	UCC	Continental	Petroleum	Needle	Coal tar pitch	None	None		Extruded	2900	Laboratory extrusion, fine mix.	1.62							6.712	590		
RX-2	RX-2	2 (diam) × 18	4	UCC	Continental	Petroleum	Needle	Coal tar pitch	None	>1	Coal tar pitch	Extruded	2900	Same as RX-1 except impregnated.	1.63							6.717	710		

TABLE 1. *(contd)*

Type	Block Numbers	Block Size, in.	Sample Scheme Figure Number	Manufacturer	Coke Source	Coke Type	Coke Shape	Binder	Additive	Impregnations Number	Impregnations Type	Forming Method	Graphitization Temperature, °C	Description	Density, g/cm^3	CTE (25-425C), in./in./°C × 10^6 Transverse	CTE Parallel	Resistivity, ohm-cm × 10^{-4} Transverse	Resistivity Parallel	Young's Modulus, psi × 10^{-6} Transverse	Young's Modulus Parallel	X-Ray Parameters, Å c	L_c	a	L_a
RX-3	RX-3	2 (diam) × 18	4	UCC	Continental	Petroleum	Needle	Coal tar pitch	None	>1	Coal tar pitch	Extruded	3100	Same as RX-2 except all flour mix.	1.59							6.706	771		
JOZ	61-20	3 1/8 × 3 1/8 × 5 1/4	1 (6)	GLCC	GLCC	Petroleum	Raw	Coal tar derivative	None	>1	Coal tar pitch	Molded		Experimental raw-coke graphite, same as 61-21 except impregnated.	1.89	5.96	5.25	9.0				6.736	404	2.462	799
JOZ	61-21	3 3/4 × 3 3/4 × 5	1 (6)	GLCC	GLCC	Petroleum	Raw	Coal tar pitch	None	None		Molded		Experimental raw-coke graphite.	1.70	5.78	4.85					6.733	390	2.462	823
No additive	61-56	3 (diam) × 6	4	SCC	GLCC	Petroleum	Needle	Coal tar pitch	None	1	Coal tar pitch	Extruded	2900	Additive series (DDR 118), base graphite without additive, mix-80% #60 flour and 20% particles through 20 and on 35 mesh screen, normal bake, Cl-purification.	1.62	2.82	0.98	16.7	5.0			6.749	302	2.4619	642
Cr_2O_3	61-67	3 (diam) × 6	4	SCC	GLCC	Petroleum	Needle	Coal tar pitch	1% Cr_2O_3	1	Coal tar pitch	Extruded	2900	Additive series (see 61-56)	1.66	3.47	1.02	19.3	7.1	0.50	1.47	6.742	293	2.4622	548
$CrCl_3 \cdot 6\ H_2O$	61-69	3 (diam) × 6	4	SCC	GLCC	Petroleum	Needle	Coal tar pitch	1% $CrCl_3 \cdot 6\ H_2O$	1	Coal tar pitch	Extruded	2900	Additive series (see 61-56)	1.70	3.51	0.98	14.4	5.5			6.742	250	2.4626	863
V_2O_3	61-70	3 (diam) × 6	4	SCC	GLCC	Petroleum	Needle	Coal tar pitch	1% V_2O_3	1	Coal tar pitch	Extruded	2900	Additive series (see 61-56)	1.54	3.55	1.26	16.3	7.6			6.731	339	2.4620	708
Al_4C_3	61-73	3 (diam) × 6	4	SCC	GLCC	Petroleum	Needle	Coal tar pitch	1% Al_4C_3	1	Coal tar pitch	Extruded	2900	Additive series (see 61-56)	1.51	3.09	1.03	18.5	13.5			6.738	270	2.4629	728
Raw coke	63-16	6 1/2 (diam) × 6	5	GLCC	Texas-Lockport	Petroleum	Raw	Coal tar pitch	None	None		Molded	2500	Experimental raw-coke graphite, base graphite, isotropic.	1.72	6.53	6.34	16.2	15.6	1.60	1.69	6.752	281	2.4606	696
Raw coke-impregnated	63-17	4 (diam) × 6	5	GLCC	Texas-Lockport	Petroleum	Raw	Coal tar pitch	None	1	Coal tar pitch	Molded	2500	Experimental raw-coke graphite, same as 63-16 except impregnated.	1.78	5.98	5.84	13.1	12.9	1.46	1.44	6.740	320	2.4603	445
Raw coke-no binder	63-19	3 × 4 × 6	6	GLCC	Texas-Lockport	Petroleum	Raw	None	None	None		Molded	2900	Experimental raw-coke graphite with no binder, same series as 63-16.	1.46	5.14	4.45	17.9	17.0	0.60	0.64	6.753	269		
50 °C/hr	63-23	3 diam	4	SCC	Sohio-Lima	Petroleum	Conventional	Coal tar pitch	None	None		Extruded	2900	Rate of rise of graphitization temperature series (DDR-164).	1.66	3.32	1.81	14.1	8.3	0.58	1.34	6.731	460	2.4591	952
30,000 °C/hr	63-29	3 diam	4	SCC	Sohio-Lima	Petroleum	Conventional	Coal tar pitch	None	None		Extruded	2900	Rate of rise of graphitization temperature series (See 63-23).	1.51	3.05	1.84	14.7	9.5			6.736	500	2.4561	675
700 °C binder	63-30	3 diam	4	SCC	GLCC	Petroleum	Needle	Coal tar pitch	None	None		Extruded	700	Maximum binder-temperature series (DDR-164), filler graphitized at 2900 °C.	1.46	4.24	1.35					6.729	490	2.4557	500
900 °C binder	63-31	3 diam	4	SCC	GLCC	Petroleum	Needle	Coal tar pitch	None	None		Extruded	900	Maximum binder-temperature series (See 63-30).	1.51	4.11	1.68					6.732	520	2.4602	780
1400 °C binder	63-32	3 diam	4	SCC	GLCC	Petroleum	Needle	Coal tar pitch	None	None		Extruded	1400	Maximum binder-temperature series (See 63-30).	1.48	3.41	1.15					6.729	485	2.4595	1305
2000 °C binder	63-33	3 diam	4	SCC	GLCC	Petroleum	Needle	Coal tar pitch	None	None		Extruded	2000	Maximum binder-temperature series (See 63-30).	1.48	3.32	1.24	36.7		0.39		6.729	368	2.4585	420
2350 °C binder	63-34	3 diam	4	SCC	GLCC	Petroleum	Needle	Coal tar pitch	None	None		Extruded	2350	Maximum binder-temperature series (See 63-30).	1.46	3.75	1.16					6.734	470	2.4580	712

TABLE 1. *(contd)*

Type	Block Numbers	Block Size, in.	Sample Scheme Figure Number	Manufacturer	Coke Source	Coke Type	Coke Shape	Binder	Additive	Impregnations Number	Impregnations Type	Forming Method	Graphitization Temperature, °C	Description
2750 °C binder	63-35	3 diam	4	SCC	GLCC	Petroleum	Needle	Coal tar pitch	None	None		Extruded	2750	Maximum binder-temperature series (See 63-30).
2900 °C binder	63-36	3 diam	4	SCC	GLCC	Petroleum	Needle	Coal tar pitch	None	None		Extruded	2900	Maximum binder-temperature series (See 63-30).
Max. shrinkage	63-37	3 diam	4	SCC	Witco	Pitch	Raw	Coal tar pitch	Fe_3O_4	None		Extruded	2900	Maximum shrinkage experimental graphite, normal bake, thermal purification.
Raw coke-no binder	63-38	4 × 4 × 6	6	GLCC	Texas-Lockport	Petroleum	Raw	None	None	None		Molded	2500	Experimental raw-coke graphite with no binder, same as 63-19 except 2500 °C.
H-205	63-50	4 (diam) × 6	4 (5)	GLCC			Non-needle	Coal tar pitch	None	1	Coal tar pitch	Molded	2800	Experimental graphite, normal bake, similar to UKAEA AGL graphite.
H-309	64-13, 64-13B	4 × 4 × 6	6	GLCC	Texas-Lockport	Petroleum	Calcined	Coal tar pitch	None	None		Molded	2500	Coking series (DDR 177), fully calcined coke.
H-313	64-17, 64-17B	4 × 4 × 6	6	GLCC	Texas-Lockport	Petroleum	Raw	None	None	None		Molded	2500	Coking series (See 64-13), raw coke.
780S	64-18,65-3	5 (diam) × 12	4	SCC	Texas	Petroleum		Coal tar pitch	None	1	Coal tar pitch	Extruded	2800	Experimental graphite.
PO3	65-1	7 (diam) × 21	5	PCC		Petroleum			None	None		Isostatically molded	2800	Special, highly impermeable graphite.
CHN	65-4	4 1/2 (diam) × 12	4	UCC			Needle	Coal tar pitch	None	None		Extruded	>2800	Experimental graphite.
Graphitization 2400 °C	65-5	3 7/8 (diam) × 6 5/8	4	SCC	SCC	Petroleum	Needle	Coal tar pitch	None	None		Extruded	2400	Graphitization temperature series, normal bake.
Graphitization 3000 °C	65-8	3 7/8 (diam) × 7 7/8	4	SCC	SCC	Petroleum	Needle	Coal tar pitch	None	None		Extruded	3000	Graphitization temperature series (See 65-5).
Isotropic	65-9	4 1/2 (diam) × 12	4	SCC	SCC	Non-Petroleum	Green	Coal tar pitch	None	None		Extruded	2750	Experimental graphite.
No binder	65-11	2 1/4 × 2 3/4 × 4	6	UCC		Petroleum	Needle	Coal tar pitch	None	None		Molded		Experimental graphite.
JOZ	65-18	7 1/4 (diam) × 7 1/2	5	GLCC	GLCC	Petroleum	Raw	Coal tar derivative	None	1	Coal tar pitch	Molded	2800	Commercial grade JOZ isotropic graphite.
DS13	65-20 66-6	6 × 6 × 3/4 3 3/4 × 3 3/4 × 1 3/4	6	PCC		Petroleum			None	None		Molded	2800	High purity special graphite, halide purification.
RP4	65-21	3 1/2 × 17 1/2 × 25	1	SCC	SCC	Petroleum	Complex	Coal tar pitch	None	None		Extruded	2800	Commercial grade isotropic graphite, halide purification.
RC5	65-22	3 1/2 × 17 1/2 × 25	1	SCC	SCC	Petroleum	Non-needle	Coal tar pitch	None	None		Extruded	2800	Isotropic experimental graphite, normal bake.
GN	65-29	4 1/4 (diam) × 9 1/2	4	BCC			Non-needle		None	Multiple	Coal tar pitch	Extruded	2650	Nuclear grade, pre-graphitized coke.
H-323	65-30	9 1/4(diam) × 6 3/8	4,5	GLCC	GLCC		Non-needle	Coal tar pitch	None	1	Coal tar pitch	Special process	2800	Experimental graphite.
MHLM	65-31	7 3/16 × 7 1/8 × 5 5/8	6	GLCC	GLCC	Petroleum	Non-needle	Coal tar pitch	None	1	Coal tar pitch	Molded	2800	Experimental graphite, gas purification.
H-319	65-32, GLY	3 (diam) × 16 7/8	4	GLCC	GLCC	Petroleum		Coal tar pitch	None	None		Special process	2800	Isotropic experimental graphite.

Type	Density, g/cm³	CTE (25-425C), in./in./°C × 10⁶ Transverse	CTE Parallel	Resistivity, ohm-cm × 10⁻⁴ Transverse	Resistivity Parallel	Young's Modulus, psi × 10⁻⁶ Transverse	Young's Modulus Parallel	X-Ray Parameters, Å c	L_c	a	L_a
2750 °C binder	1.47	3.23	1.01					6.728	490	2.4643	1485
2900 °C binder	1.50	3.45	0.96	23.6	10.2	0.70	1.10	6.726	600	2.4604	705
Max. shrinkage	1.63	6.00	3.68					6.744	272	2.4595	505
Raw coke-no binder	1.35	6.19	4.82	39.4	31.2	0.41	0.46	6.768	281	2.4610	570
H-205	1.75	6.30	5.55	18.3	15.2			6.768	212	2.4613	570
H-309	1.55	4.85	3.41	25.5	20.7	0.56	0.56	6.740	286	2.4600	>2000
H-313	1.53	6.10	4.99	14.1	11.8	1.30	1.18	6.740	252	2.4611	995
780S	1.81	3.18	2.11	14.8	10.2	1.48	1.75				
PO3	1.83	4.09	3.80		22.9			6.751	193		
CHN	1.85	3.50	2.30								
Graphitization 2400 °C	1.81	3.00	1.37	25.5	10.1			6.734	256	2.4619	427
Graphitization 3000 °C	1.83	2.42	0.94	20.1	8.1			6.728	322	2.4614	463
Isotropic	1.91	6.32	4.84	12.7	9.6	1.55	2.28	6.756	213	2.4616	322
No binder	1.64	2.76	1.11	28.1				6.738	298	2.4664	263
JOZ	1.72	6.65	5.83	14.8	12.9	1.34	1.37	6.749	256		
DS13	1.82	5.00	3.76	17.0	13.6	0.42	1.88	6.740	224		
RP4	1.73	4.85	3.85	10.4	9.1	1.27	1.59	6.735	260		
RC5	1.73	5.26	4.88	9.9	9.9	1.36	1.25	6.737	287		
GN	1.87	2.81	1.99	13.7	10.8	1.25	1.74	6.736	262		
H-323	1.72	4.90	4.50	13.6	13.0	1.14	1.26	6.747	236		
MHLM	1.73	3.55	3.09	11.6	9.4			6.732	320		
H-319	1.78	3.54	3.23	10.0	9.2	1.20	1.90	6.732	297	2.458	

TABLE 1. *(contd)*

Type	Block Numbers	Block Size, in.	Sample Scheme Figure Number	Manufacturer	Coke Source	Coke Type	Coke Shape	Binder	Additive	Impregnations Number	Impregnations Type	Forming Method	Graphitization Temperature, °C	Description	Density, g/cm³	CTE (25-425C), in./in./°C × 10⁶ Transverse	CTE Parallel	Resistivity, ohm-cm × 10⁻⁴ Transverse	Resistivity Parallel	Young's Modulus, psi × 10⁻⁶ Transverse	Young's Modulus Parallel	X-Ray Parameters, Å c	L_c	a	L_a
9567	65-37, 66-12	4 3/4 × 12 7/16 × 20	1,4	SCC			Needle	Coal tar pitch	~1% FeO	>1	Coal tar pitch	Extruded	2800	Experimental graphite, available in large sizes.	1.71	3.62	1.42	9.6	5.8	0.90	1.70	6.722	376		
MSRE	65-38, 66-7	2 1/4 × 2 1/4 × 4	1	UCC		Petroleum		Coal tar pitch	None	2	Resin	Extruded	2800	MSRE core graphite, low permeability, fine grain, gas purified.	1.86	3.43	0.84	17.2	5.7			6.734	313		
AXF-8Q1 (EP-1924-HP)	65-42	2 (diam) × 6	5,4	POCO	Proprietary	Proprietary	Approximately Spherical	Proprietary	None	None		Isostatically Molded	>2500	Fine grain, high strength, isotropic, high CTE, largest particles <50 microns, halide purification, total ash 5 ppm.	1.79	7.05	7.16	16.1	15.4	1.68	1.75				
EP-192C-HP	66-4	1 1/2 × 4 × 18	6,1	POCO	Proprietary	Proprietary	Approximately Spherical	Proprietary	None	None		Isostatically Molded	>2500	Same as 65-42 except lower density.	1.51	6.82	6.52	17.0	16.4	1.10	1.16				
DS14	66-5	3 3/4 × 3 3/4 × 1 3/4	4,5	PCC		Petroleum			None	None		Molded	2800	Same as 65-20 except flake graphite added in filler.	1.69	4.19	2.32	29.2	16.6	1.00	1.66				
H-327A	66-9	12 3/4 (diam) × 4	4	GLCC		Petroleum	Needle	Coal tar pitch	None	>1	Coal tar pitch	Extruded	2800	Commercial graphite available in large size on developmental basis.	1.78	3.37	1.22	11.3	5.6			6.716	770	2.460	
H-328	66-10	17 3/8 (diam) × 4	4,5	GLCC	GLCC		Isotropic		None	1	Coal tar pitch	Molded	2800	Developmental.	1.72	5.74	5.67	12.0	11.8	1.50	1.56	6.742	360	2.460	
H-207-85	66-11, GLZ	6 (diam)	4	GLCC	GLCC		Isotropic	Coal tar pitch	None	>1	Coal tar pitch	Molded	2800	Developmental.	1.82	5.81	4.73	10.7	9.1	1.65	1.56	6.750	224		
H-349	66-13		4	GLCC	GLCC	Petroleum	Needle	Coal tar pitch	None			Special process		Special process, baked under pressure.	1.64	2.87	1.26	16.0	8.2						
9640	66-14	8 1/2 (diam) × 9	4	SCC	SCC		Needle		None			Molded (Not conventional)	2800	Needle coke isotropic.	1.58	3.8	3.6	15.7	15.3		1.24				
9650	66-15	4 1/4 × 4 × 8	4	SCC	Proprietary		Raw		None			Molded	2800	Raw coke.	1.92	7.4	7.2		40.2		0.85				
9751	67-1	2 5/8 × 12 × 12	4	SCC	SCC				None	None		Molded	2800	Isotropic, gas-purified, no impregnation.	1.73	6.9	6.2		19.3						
RC-4	67-3	12 (diam) × 10	1	SCC	SCC	Petroleum	Complex	Coal tar pitch	None	None		Extruded	2800	Commercial grade isotropic, same as 65-21 except not purified.	1.73										

All the data tabulated in BNWL-1056B, Appendix C, are presented graphically in the following subsections or in BNWL-1056B, Appendix E. To facilitate handling of the large amount of data involved, a computer program was used for plotting the graphs. For each of the temperature intervals shown, the computer grouped all the data into neutron fluence intervals of 0.5×10^{21} nvt (e.g., 0-0.5, 0.51-1.0, 1.01-1.50 etc.). The mean of the study parameters (e.g., length change, etc.) and the mean fluences were calculated and then plotted. The small circled numbers on the graphs next to the data points indicate the number of individual data points averaged to give mean values used in constructing the plots. In addition, the computer calculated a best-fit third-order polynomial curve to the data. Curve equations tabulated in BNWL-1056B, Appendix D, are those comprising data points sufficient to be meaningful. These equations should be useful to engineers and designers making dimensional change and stress calculations. However, the equations are not valid for large extrapolations beyond the last data point.

For the convenience of the reader a duplicate set of all the graphs for the CSF reference graphite are provided in BNWL-1056B, Appendix F. These can be easily removed, if so desired, and used as overlay graphs to provide ready comparisons to the behavior of other graphites.

LENGTH CHANGE

The dimensional behavior of the various irradiated graphites continues to follow the general pattern reported earlier.(5,8,9) In the transverse direction, the material expands very slightly, contracts, goes through a turnaround, and then expands very rapidly. In the parallel direction, the graphites generally contract at an increasing, then a decreasing rate and, as reported herein, also pass through a turnaround and expand. Between 300 to 800 °C, the contraction rate decreases as the temperature increases. The turnaround is reached at roughly the same fluence for the different temperatures, but the net expansion after turnaround is greater at 800 °C. Above 800 °C, graphites contract more rapidly, but reach turnaround at generally lower fluences and then expand very rapidly.

The length-change data for CSF graphite, considered the reference graphite, are presented in Figures 1 and 2. In the transverse direction, CSF graphite behaves in the general manner described above. The contraction rate decreases as the irradiation temperature is increased from 400 to 800 °C. Turnaround first occurs at 800 °C, although it occurs at approximately 1×10^{22} nvt for all samples in this temperature range. The general dimensional-change behavior is similar for samples irradiated at 850 to 1275 °C except that the damage is accelerated, and turnaround occurs at a fluence of 4×10^{21} nvt. The expansion after turnaround increases as irradiation temperature increases.

The behavior of parallel samples follows the same general trend, except that turnaround occurs at a higher fluence and at a total contraction nearly four times as large as for transverse samples for comparable temperatures.

The length-change data for NC8 graphite, a needle-coke anisotropic material, are presented in Figures 3 and 4. In the transverse direction, turnaround at 400 to 750 °C again occurs at about 1×10^{22} nvt. However, the earliest turnaround occurs at 400 to 475 °C, and the expansion at 400 °C approaches that at 650 °C. At 1025 to 1075 °C, turnaround occurs at 3×10^{21} nvt and the expansion rate is very rapid. In the parallel direction, the 400 to 475 °C data show significantly more contraction than the 575 to 825 °C data, and turnaround at the higher temperature occurs at about 2.2×10^{22} nvt. Progressively

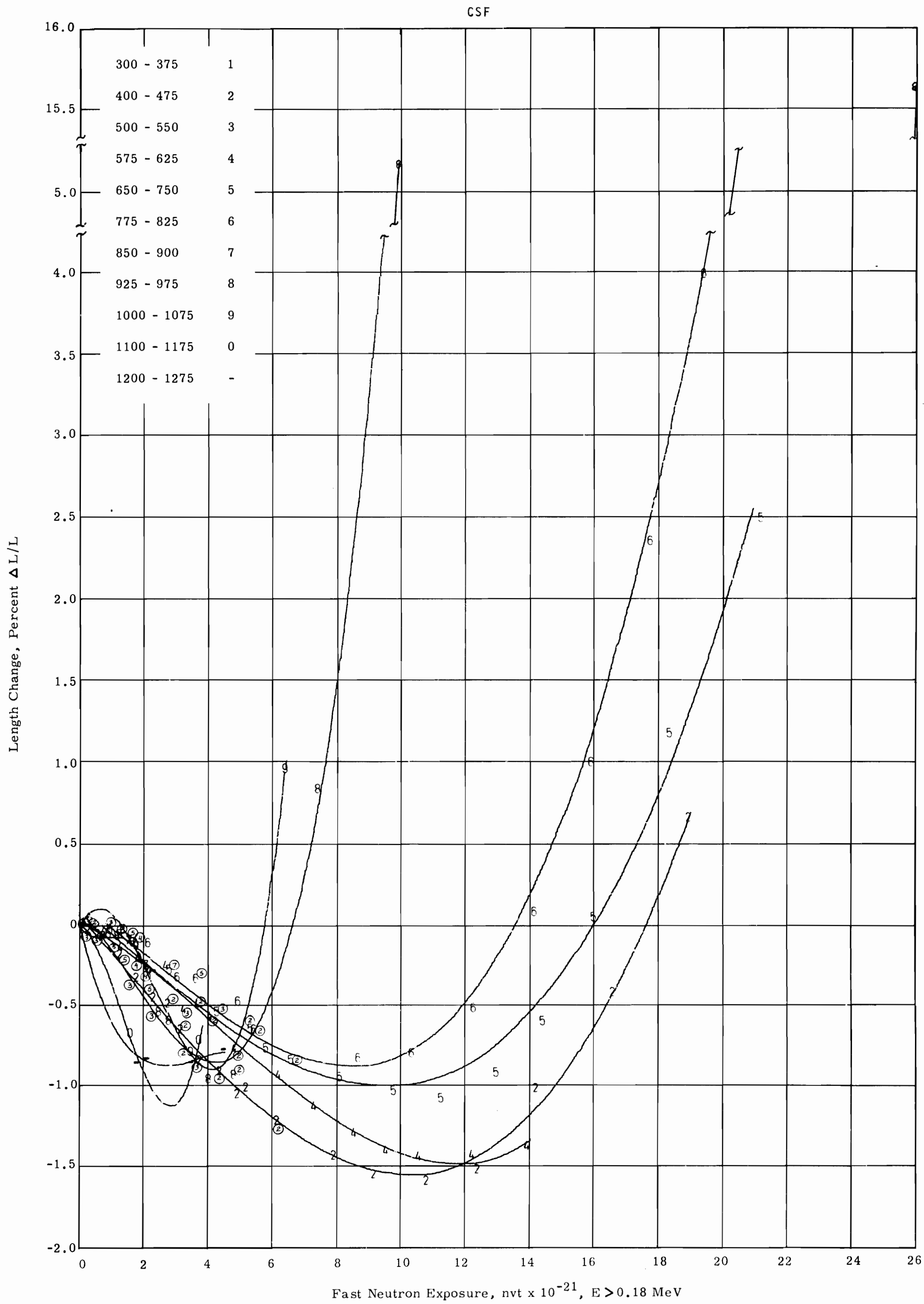

FIGURE 1. Length Change of CSF Graphite (Transverse).

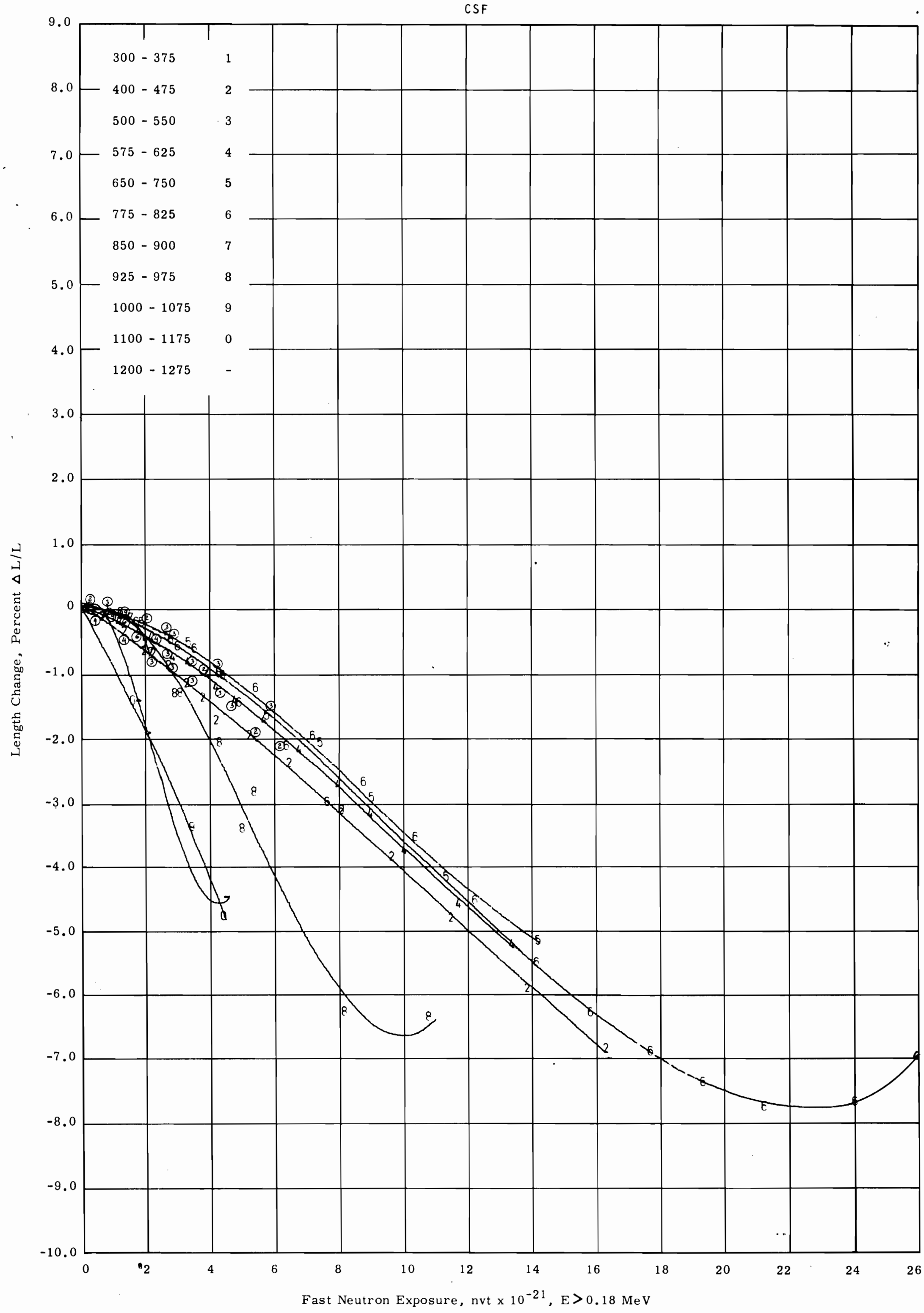

FIGURE 2. Length Change of CSF Graphite (Parallel).

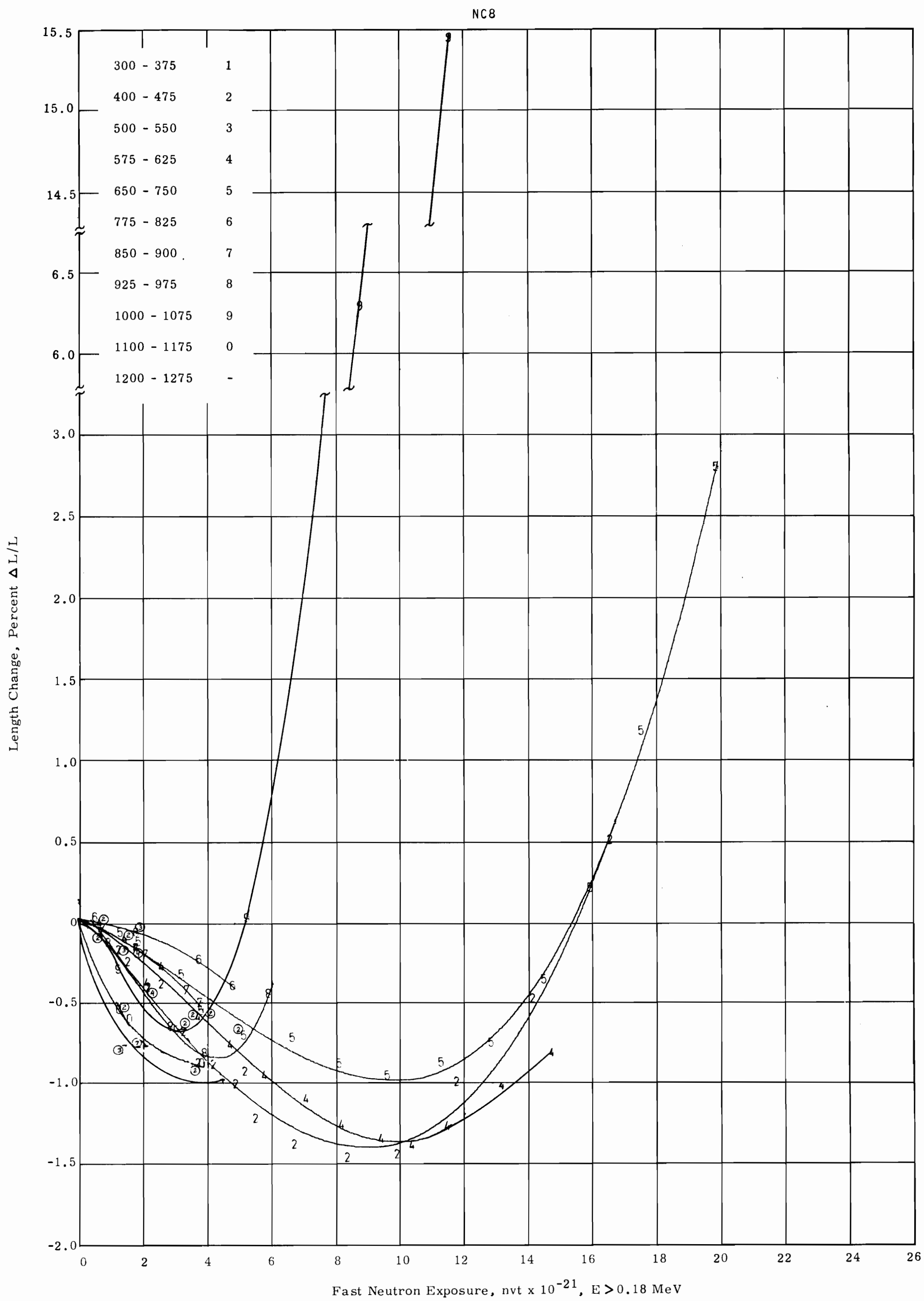

FIGURE 3. Length Change of NC8 Graphite (Transverse).

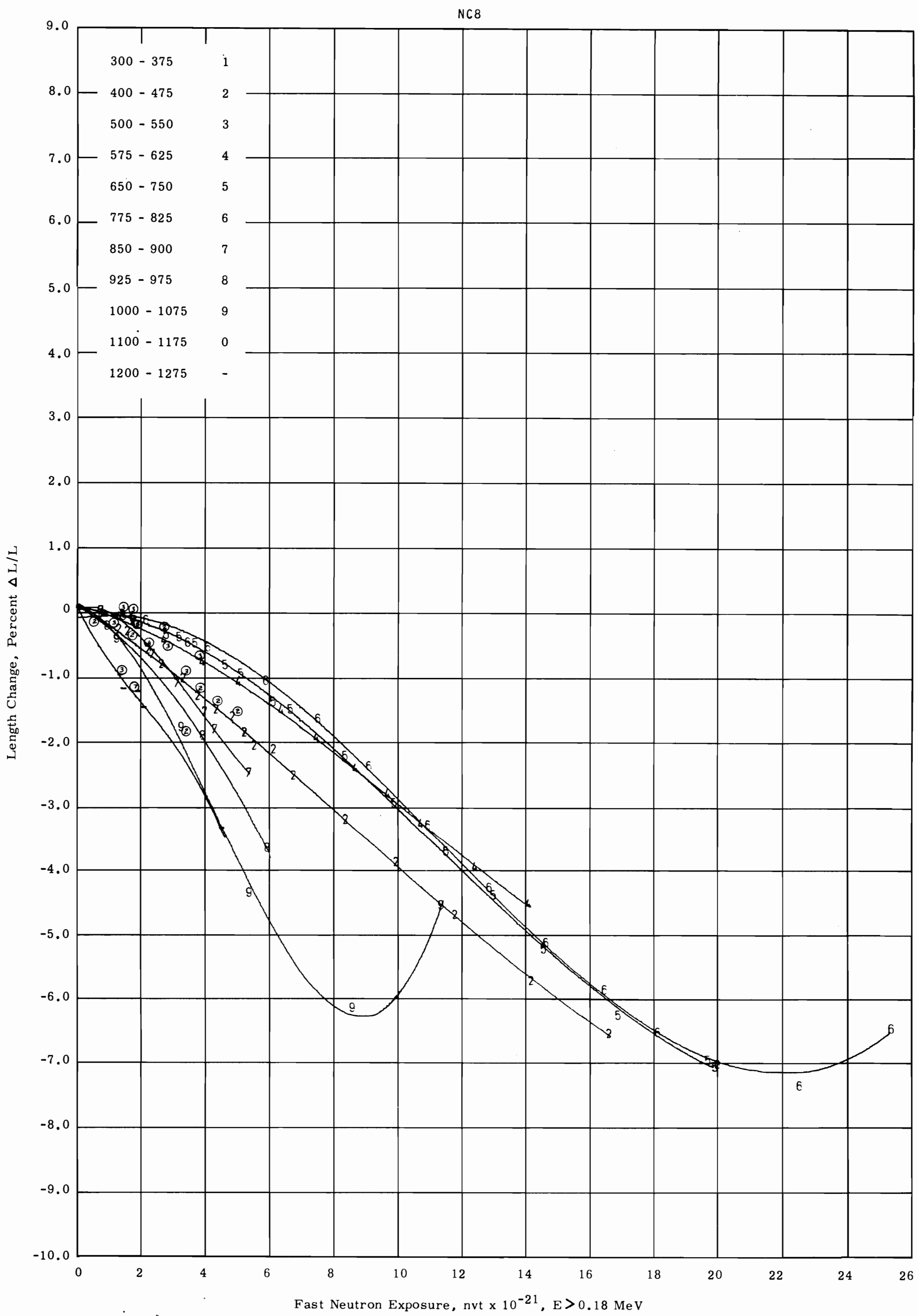

FIGURE 4. Length Change of NC8 Graphite (Parallel).

larger contractions are shown at 850 to 900 °C, 925 to 975 °C, and 1000 to 1275 °C. At 1000 to 1075 °C, the samples have gone through turnaround at a fluence of 9×10^{21} nvt.

The data for NC7 graphite (the prototype for NC8) are shown in Figures 5 and 6. The most interesting data are for the 775 to 825 °C sample which, at a fluence of 2.4×10^{21} nvt, has expanded nearly 20% in the transverse direction.

The data for TSX, the N-Reactor graphite, are presented in Figures 7 and 8. In the transverse direction, the temperature effect is not as pronounced in the range of 400 to 825 °C as for CSF. Turnaround occurs more quickly at 400 °C and at fluences well below 1×10^{22} nvt. The contraction rates above 850 °C are greater than at 800 °C, but turnaround occurs at about 3×10^{21} nvt. Behavior in the parallel direction nearly duplicates that of CSF parallel except that at 925 to 975 °C considerably more contraction occurs and turnaround has not been reached at 1×10^{22} nvt.

The length-change data for poorly graphitized TSGBF graphite are also presented in Figures 7 and 8. Dimensional changes occur very rapidly in this material. In the transverse direction, turnaround occurs at a fluence of 5×10^{21} nvt in the 775 to 825 °C range, and at 6×10^{21} nvt for the 650 to 750 °C range. However, startling behavior is noted at 925 to 975 °C where turnaround occurs prior to 3×10^{21} nvt and expansion proceeds at a rate greater than $5\%/10^{21}$ nvt until at 9×10^{21} nvt an expansion of nearly 35% is reached. In the parallel direction, the behavior at temperatures of 925 to 1075 °C is most significant. The samples contract 4.5% by 5×10^{21} nvt, and yet expand to nearly 14% by 9×10^{21} nvt. These rapid dimensional changes indicate that, for improved dimensional stability, the materials must be well graphitized.

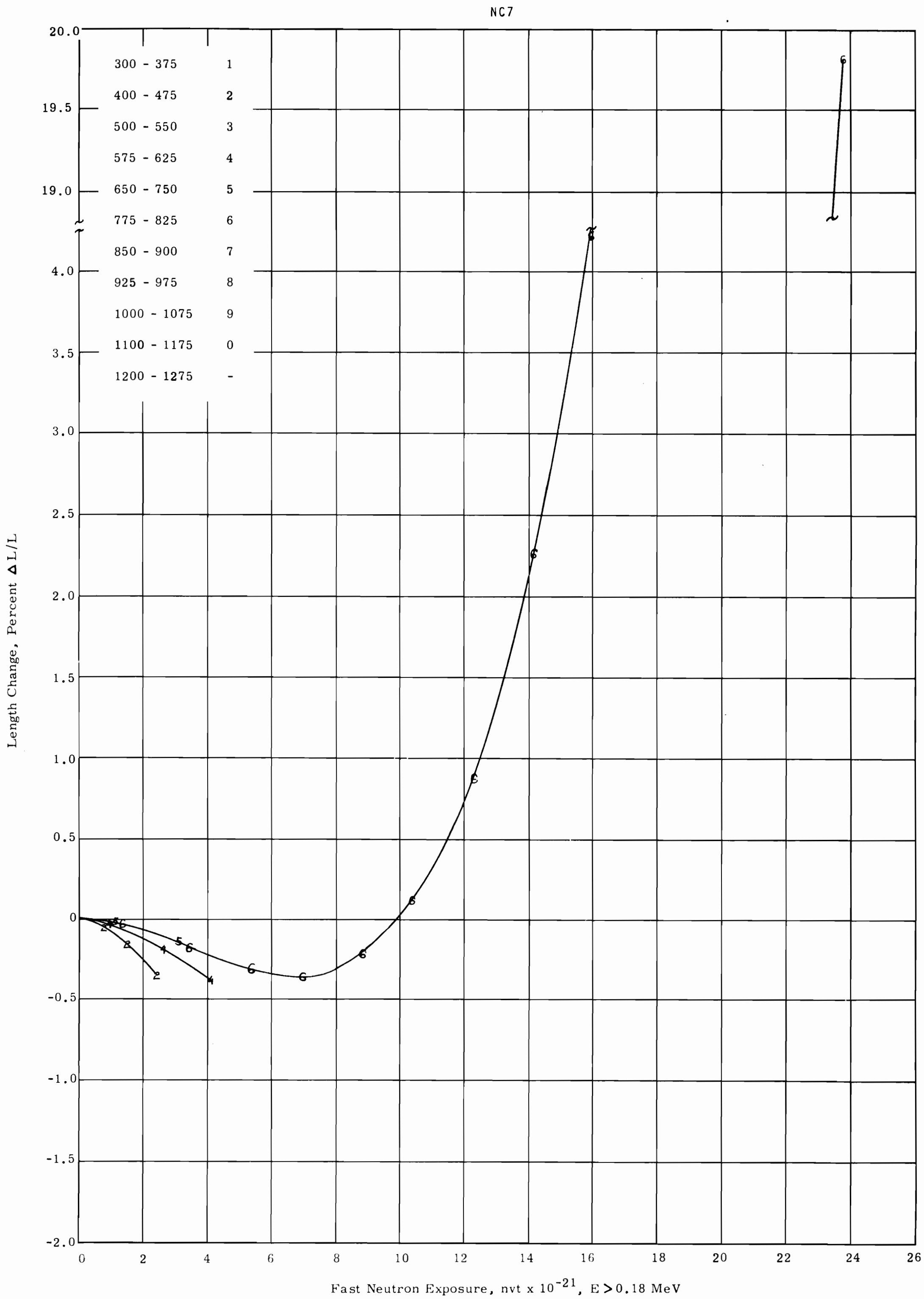

FIGURE 5. Length Change of NC7 Graphite (Transverse).

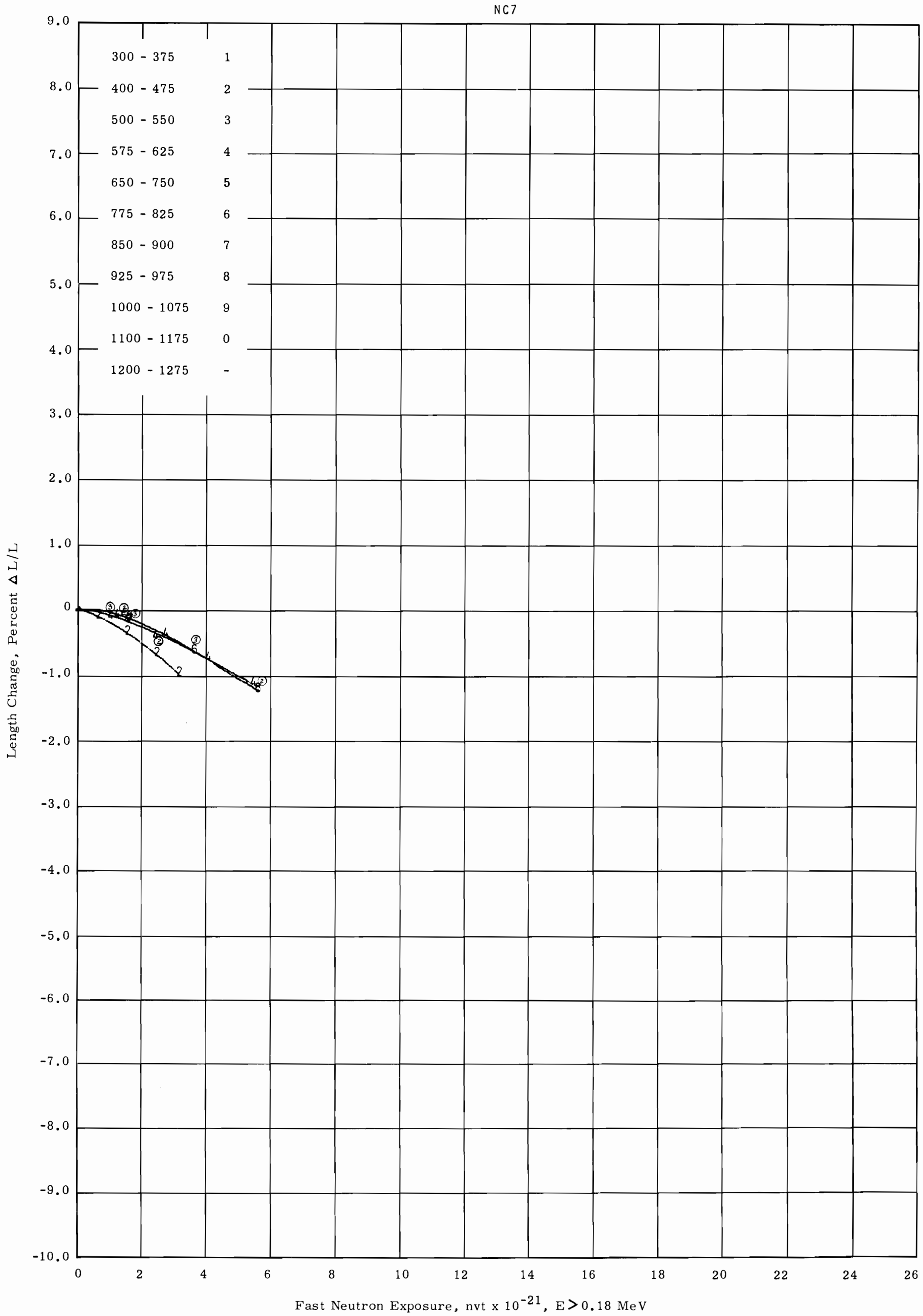

FIGURE 6. Length Change of NC7 Graphite (Parallel).

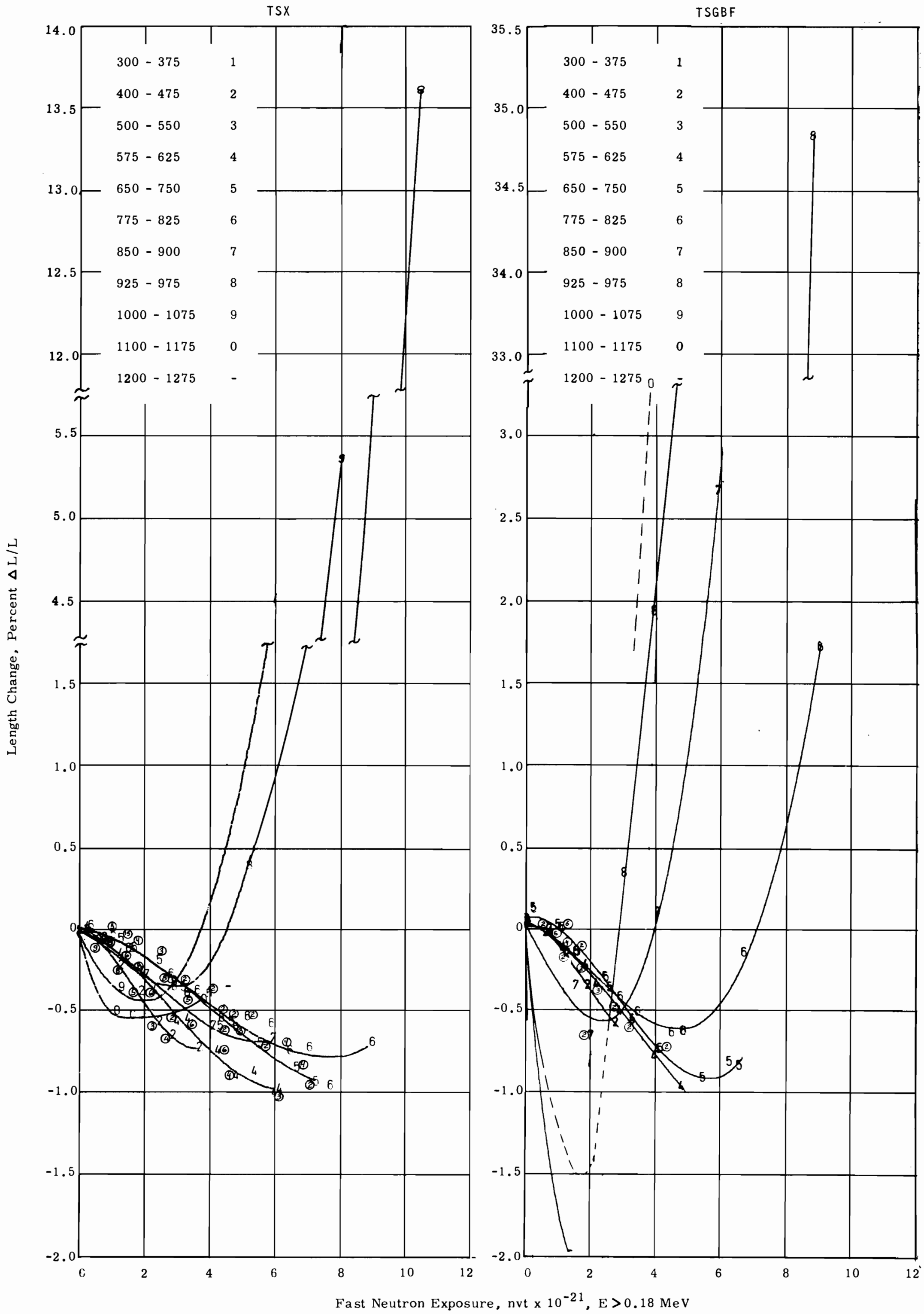

FIGURE 7. Length Change of TSX and TSGBF Graphites (Transverse).

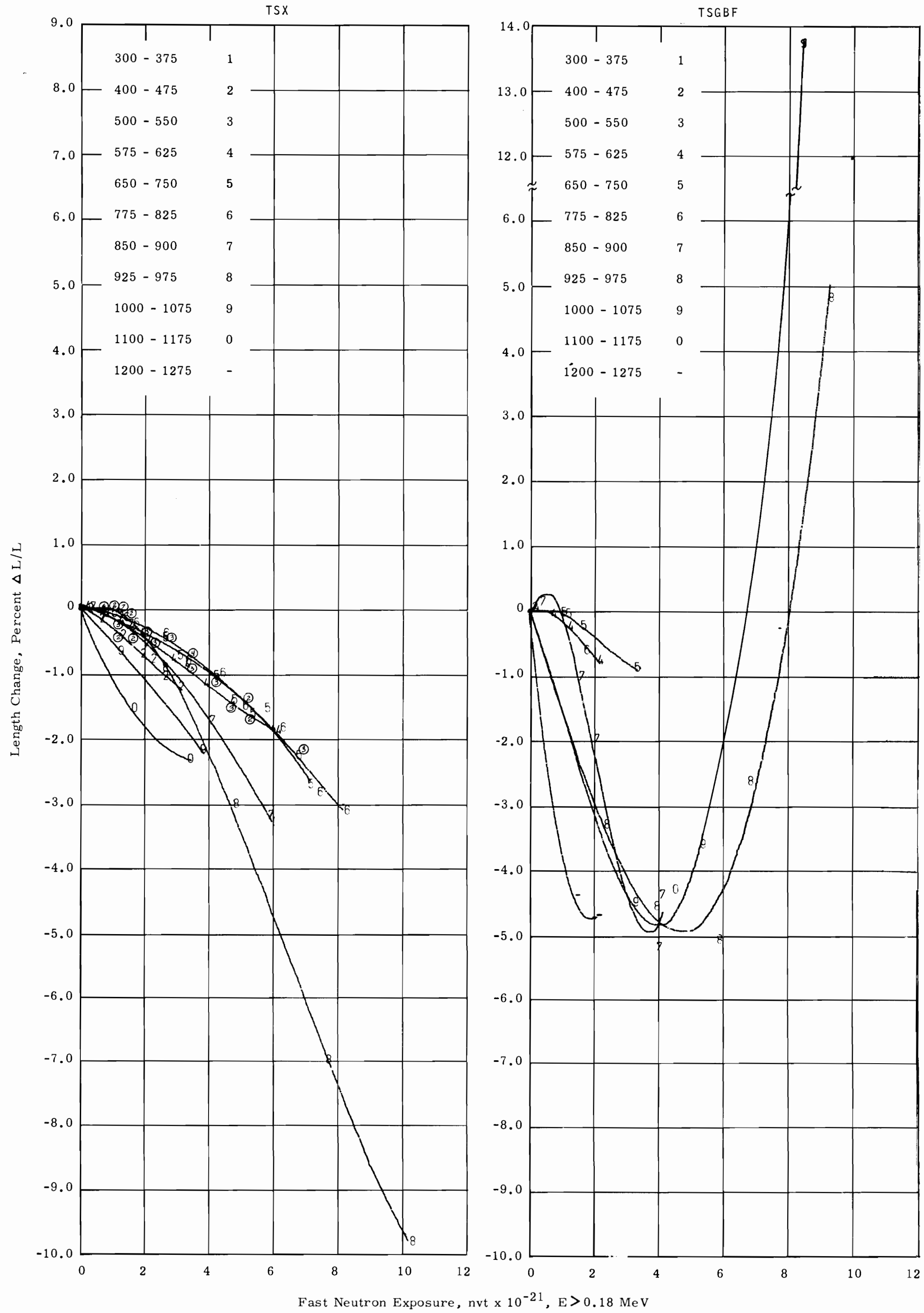

FIGURE 8. Length Change of TSX and TSGBF Graphites (Parallel).

The dimensional behavior of graphites, embodying in the mix additives removed by graphitization, is shown in Figures 9 and 10. In the transverse direction, 61-70 (V_2O_3 additive) expands slightly more than CSF at 925 to 975 °C, while 61-73 (Al_4C_3 additive) expands slightly less. In the parallel direction, 61-73 contracts more than CSF and 61-70 contracts more than 61-73. Therefore, additives do not seem beneficial at these temperatures and fluences.

The length-change data for five raw-coke graphites are presented in Figures 11 through 14. The first four materials (63-16, 63-17, 63-19, and 63-38), by exhibiting nearly the same behavior in both the transverse and parallel direction, are shown to be quite isotropic. All these materials tend to expand rather than to contract, and to show slightly less length change than CSF transverse samples. The last material (65-18) behaves quite anisotropically and, in both orientations, expands more than CSF. In general, these raw-coke graphites appear to contract somewhat less than CSF but after turnaround expand about the same or more than CSF, and hence appear to offer only minor advantages for long-term stability.

The dimensional behavior for the two extremes of the coking series of graphites is shown in Figures 15 and 16. The H309 graphite (64-13) was made from a fully calcined coke, while H313 (64-17) was made from a raw coke. The two materials show very similar anisotropic behavior. In the transverse direction, they both expand more rapidly than CSF and, in the parallel direction, reach turnaround much more rapidly than CSF.

The length-change data for two fairly isotropic graphites available in large sizes are shown in Figures 17 and 18 (RP4 and RC5). Both materials behave anisotropically under irradiation. RP4 behaves quite similarly to CSF except for the more rapid turnaround at all but temperatures from 1000 to 1075 °C

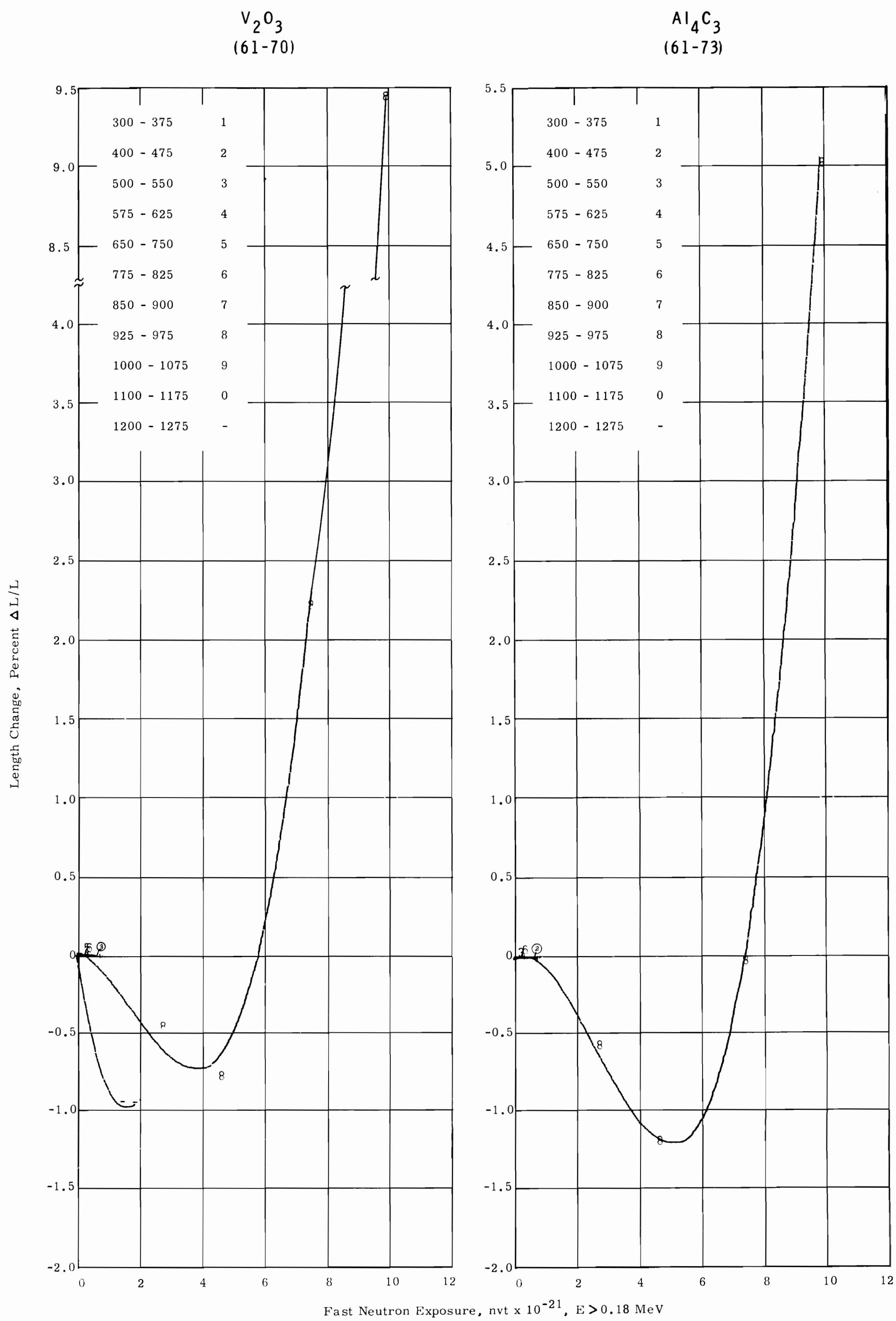

FIGURE 9. Length Change of Additive Graphites (Transverse).

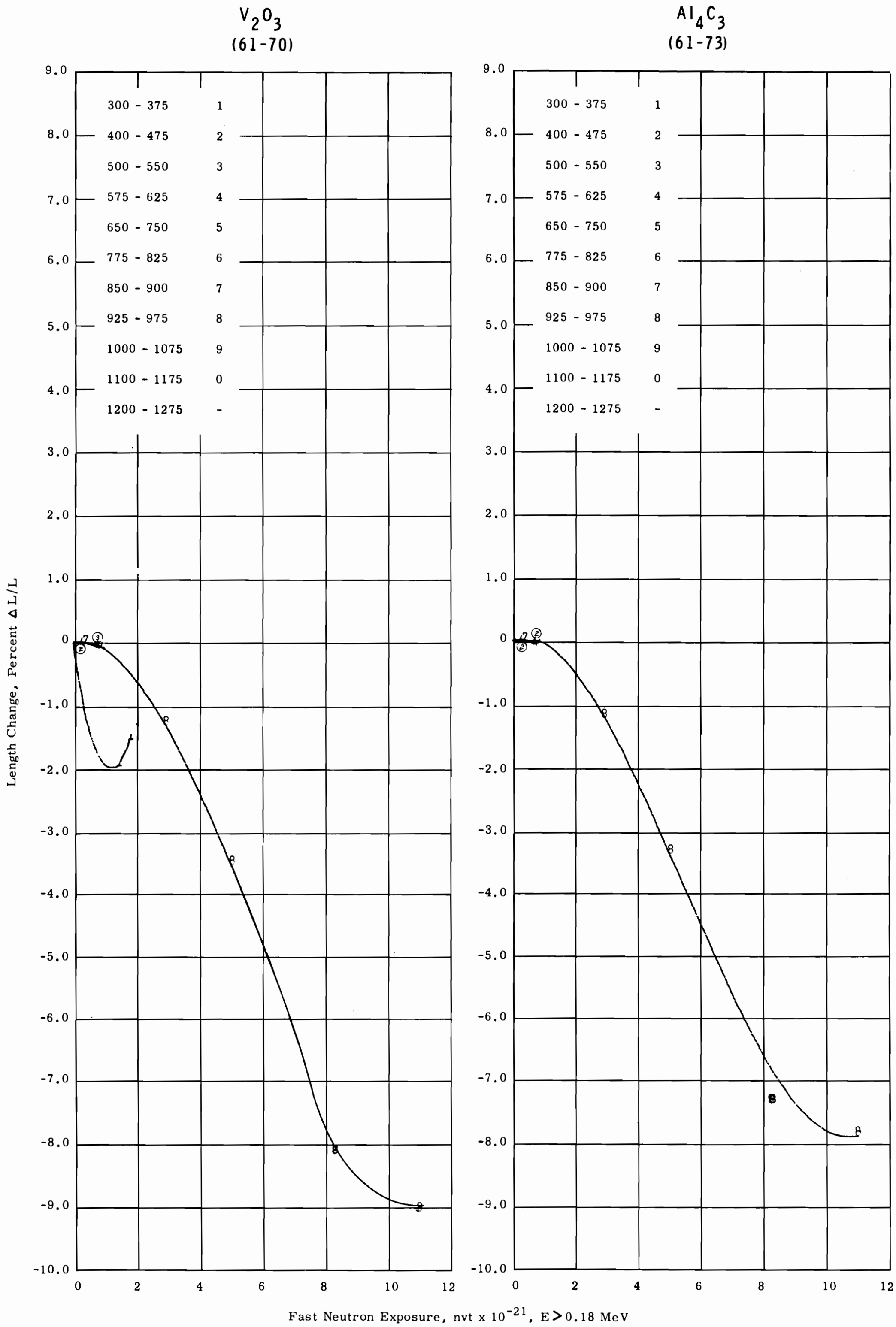

FIGURE 10. Length Change of Additive Graphites (Parallel).

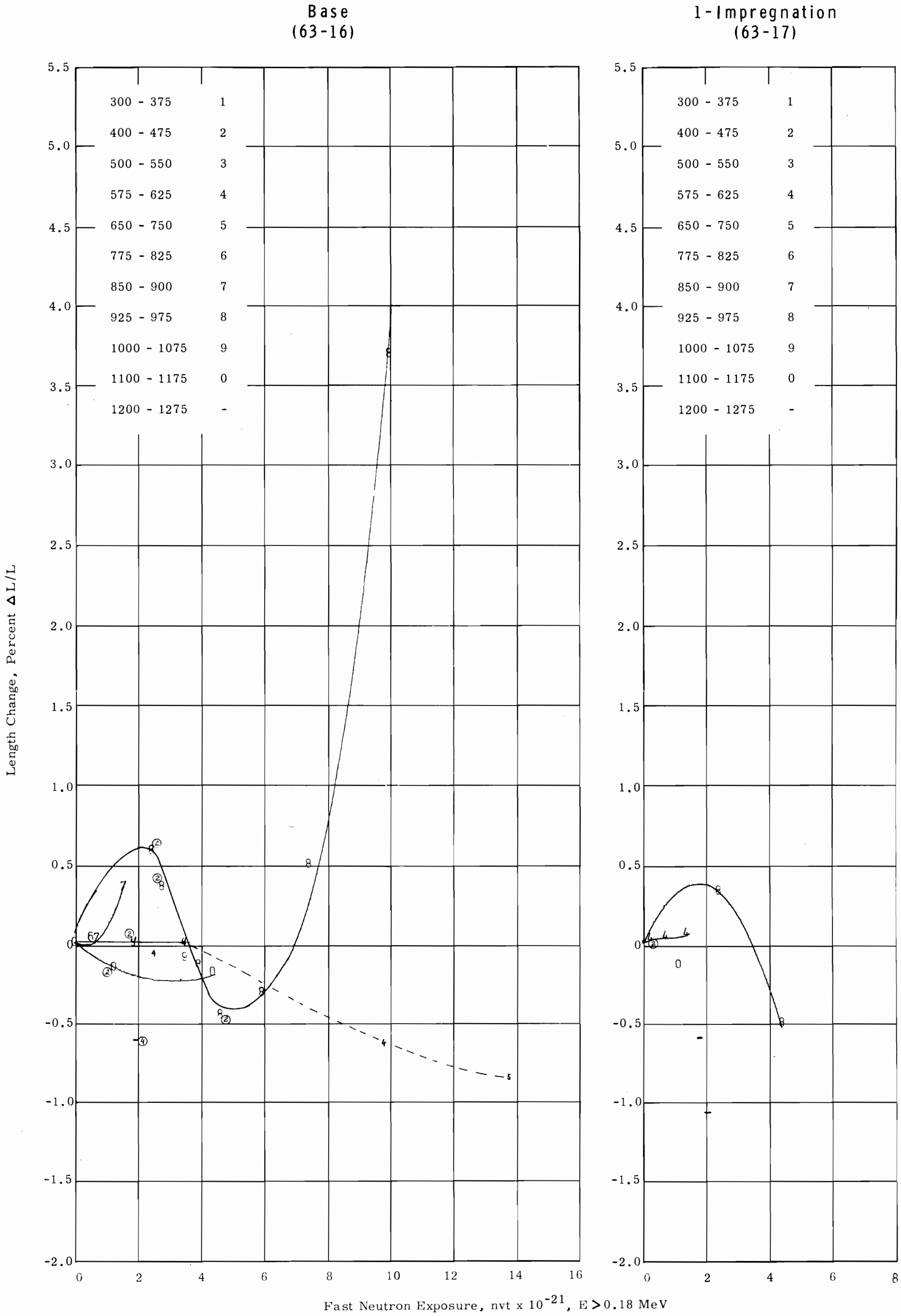

FIGURE 11. Length Change of Raw Coke Graphites (Transverse).

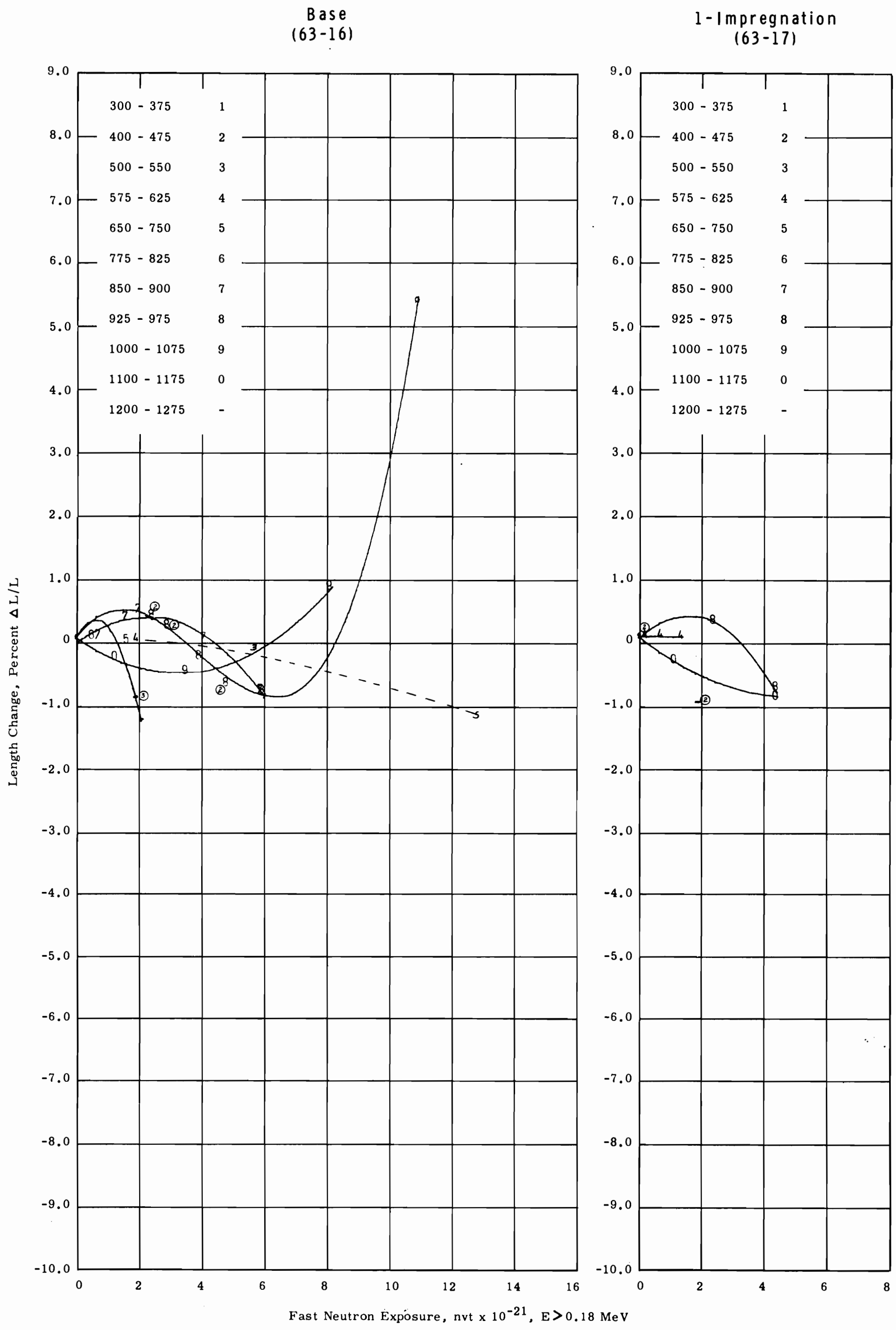

FIGURE 12. Length Change of Raw Coke Graphites (Parallel).

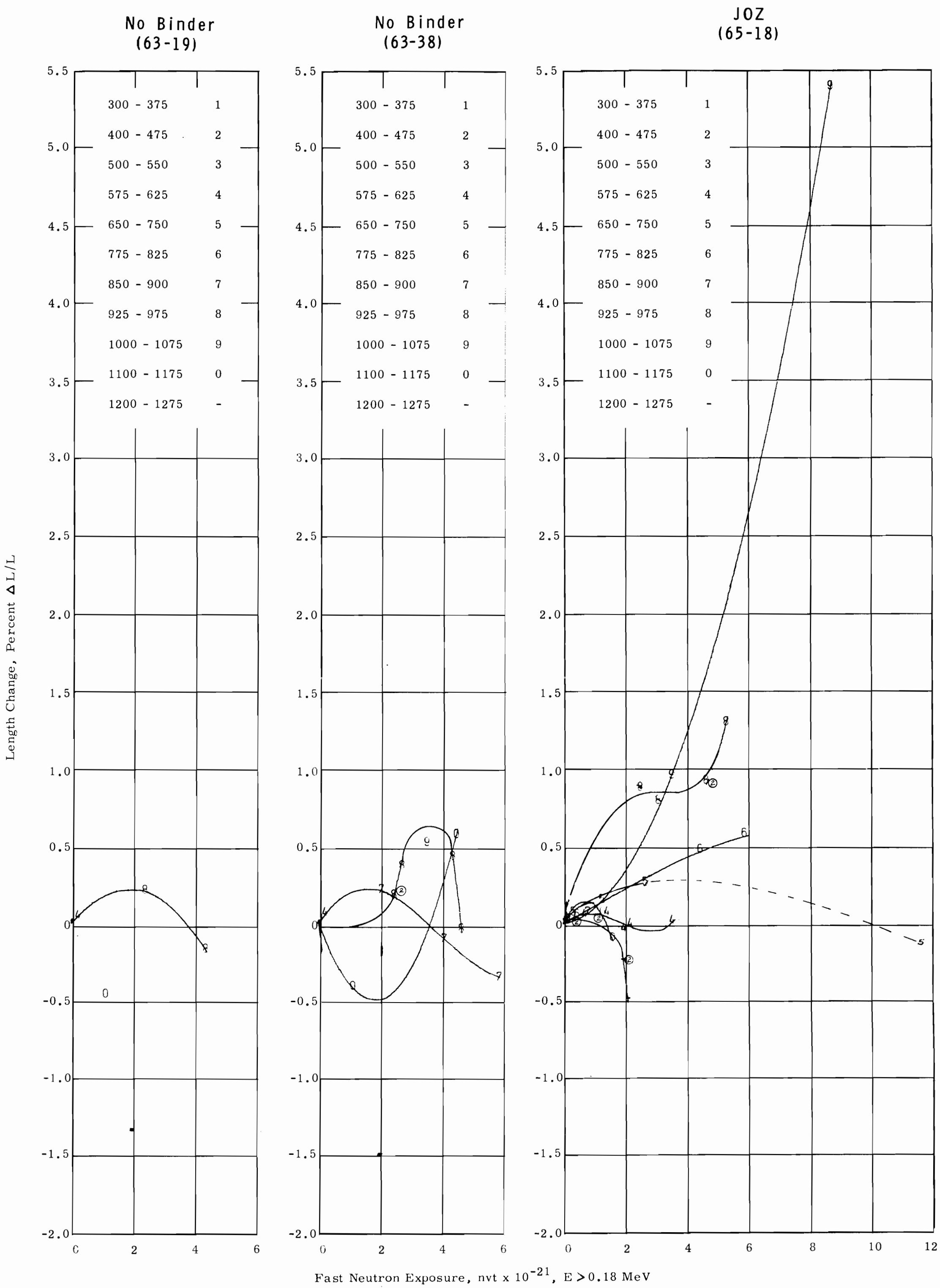

FIGURE 13. Length Change of Raw Coke Graphites (Transverse).

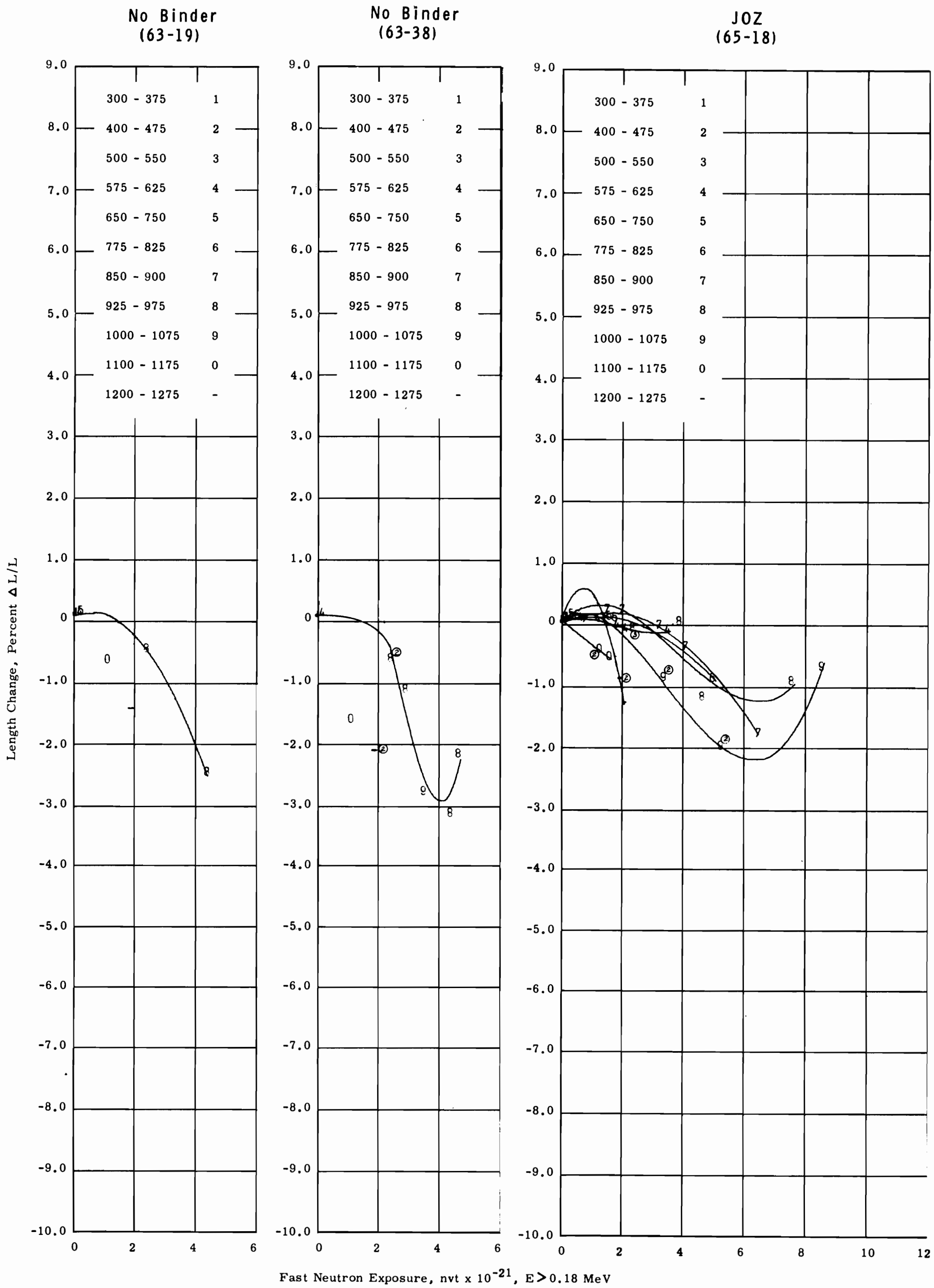

FIGURE 14. Length Change of Raw Coke Graphites (Parallel).

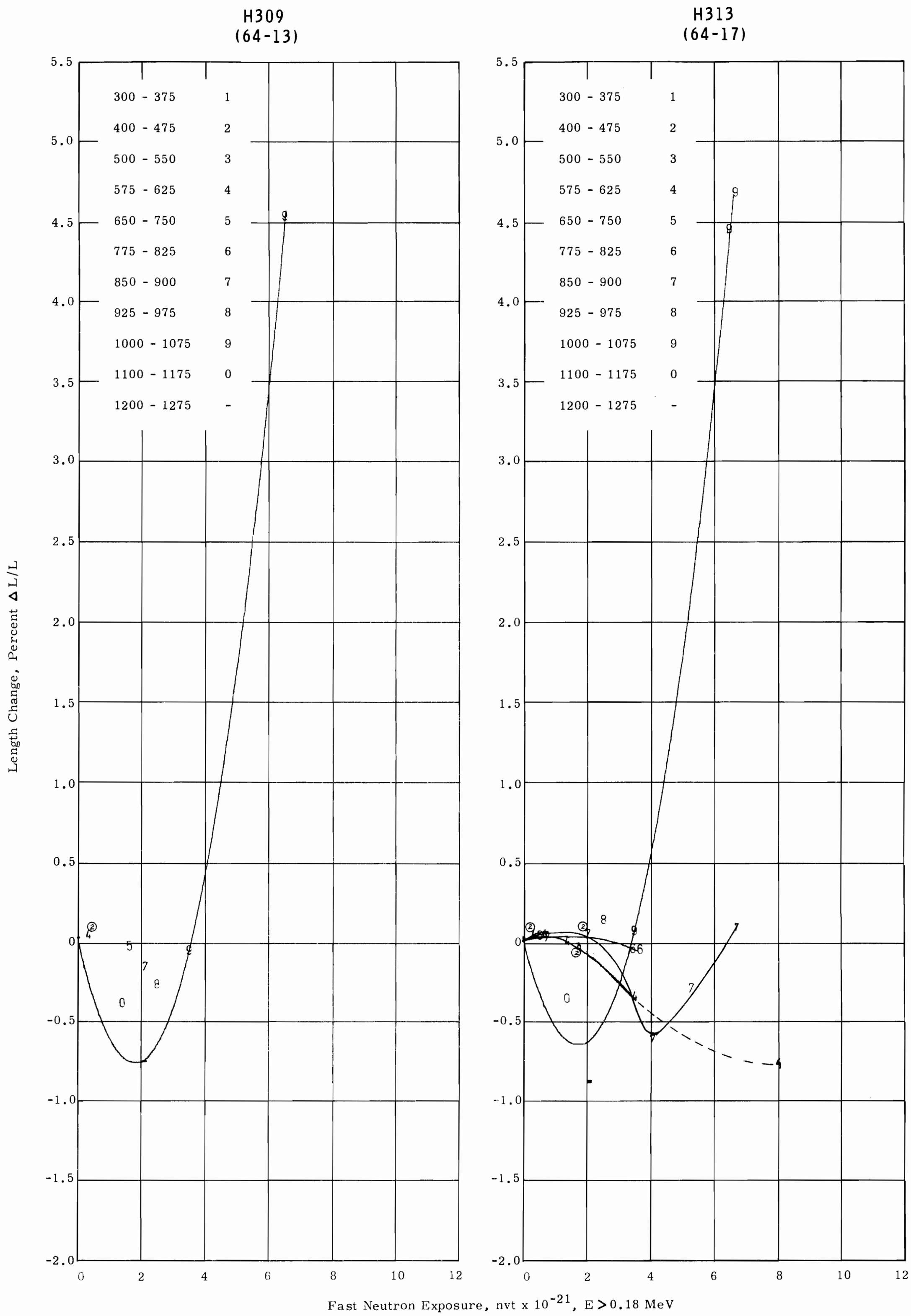

FIGURE 15. Length Change of Coking Temperature Series Graphites (Transverse).

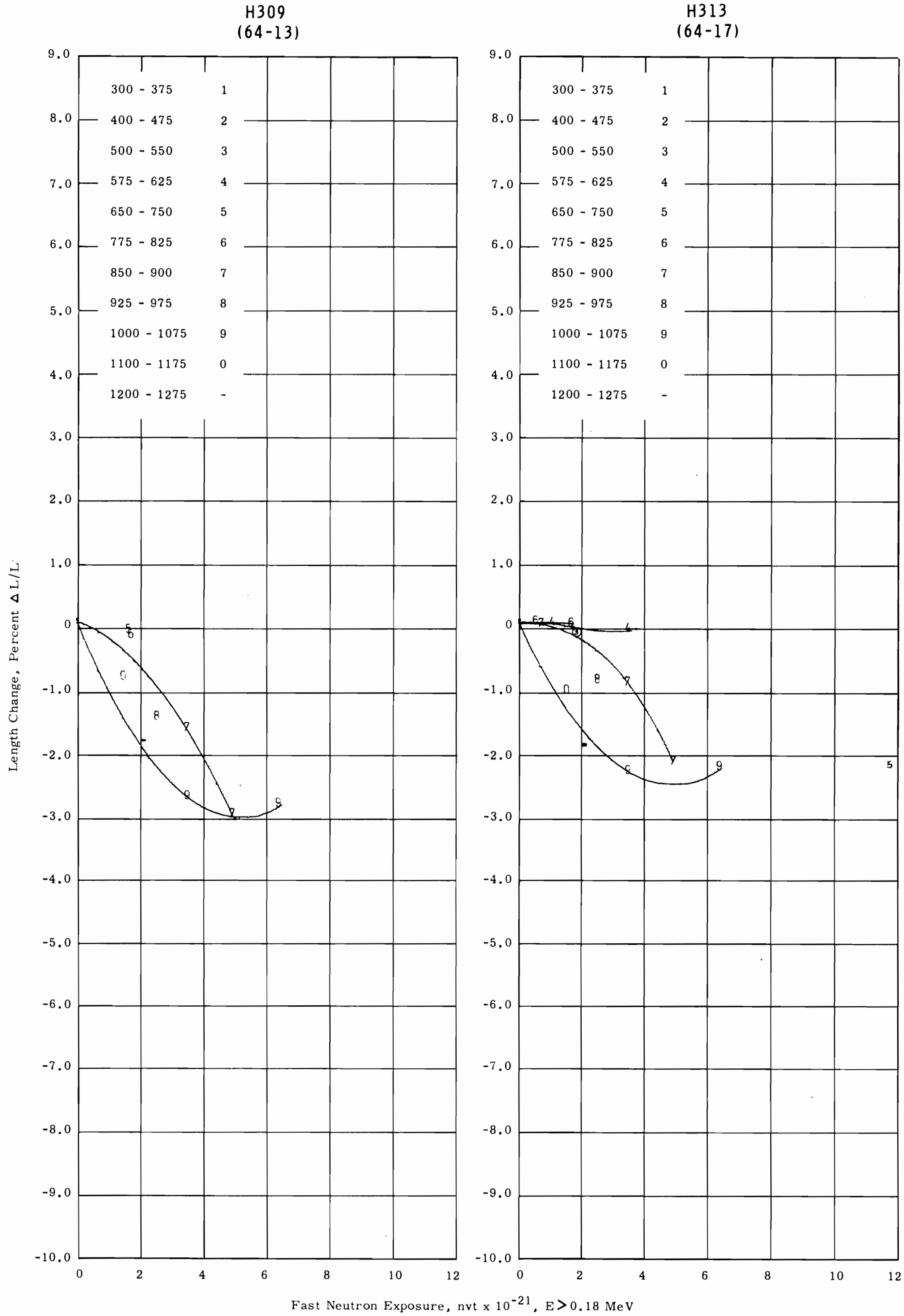

FIGURE 16. Length Change of Coking Temperature Series Graphites (Parallel).

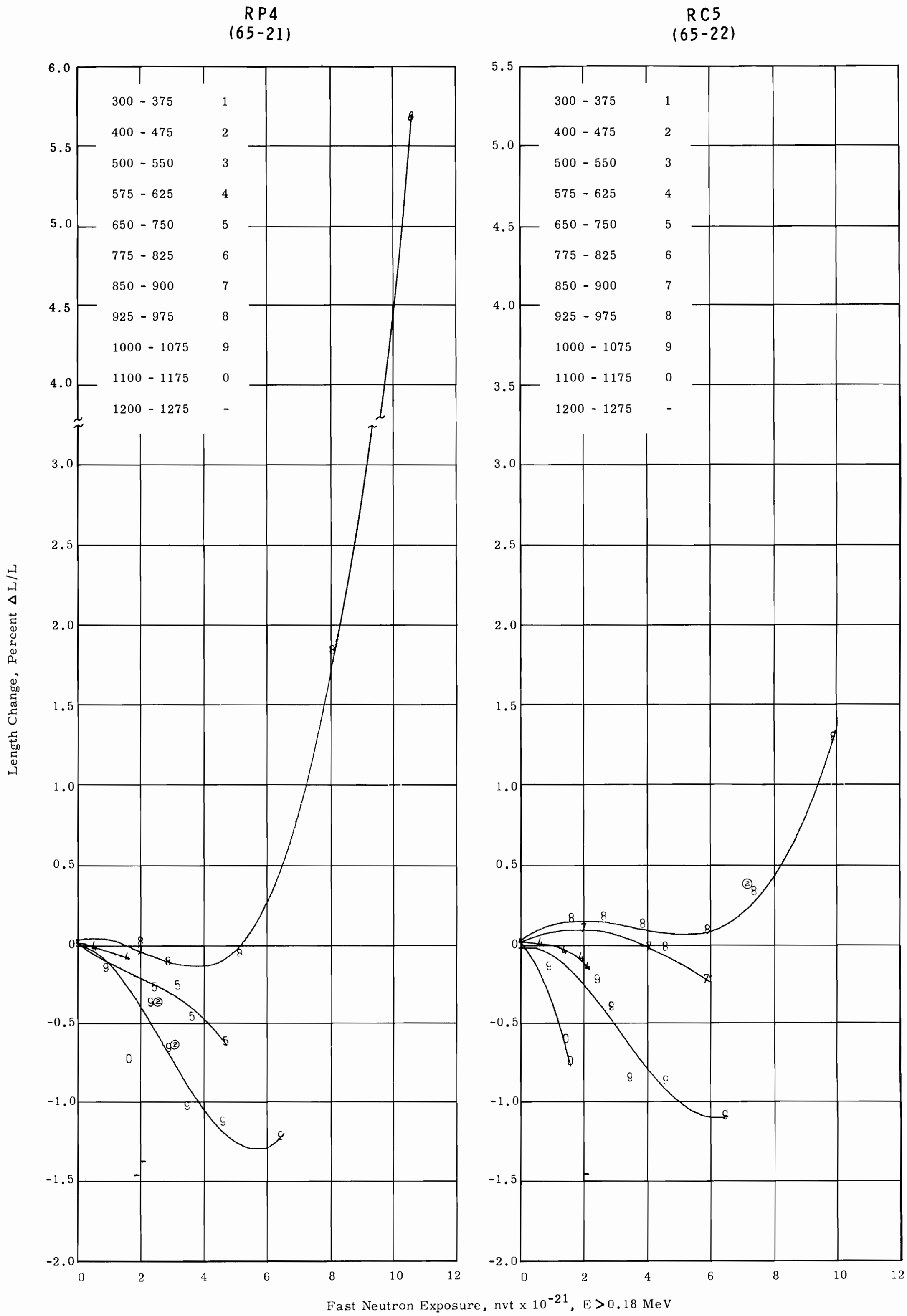

FIGURE 17. Length Change of Isotropic Graphites (Transverse).

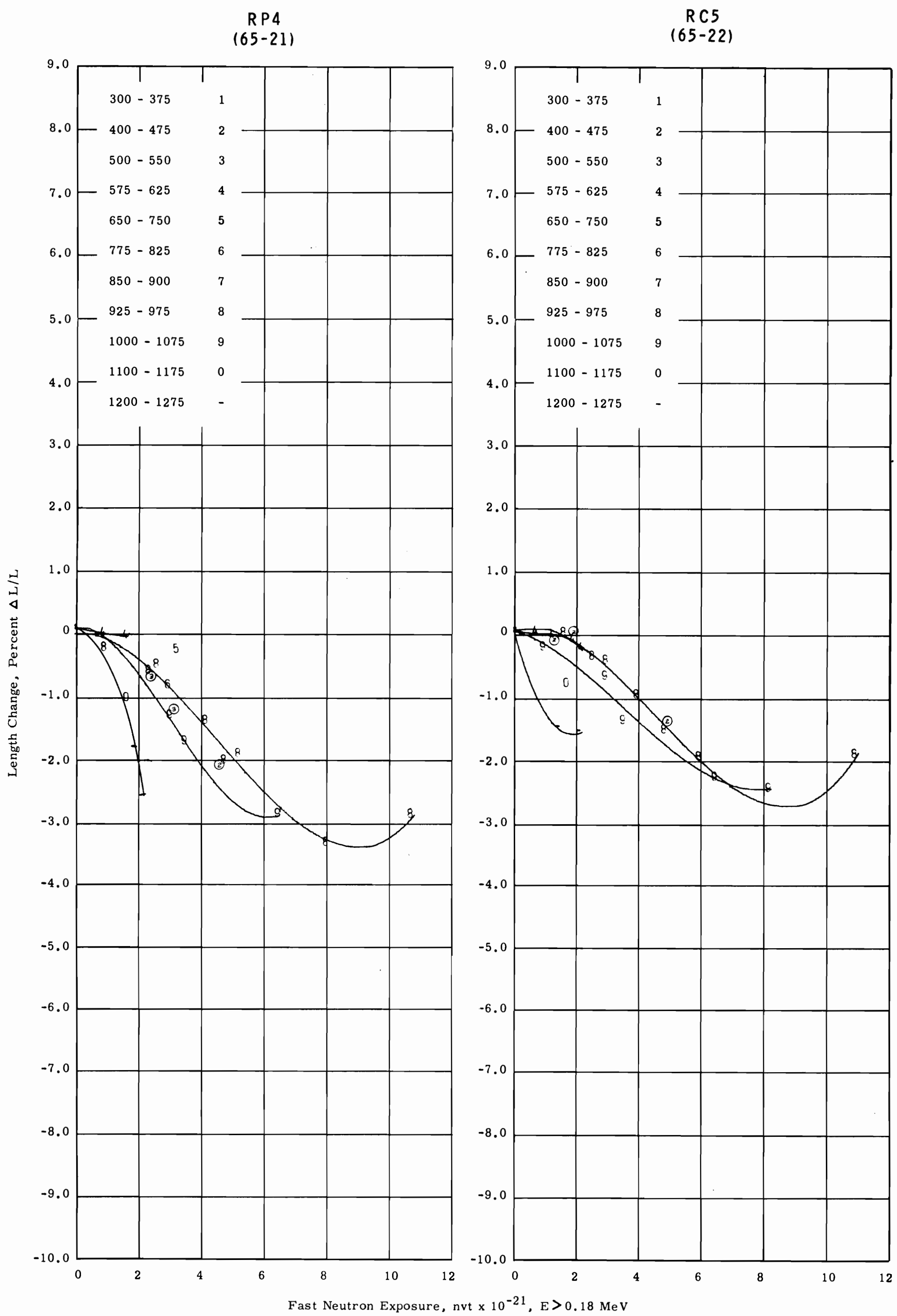

FIGURE 18. Length Change of Isotropic Graphites (Parallel).

in the transverse direction. RC5 in the transverse direction shows less contraction followed by less expansion than CSF at temperatures below 975 °C. RC5, at 1000 to 1075 °C, contracts more than CSF and turns around less rapidly, and at 1100 to 1175 °C behaves almost the same as CSF. Likewise, in the parallel direction at temperatures of 925 to 1075 °C, RC5 contracts less than CSF and at 1200 to 1275 °C behaves nearly the same.

The dimensional behavior of two other isotropic graphites which behave very isotropically under irradiation (65-42 and 66-4) is shown in Figures 19 and 20. Both materials show very small length changes, with 66-4 showing less than 65-42. The slight expansions are significantly different from the behavior of CSF. Of all the materials tested, these are the only ones showing significantly different behavior from the general contraction, turnaround, and expansion.

The length-change data for two specialty graphites DS13 and H349 are shown in Figures 21 and 22. The latter contracts more rapidly in both directions than CSF. In the parallel direction, DS13 goes through turnaround much more rapidly than CSF. Thus these specialty materials do not exhibit improved dimensional behavior.

The length-change data for GN, a special nuclear grade graphite, and MSRE, the graphite used in the Molten Salt Reactor Experiment, are shown in Figures 23 and 24. The GN graphite (65-29) reaches turnaround much more rapidly than CSF in both orientations. The MSRE graphite (65-38) shows a widely divergent behavior by expanding extremely rapidly in the transverse direction and contracting very rapidly in the parallel direction. However, this temperature range is above that in the Molten Salt Reactor Experiment.

The dimensional behavior of the two extremes of a binder-temperature series of graphite (63-30 and 63-36) and the two

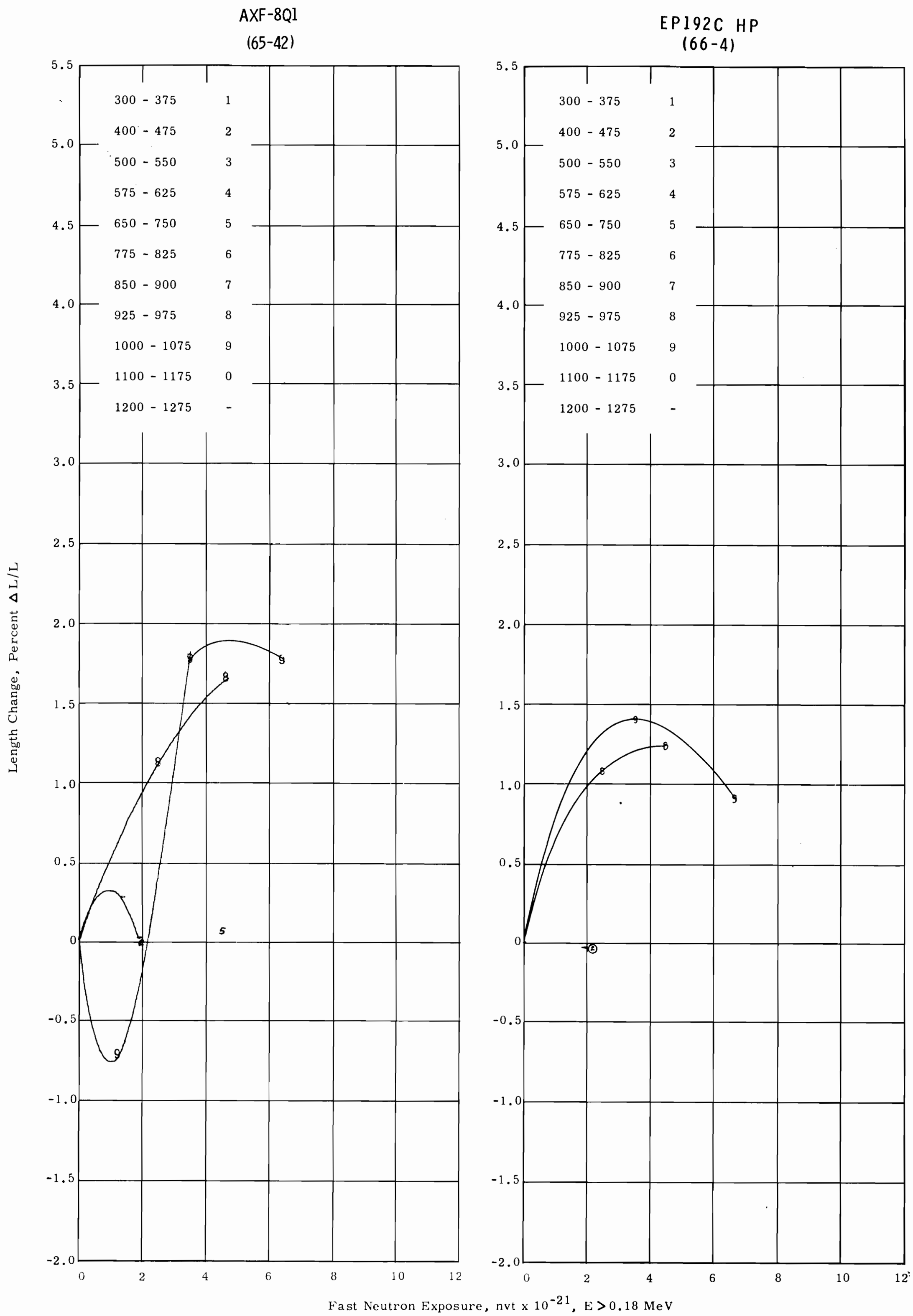

FIGURE 19. Length Change of Isotropic Graphites (Transverse).

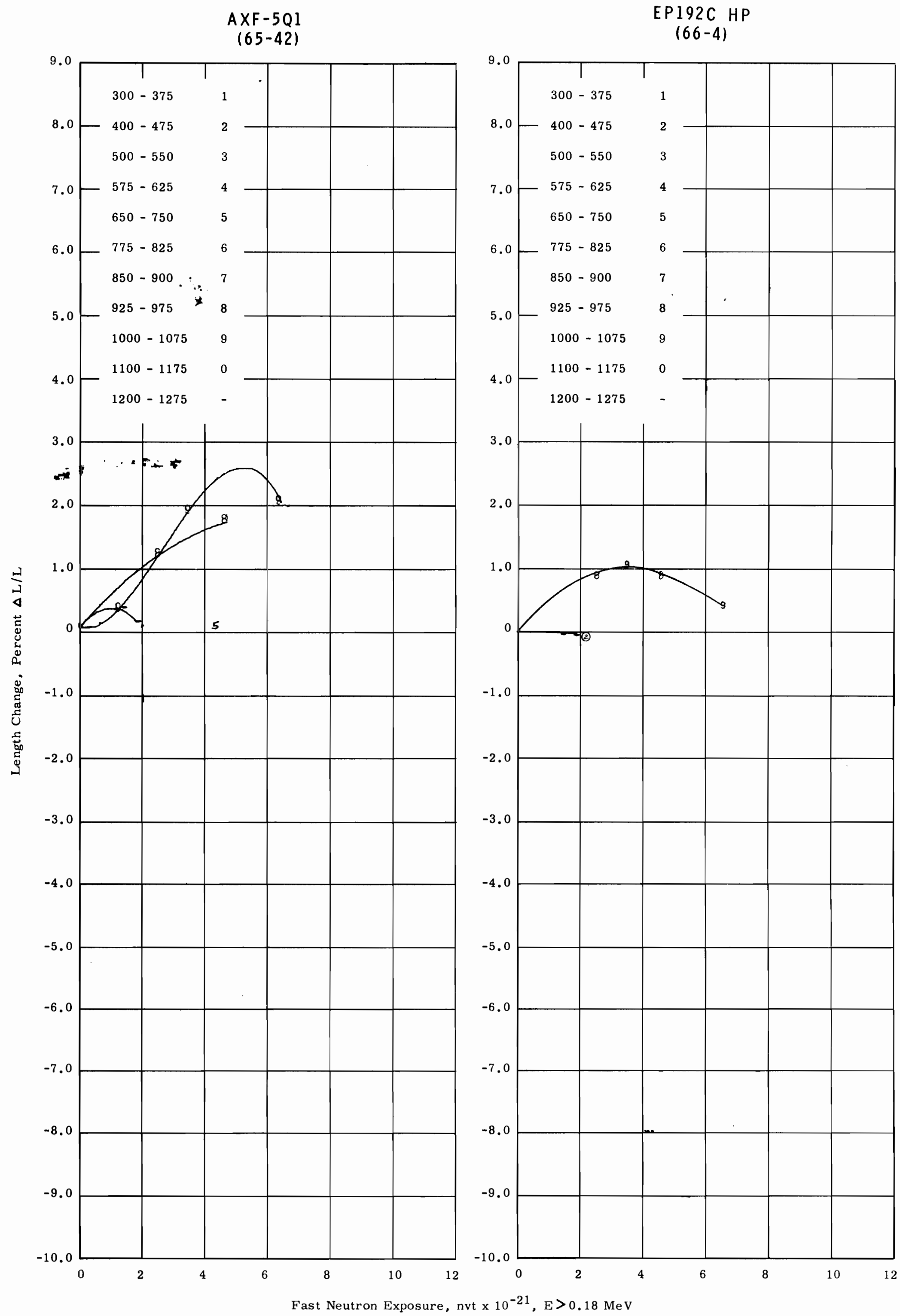

FIGURE 20. Length Change of Isotropic Graphites (Parallel).

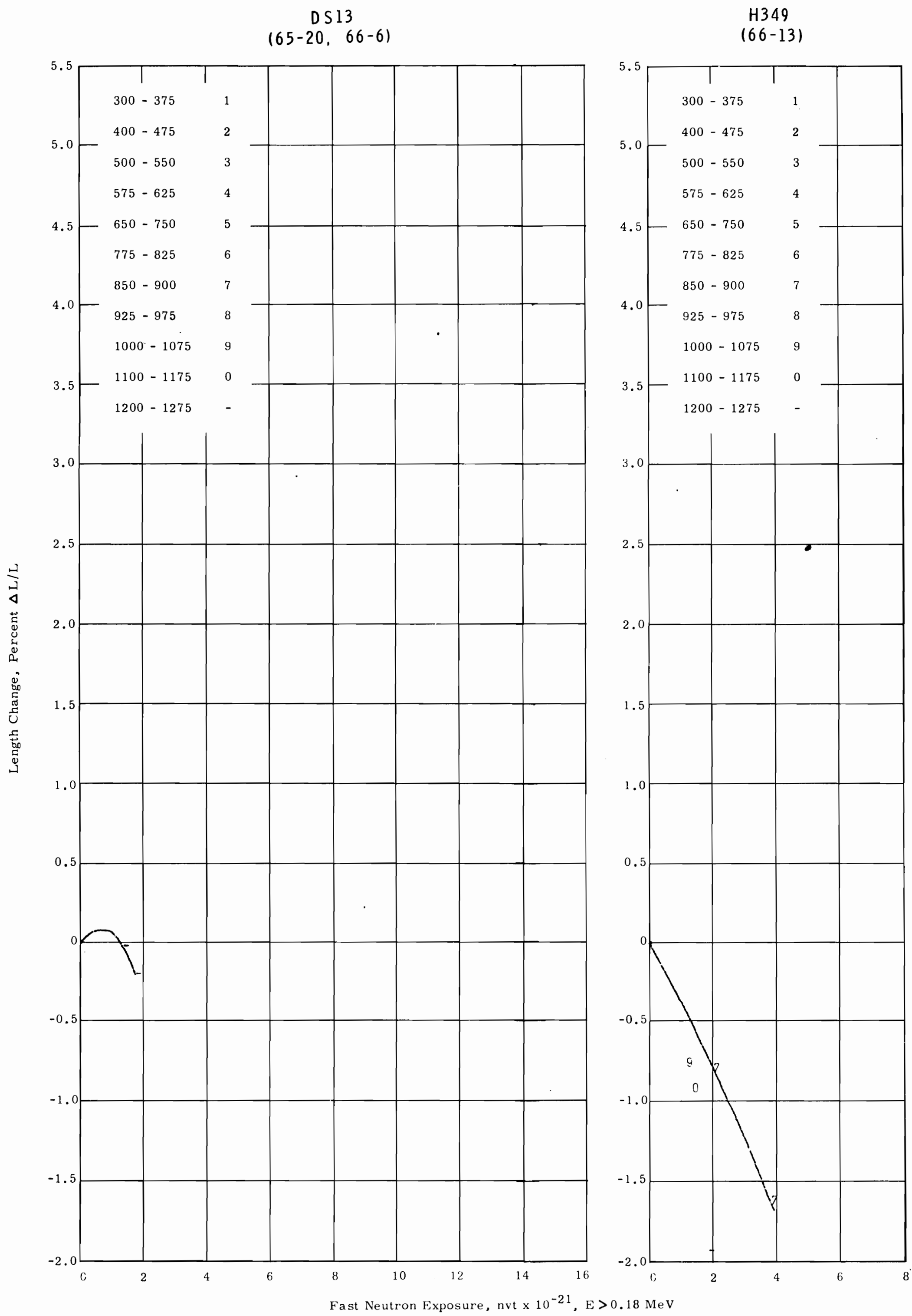

FIGURE 21. Length Change of Specialty Graphites (Transverse).

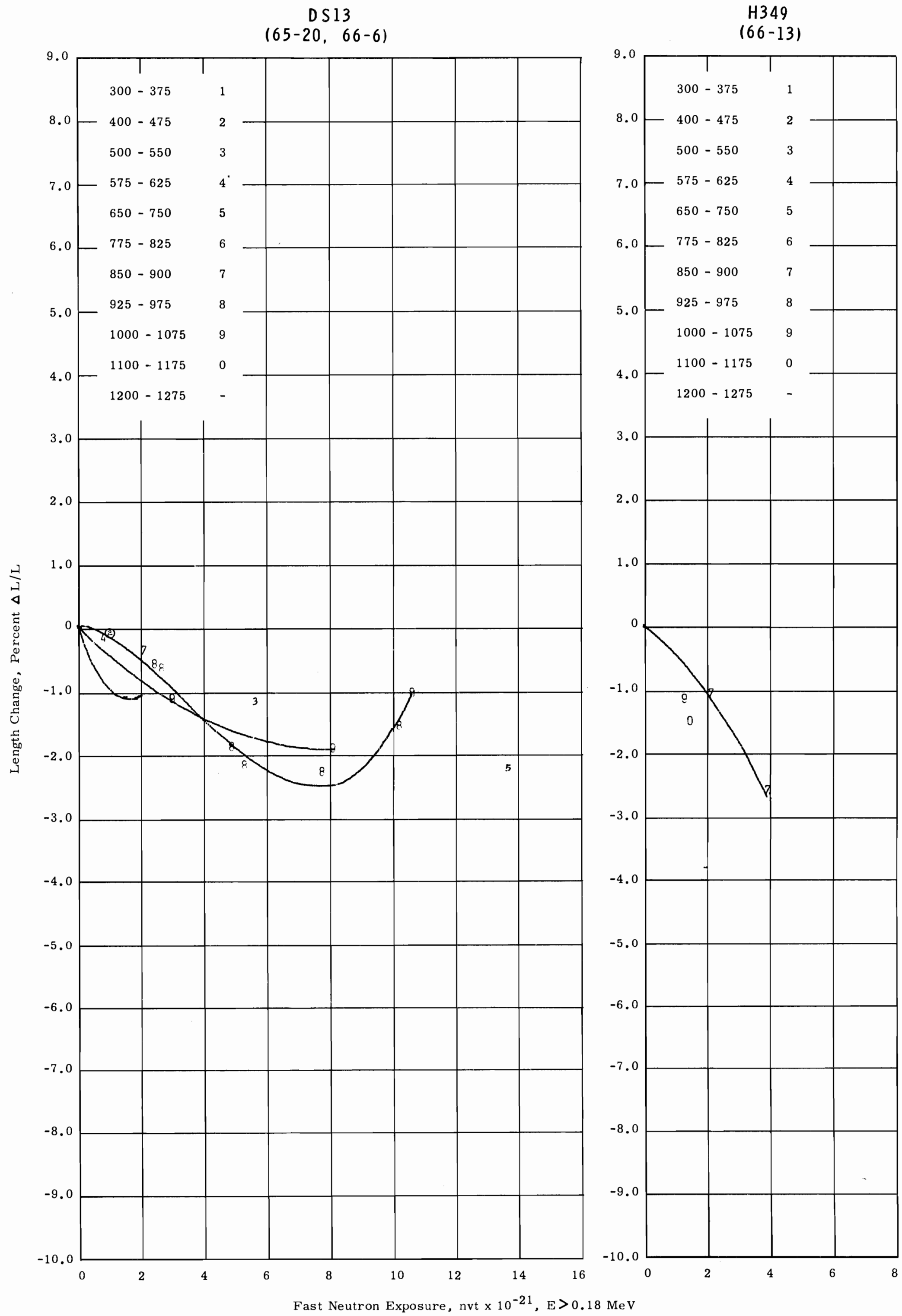

FIGURE 22. Length Change of Specialty Graphites (Parallel).

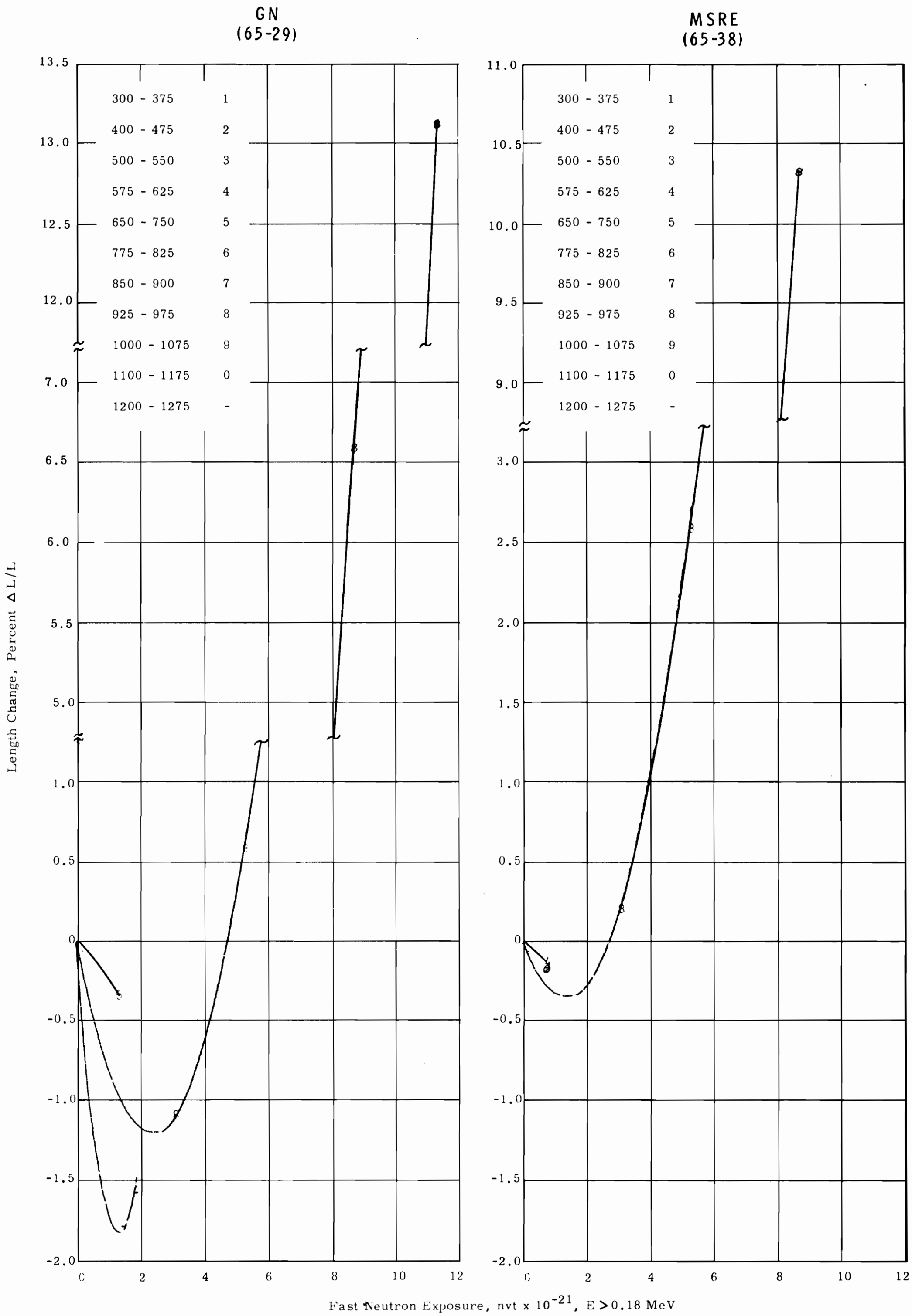

FIGURE 23. Length Change of Nuclear-Grade Graphites (Transverse).

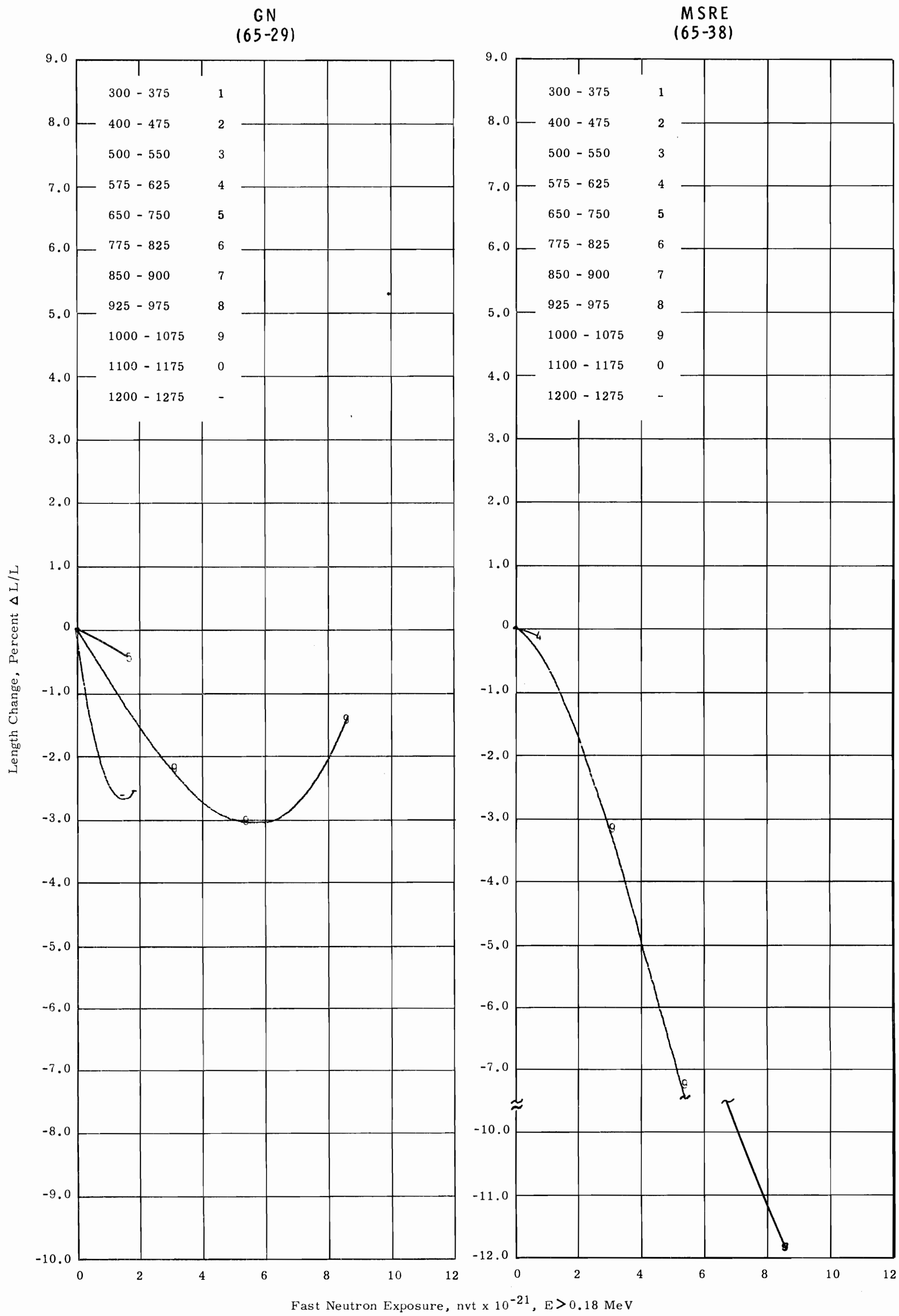

FIGURE 24. Length Change of Nuclear-Grade Graphites (Parallel).

extremes of a graphitization temperature series of graphites (65-5 and 65-8) are presented in Figures 25 and 26. A comparison of the data shows, for both orientations in both series, the least contraction in material processed at the higher temperature, thus confirming that contraction is minimized by higher graphitization temperature. However, expansion begins at low fluences in relation to CSF graphite.

The length-change data for two experimental graphites are shown in Figures 27 and 28. The 9567 (65-37) graphite, available in large sizes of interest for future gas-cooled reactors, shows anisotropic behavior very similar to that for CSF graphite.

The general turnaround behavior characteristic of all 58 different grades of graphite irradiated under this program is shown in Figures 29 and 30 for the transverse and parallel orientations, respectively. The spectrum of graphites represents a wide variety of cokes, binders, and processing conditions. The shaded areas represent the dimensional change data for all grades being irradiated. The unbounded margin on the right side of the parallel bands indicates that not all parallel samples have yet reached turnaround. However, many parallel samples within the shaded area have turned around and all undoubtedly will, but at an exposure higher than that for the transverse direction. As shown, the damage rate for both orientations at irradiation temperatures above 800 °C is appreciably higher. This transition from the low damage rate to the higher one takes place over an extremely narrow temperature range. Within the two temperatures bands, the data are all grouped closely, especially in the transverse orientation.

In summary the following general observations on length change can be made:

- Expansion becomes the dominating dimensional behavior in all directions as neutron fluences are increased.

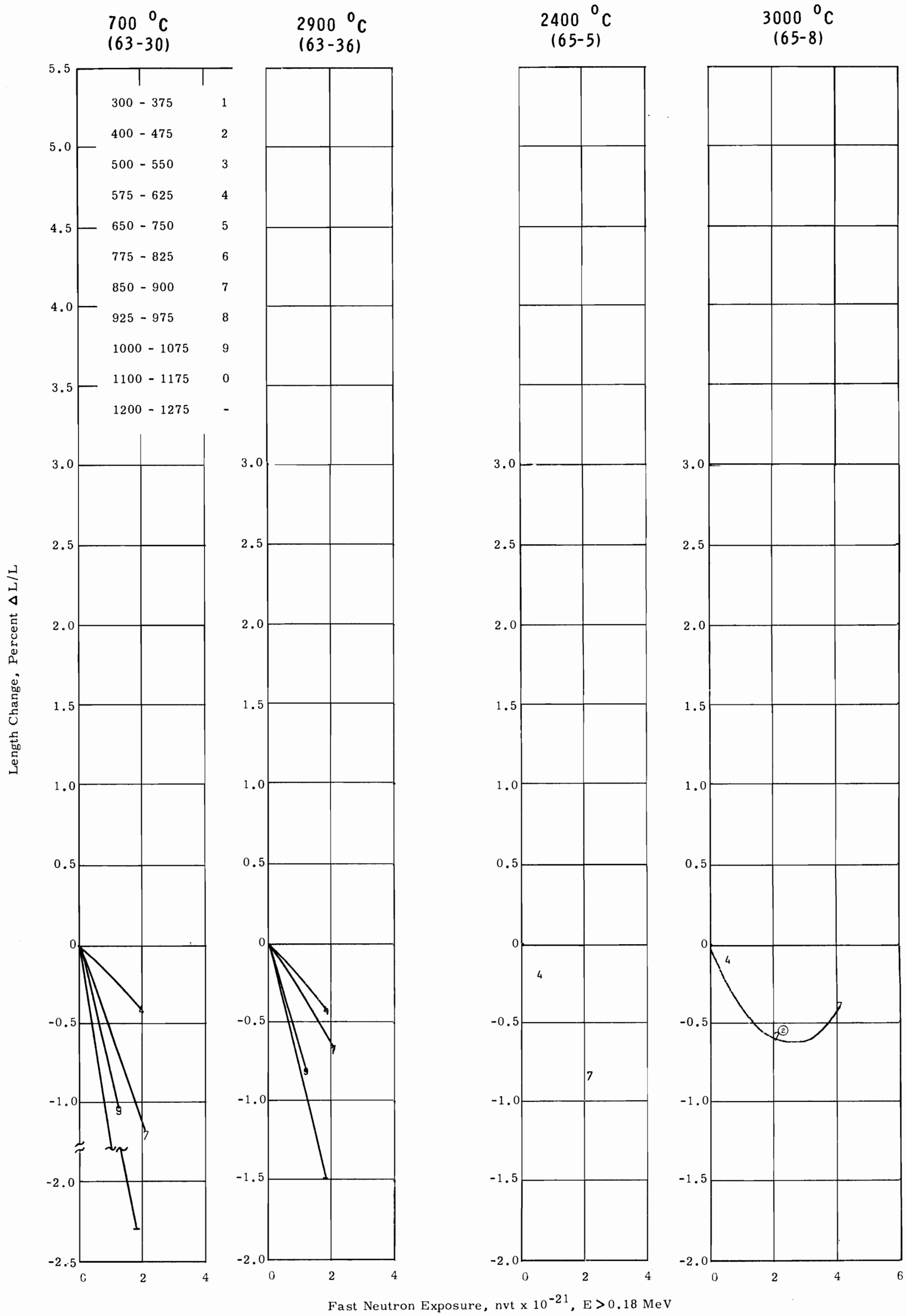

FIGURE 25. Length Change of Temperature Series Graphites (Transverse).

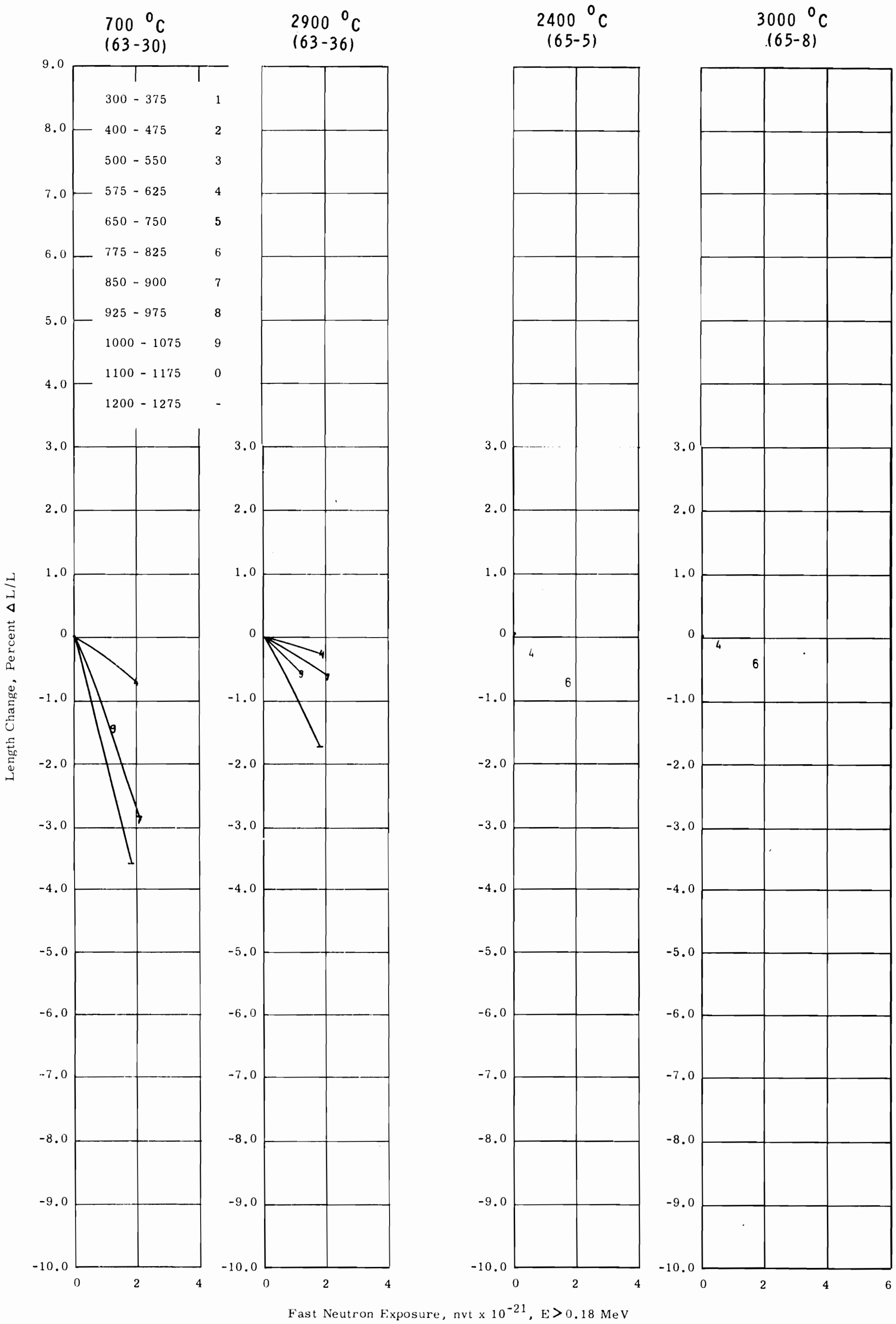

FIGURE 26. Length Change of Temperature Series Graphites (Parallel).

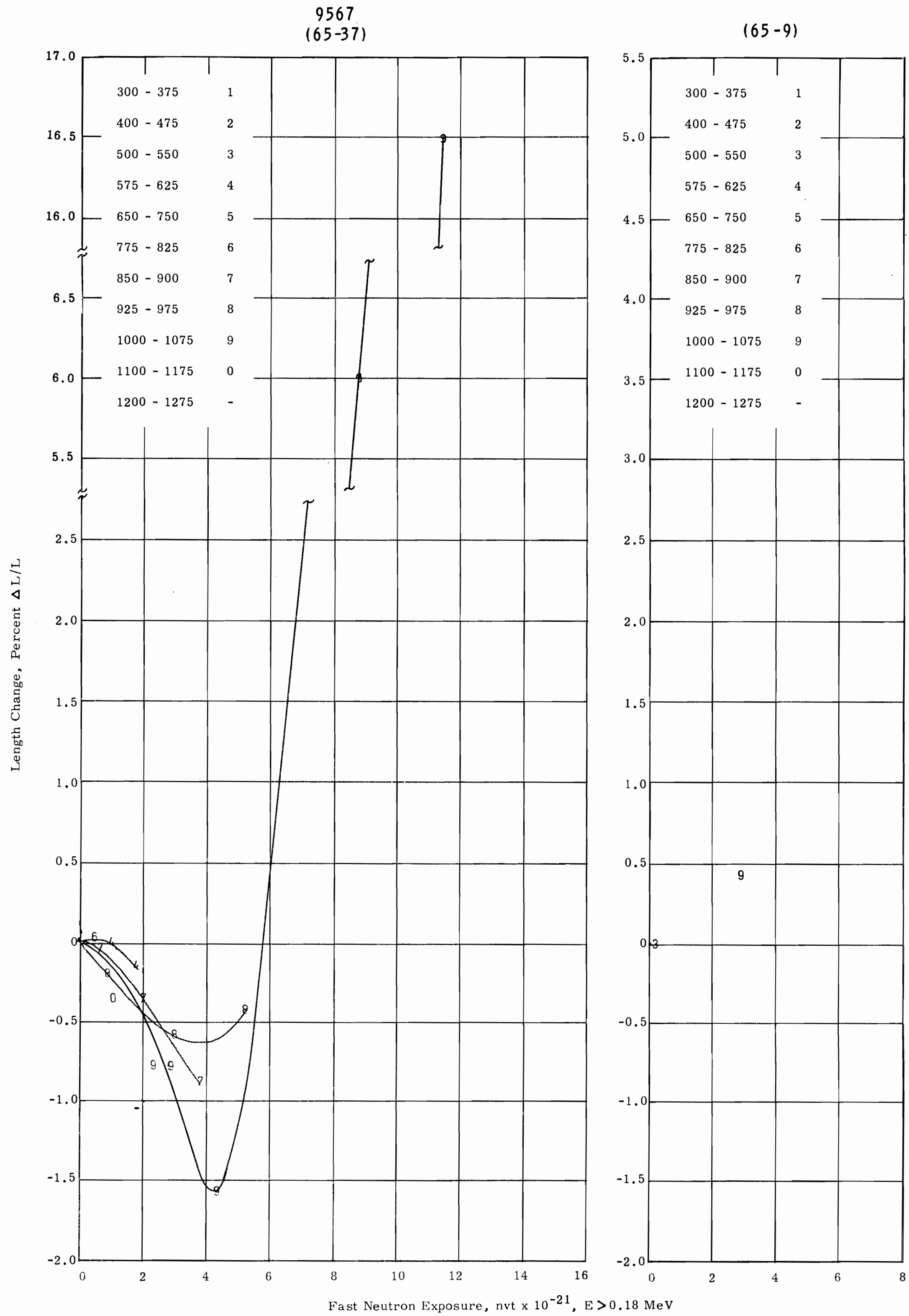

FIGURE 27. Length Change of Experimental Graphites (Transverse).

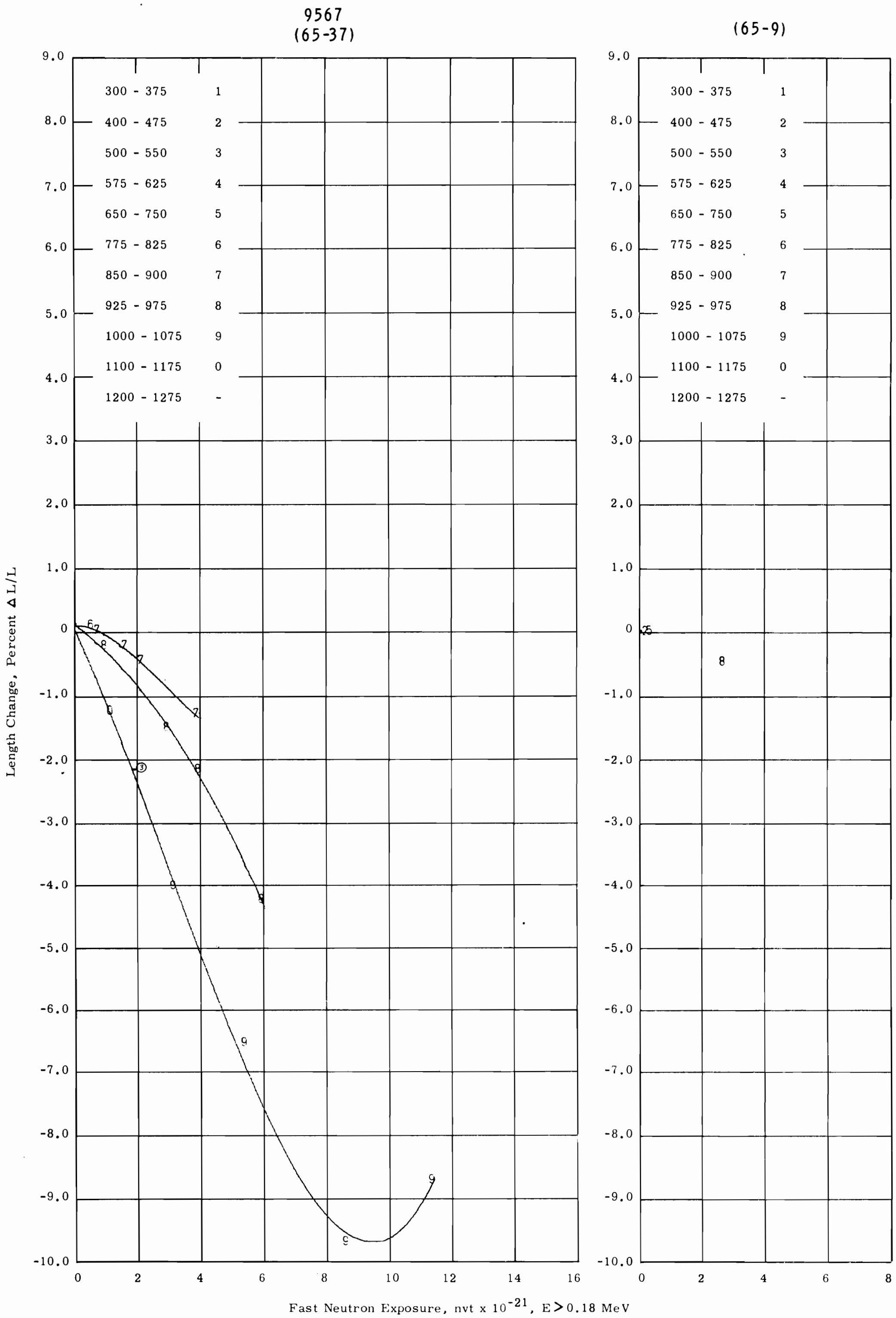

FIGURE 28. *Length Change of Experimental Graphites (Parallel).*

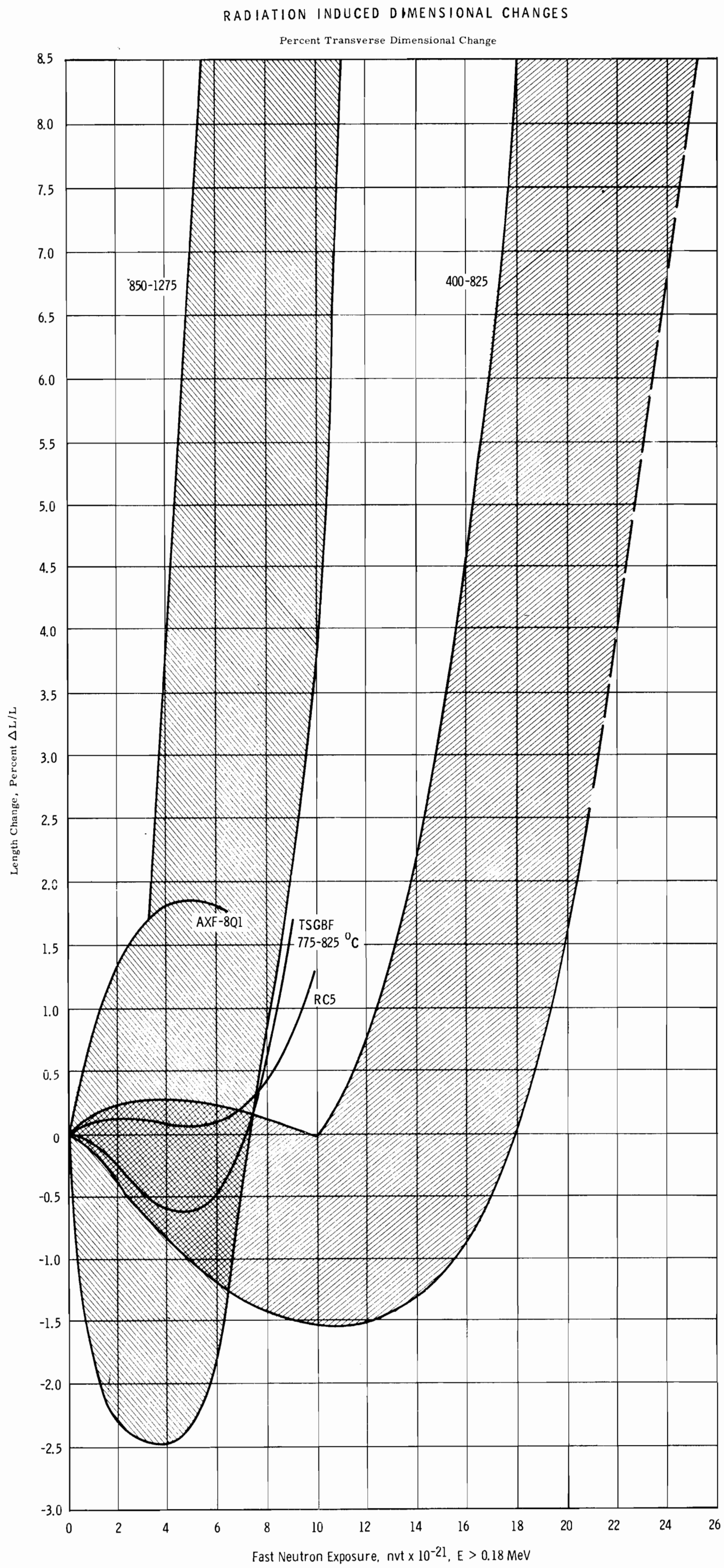

FIGURE 29. Length Change of All Graphites (Transverse).

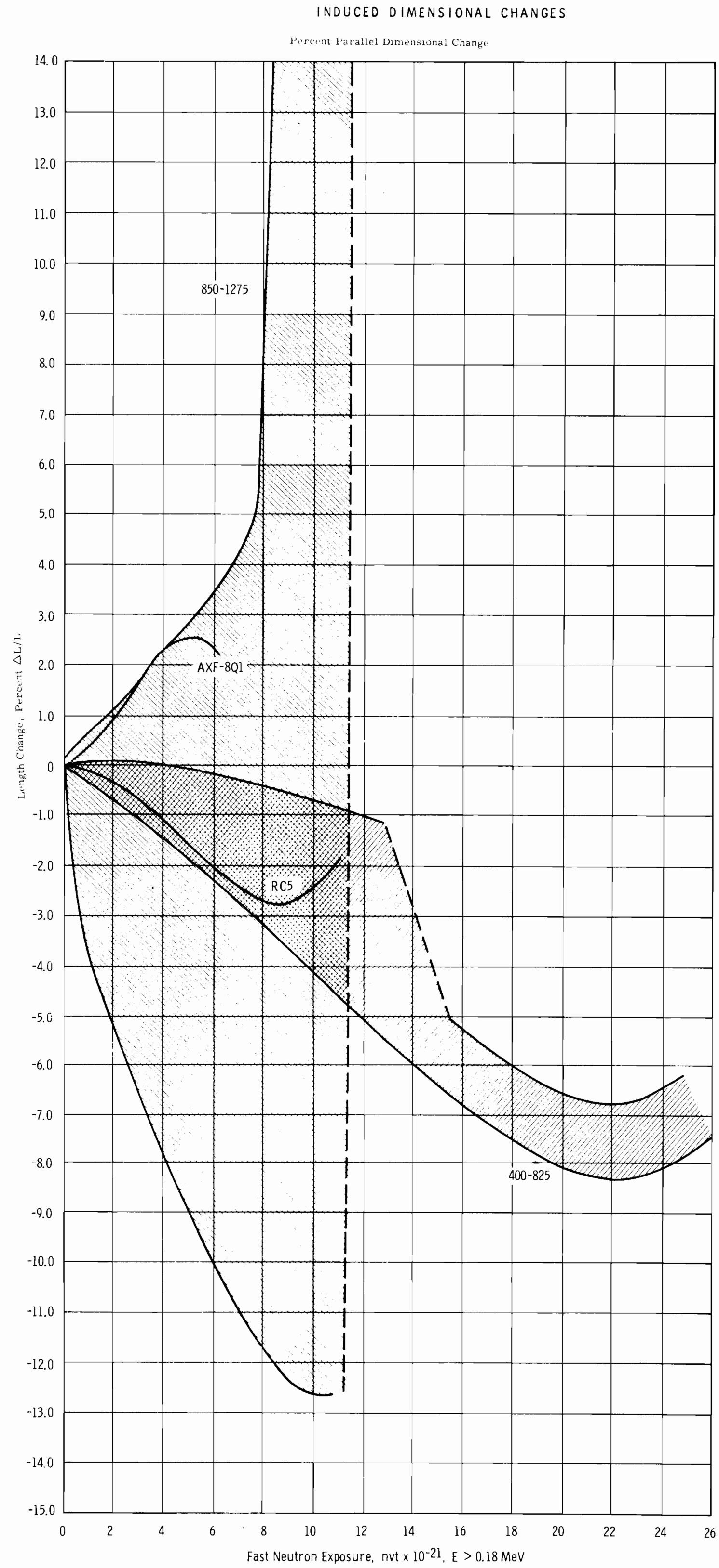

FIGURE 30. Length Change of All Graphites (Parallel).

- Above 800 °C, dimensions change much more rapidly with irradiation than at lower temperature.
- Poorly graphitized materials show larger changes than well graphitized materials.
- Isotropic graphites generally contract less than CSF and other typical grades.
- Raw-coke graphites generally contract less than CSF and other typical grades.
- Factors leading to lower contraction may be detrimental in the long-term because expansions eventually become controlling.

Effect of Sample Size on Length Change

A number of the "telephone-dial" sample holders (see BNWL-1056B, Appendix B) were measured to obtain additional information on the effect of sample size. It has been reported that large blocks, 4 × 4 × 24 in., contracted approximately twice that of small 0.43 in. diameter × 4 in. samples,(10) that the 0.43 in. diameter × 4 in. samples contracted 20 to 30% more than 0.262 in. diameter × 1 3/4 in. long samples,(11) and that 1/8 in. diameter transverse samples contracted more and 1/8 in. diameter parallel samples contracted less than samples 11/32 to 17/32 in. in diameter.(12) Consequently, the lengths (parallel direction) and diameters (transverse direction) were measured on the five dials in the H-3-12 (1) and H-3-23 (4) capsules. The results, as tabulated in BNWL-1056B, Appendix C, indicate that contractions measured on the 1.7 in. diameter × 2 in. long dials agree with data from the 1/4 in. diameter × 1 3/4 in. long rod samples within the standard deviation of the measurements on the dials.

Effect of Variation in Irradiation Temperature on Length Change

During the course of these studies, a number of samples were repositioned in the capsules to determine the effects of variations in irradiation temperatures on dimensional behavior. This behavior is of interest due to the fact that in nearly all graphite reactors operating temperatures have been increased after an initial operating period. Transverse and parallel samples of CSF, NC8, TSX, TSGBF, and RP4 were included. Both irradiation temperature increases and decreases were investigated. The results, for TSX graphite, are shown in Figure 31 and, for the other samples, in BNWL-1056B, Figures E7 through E9. Each sample is shown by a separate symbol, and the subsequent irradiations are connected by segmented lines. The number by the symbol at the lowest neutron fluence is the irradiation temperature to that time. The numbers beside the subsequent symbol are the new irradiation temperature followed by the mean irradiation temperature in parentheses. The standard length change data are shown as solid lines with temperature ranges indicated. Although exceptions were found, the general behavior indicated that contraction rate changes corresponding to that of samples irradiated exclusively at the new temperature accompany irradiation temperature changes, and that the total contraction is generally between that for samples irradiated exclusively at the old temperature and those irradiated exclusively at the new temperature.

VOLUME CHANGE

Using the length-change data presented in the previous figures, an analysis of the resultant volume change was made to give an indication of the bulk behavior of the graphites. The equation used was:

$$\frac{\Delta V}{Vo} = \left(1 + \frac{\Delta L}{L_1}\right)^2 \times \left(1 + \frac{\Delta L}{L_2}\right) - 1$$

where V = volume

L_1 = length transverse to the extrusion axis or molding force.

L_2 = length parallel to the extrusion axis or molding force.

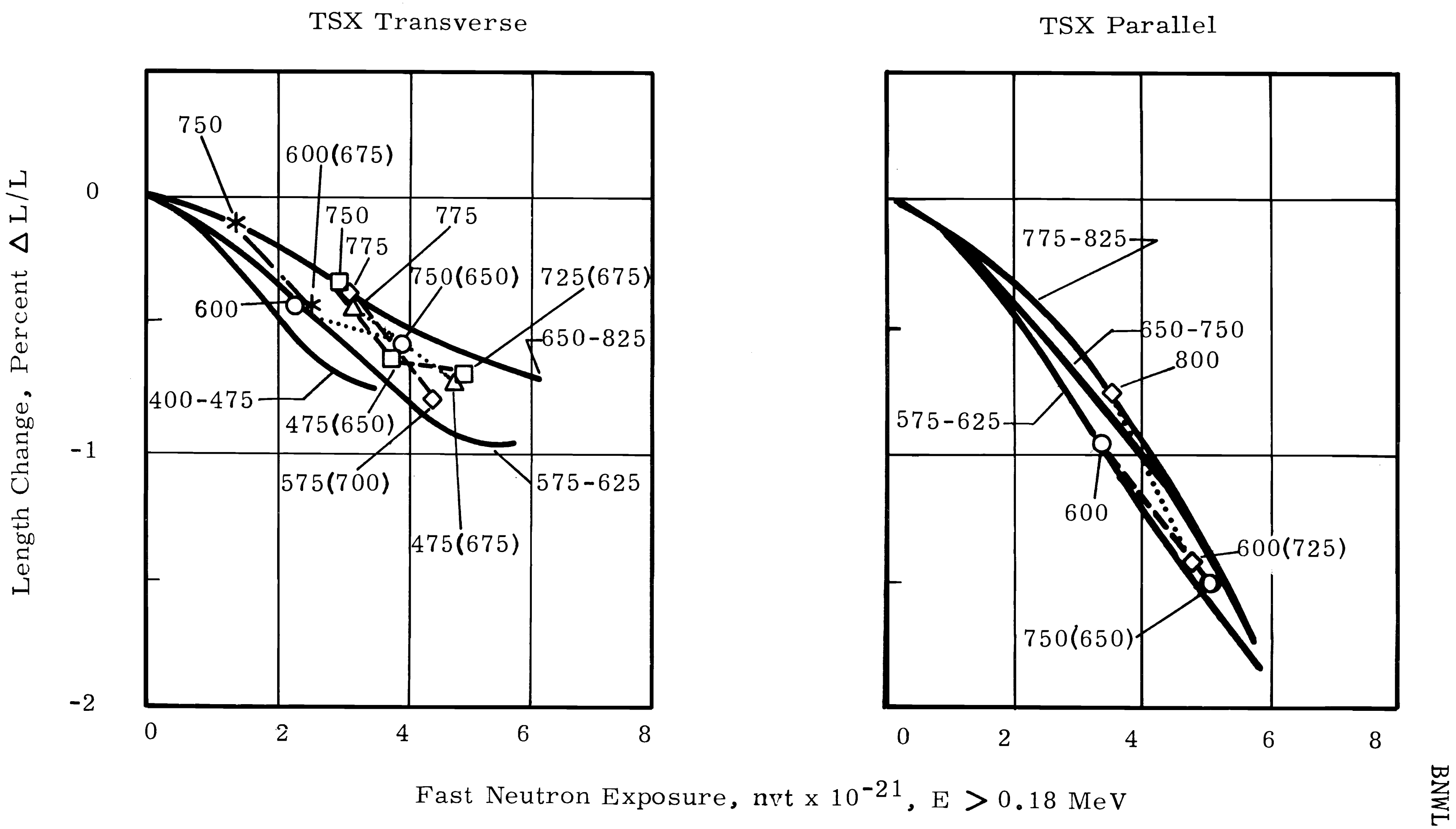

FIGURE 31. *Length Change of TSX Graphite - Sample Irradiation Temperature Changed.*

The volume-change curves for CSF graphite are presented in Figure 32. The isotherms follow a regular pattern in order of decreasing contraction at low fluences until turnaround is reached. At 775 to 825 °C, the bulk expansion of nearly 25% indicates a significant decrease in sample density.

The volume-change data for NC8 graphite (Figure 33) and for TSX graphite (Figure 34) show large bulk expansions at fluences of 1×10^{22} nvt for the higher irradiation temperatures. As would be expected from the length change data, TSGBF graphite (Figure 34) shows very rapid changes from contraction to expansion and at 925 to 975 °C shows a remarkable 80% expansion at about 8×10^{21} nvt. Thus, the rapid weakening of the material at the higher temperatures (see Strength Section) is not surprising.

The volume changes for RC5 graphite are relatively small (Figure 35), while those for AXF-8Q1 and EP192C HP graphites shown in Figure 36 are much different from all other graphites.

The general volume-change behavior of all graphites is shown in Figure 37. As would be expected the data are all grouped closely within two temperature bands. The two exceptions to the general trend at the higher temperatures are indicated.

COEFFICIENT OF THERMAL EXPANSION

The behavior of the mean coefficient of thermal expansion (CTE) from 25 °C to 425 °C as a function of neutron fluence is shown in Figures 38 through 45 and BNWL-1056B, Figures E19 through E34. In CSF transverse graphite (Figure 38), the CTE decreases and then begins increasing at about the same exposure where the length is passing turnaround. On the other hand, the CTE for CSF graphite exhibits little change in the parallel direction up to fluences of 2×10^{22} nvt as shown in Figure 39. Hanford data obtained at approximately 1×10^{21} nvt[13] indicate

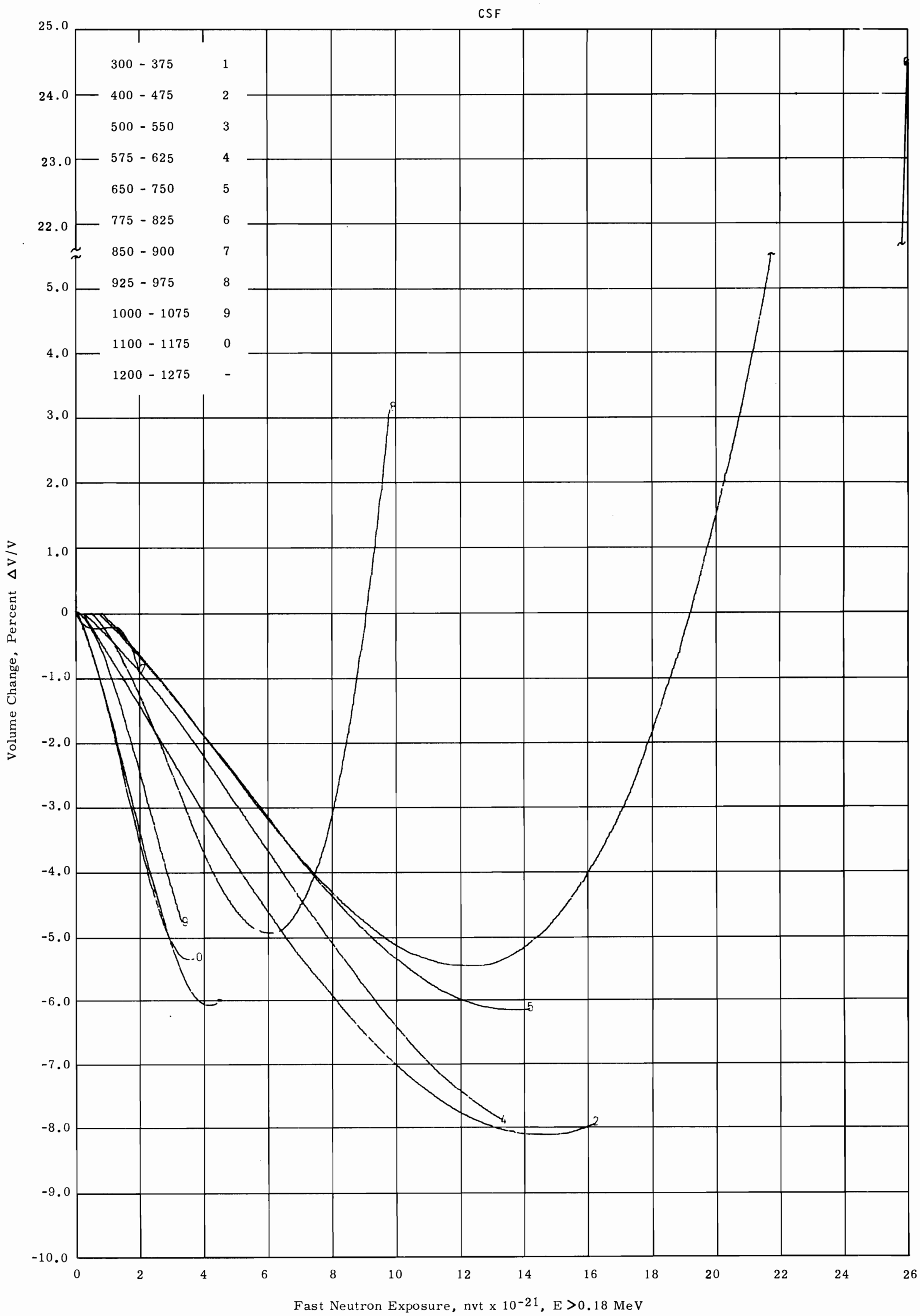

FIGURE 32. Volume Change of CSF Graphite.

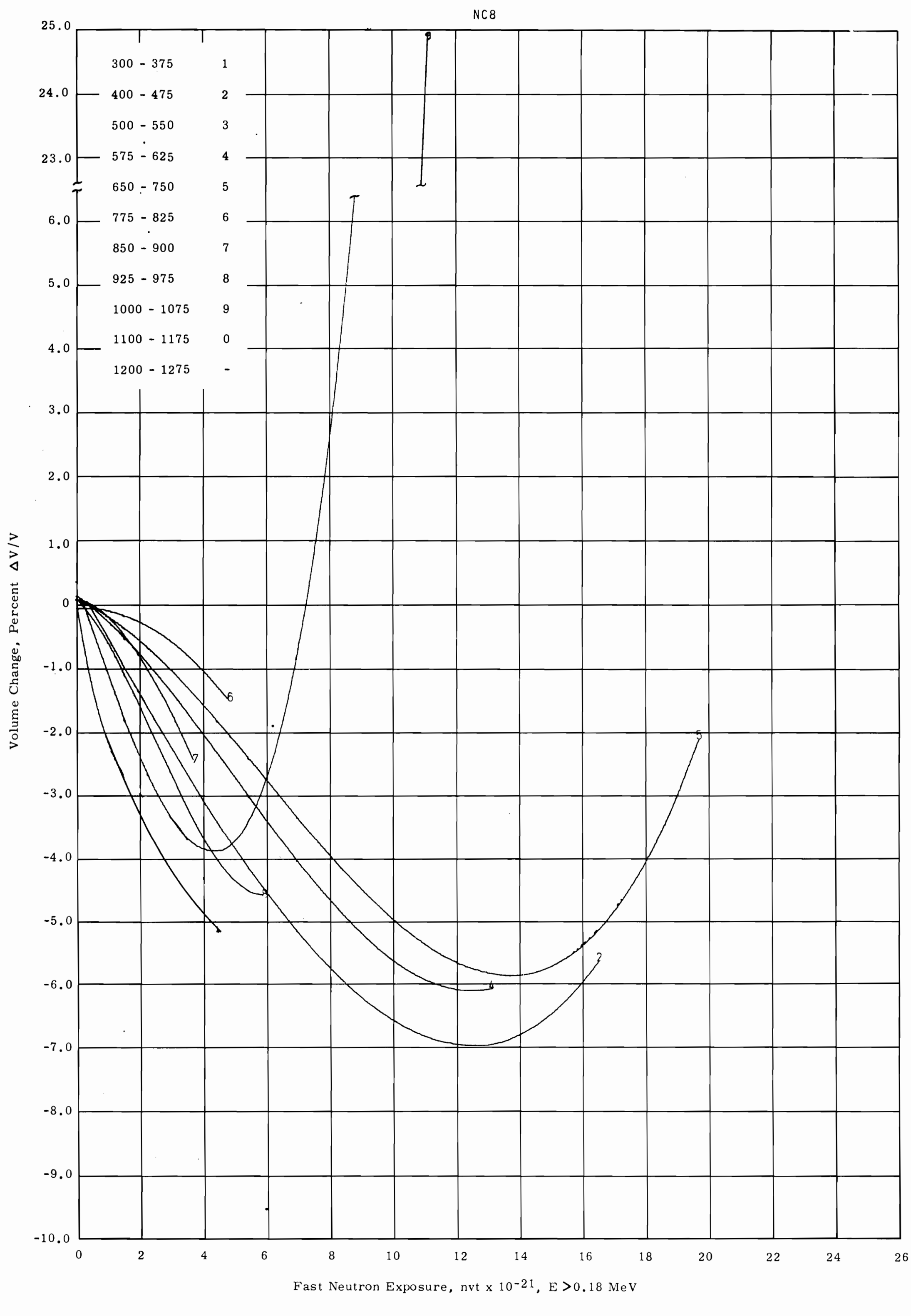

FIGURE 33. Volume Change of NC8 Graphite.

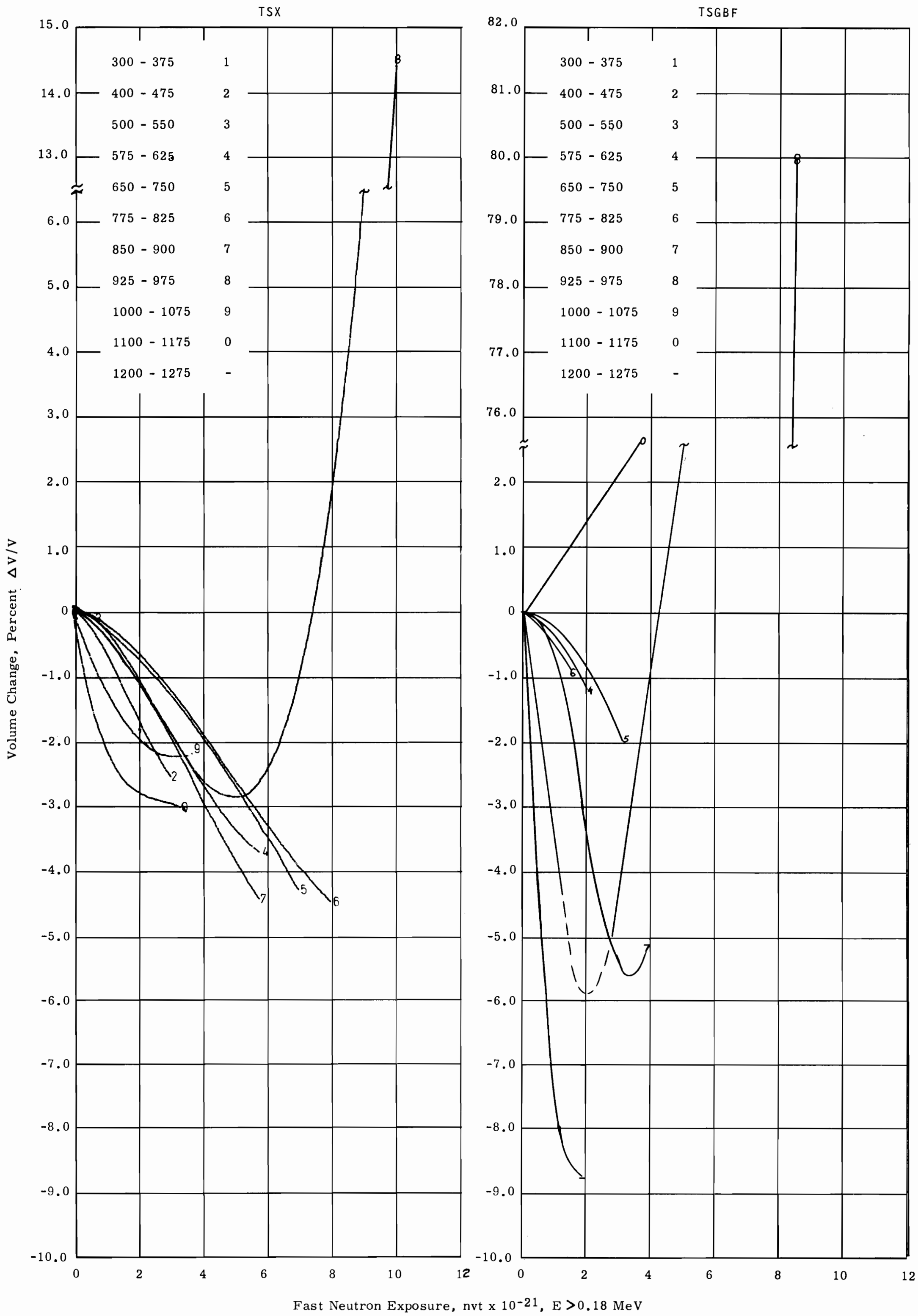

FIGURE 34. Volume Change of TSX and TSGBF Graphites.

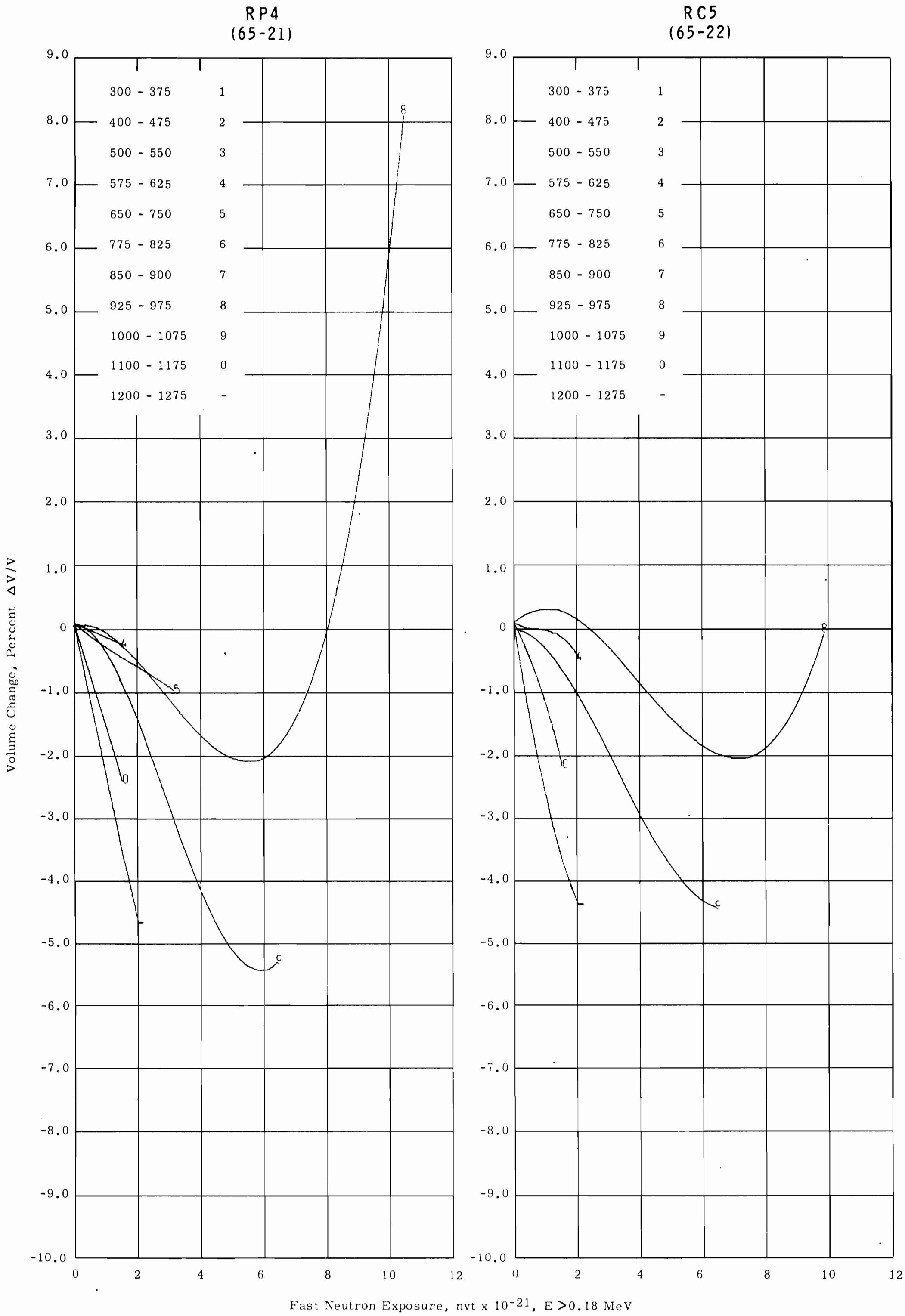

FIGURE 35. Volume Change of Isotropic Graphites.

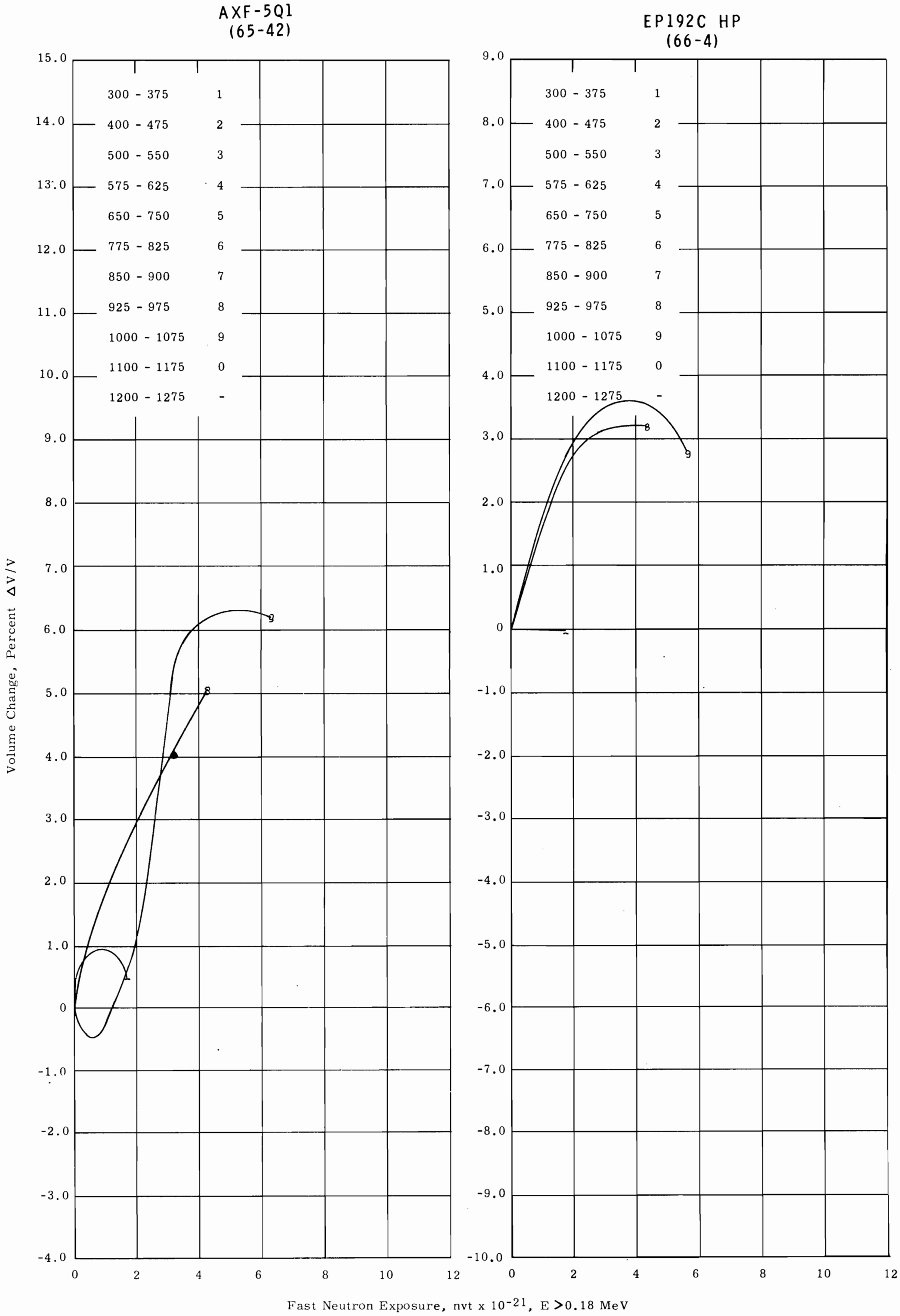

FIGURE 36. Volume Change of Isotropic Graphites.

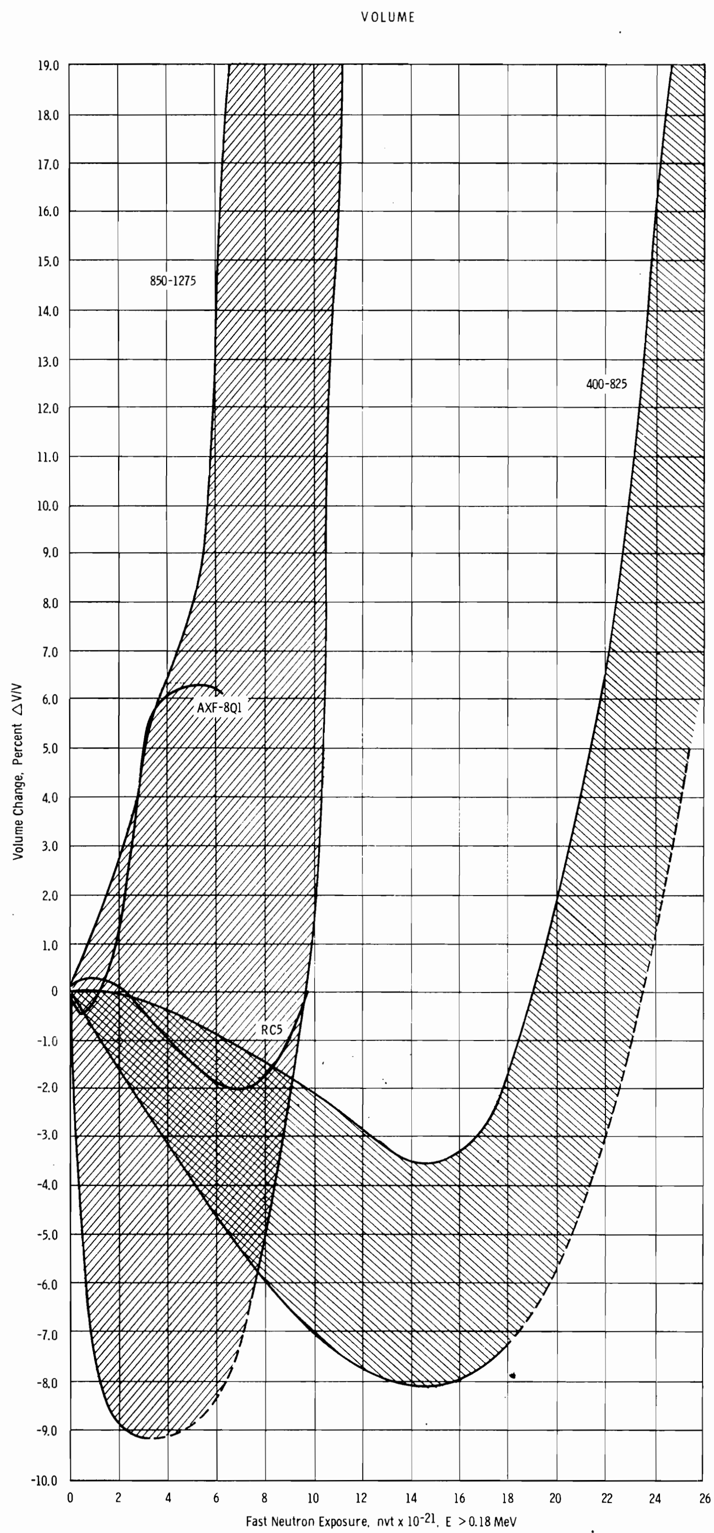

FIGURE 37. *Volume Change of All Graphites.*

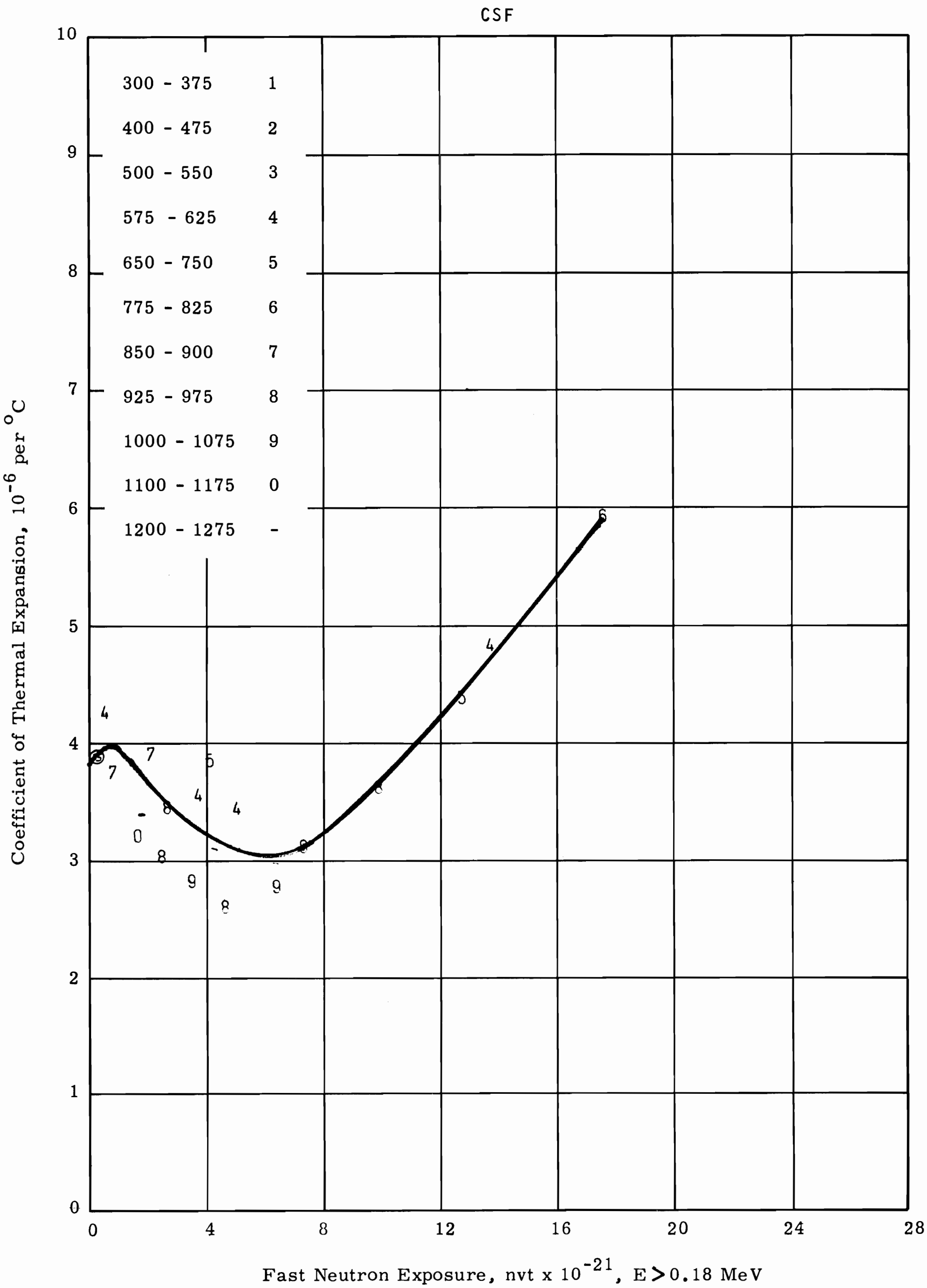

FIGURE 38. *Coefficient of Thermal Expansion of CSF Graphite (Transverse).*

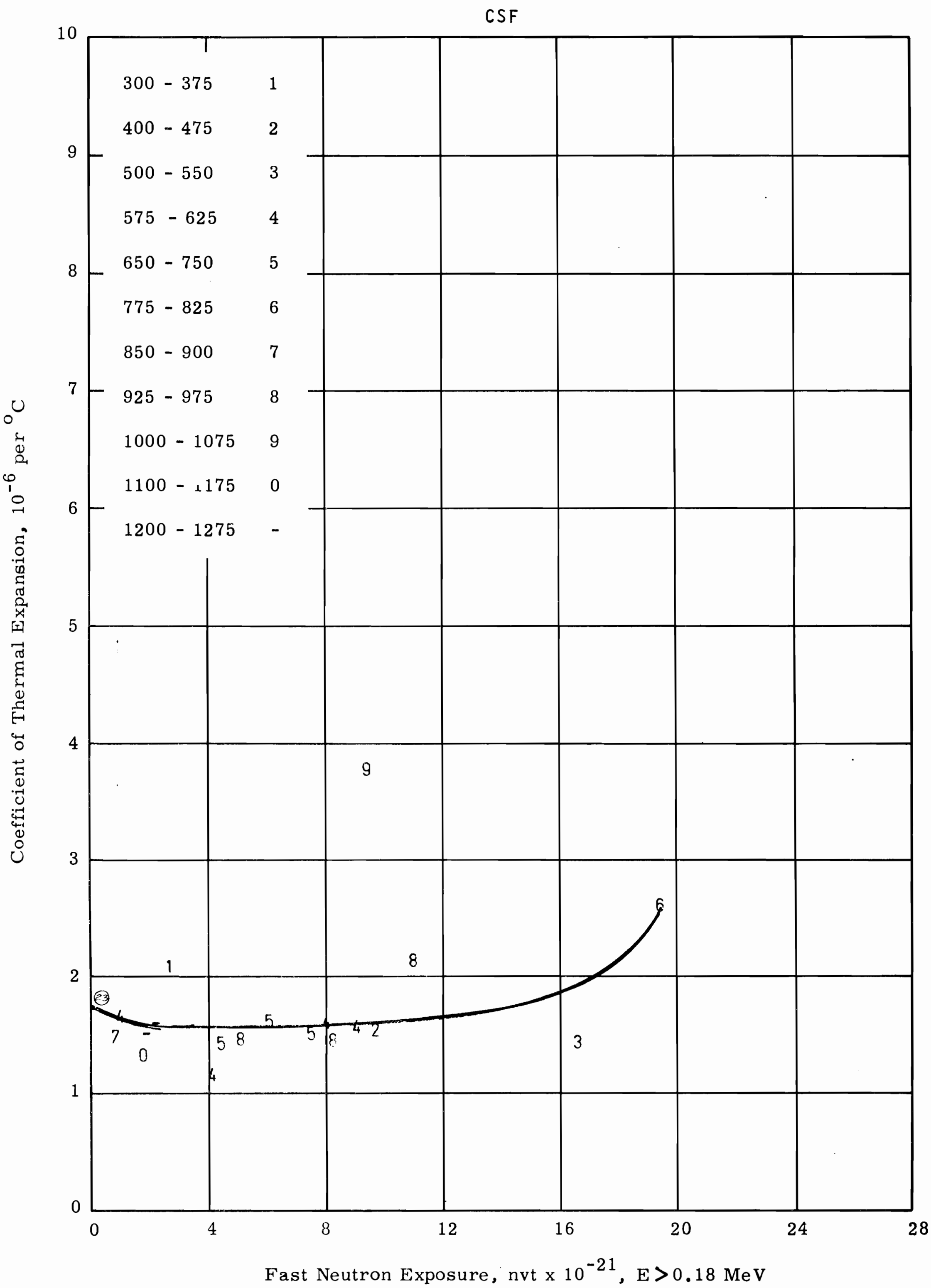

FIGURE 39. Coefficient of Thermal Expansion of CSF Graphite (Parallel).

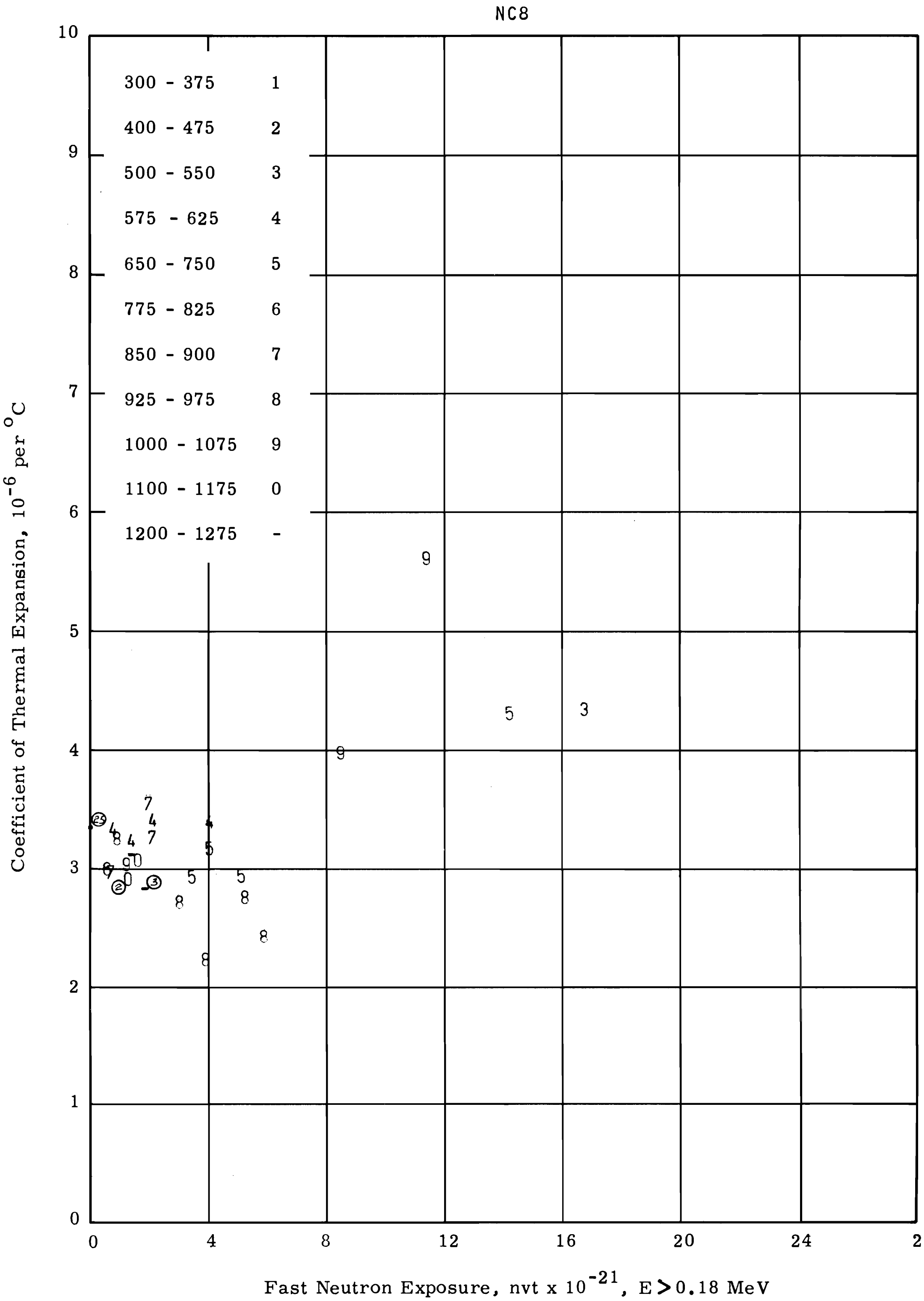

FIGURE 40. Coefficient of Thermal Expansion of NC8 Graphite (Transverse).

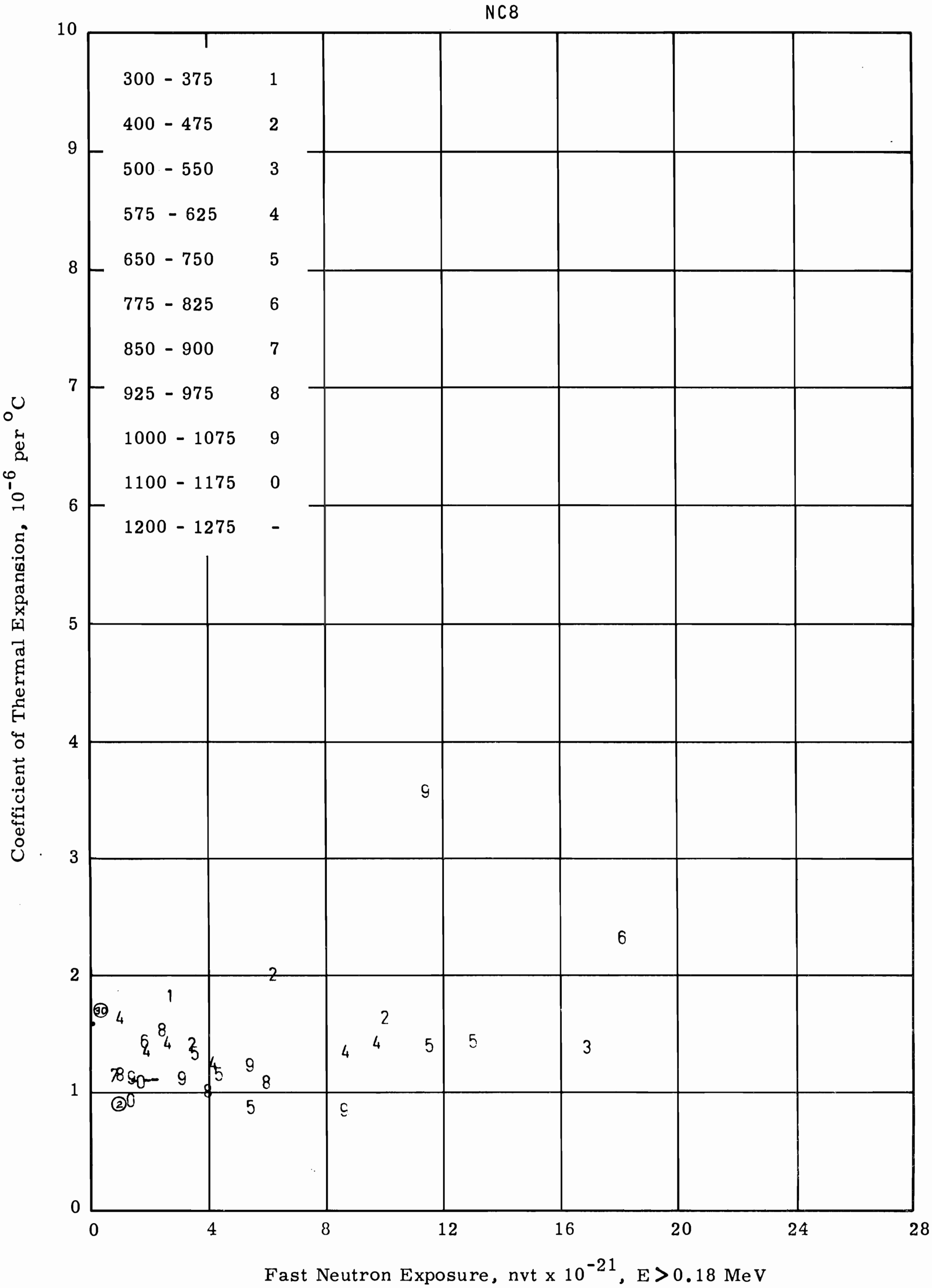

FIGURE 41. *Coefficient of Thermal Expansion of NC8 Graphite (Parallel).*

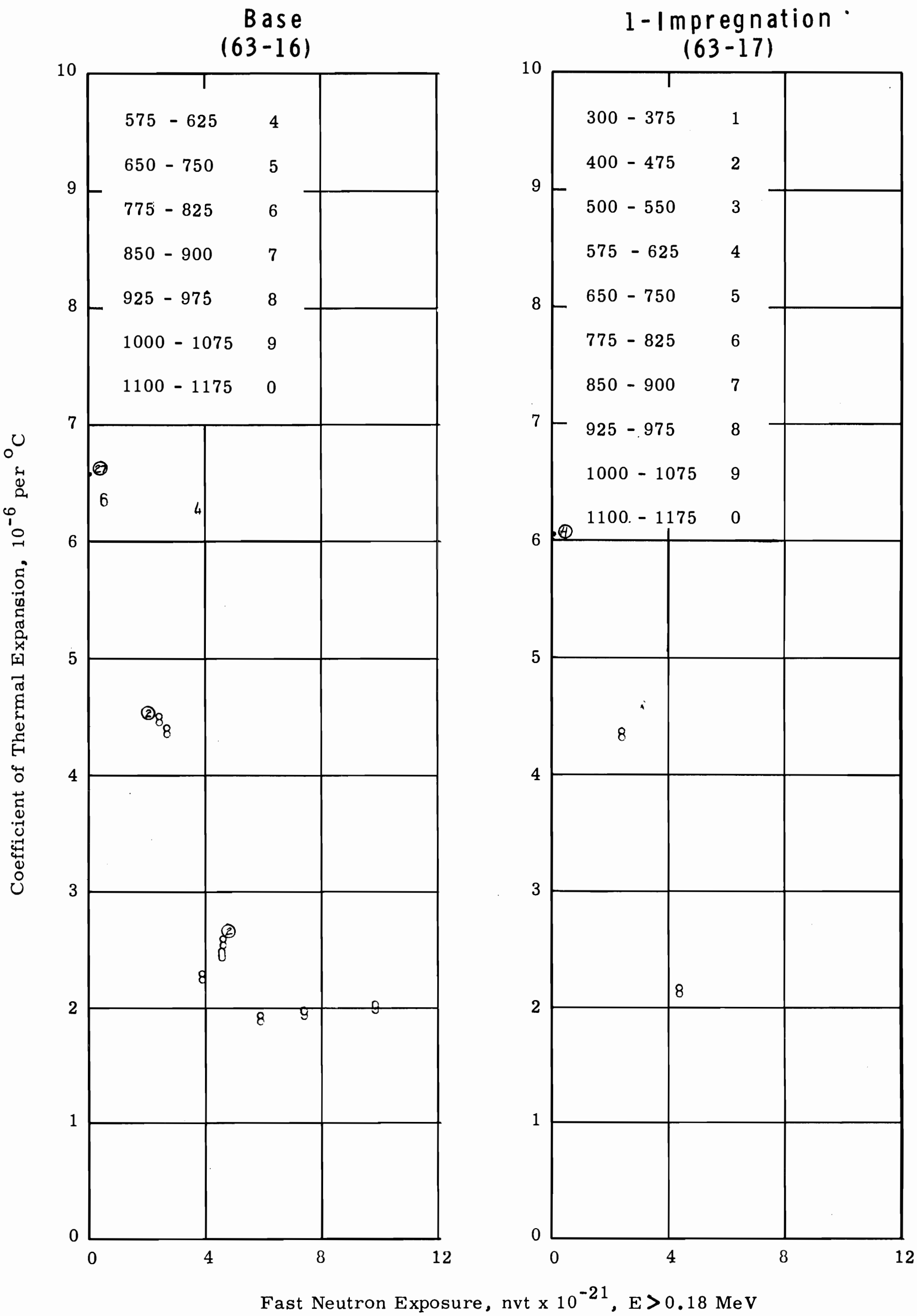

FIGURE 42. Coefficient of Thermal Expansion of Raw Coke Graphites (Transverse).

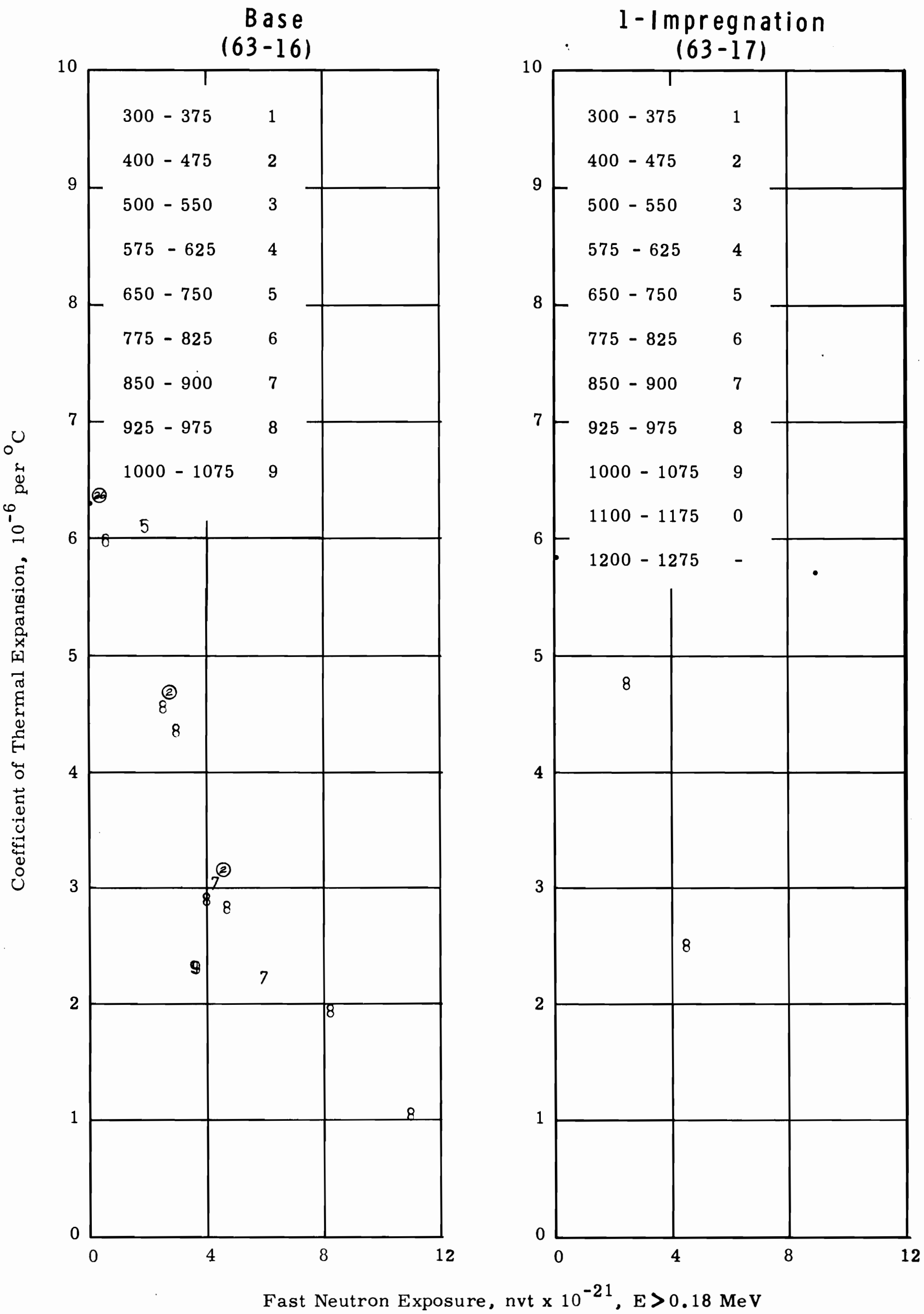

FIGURE 43. Coefficient of Thermal Expansion of Raw Coke Graphites (Parallel).

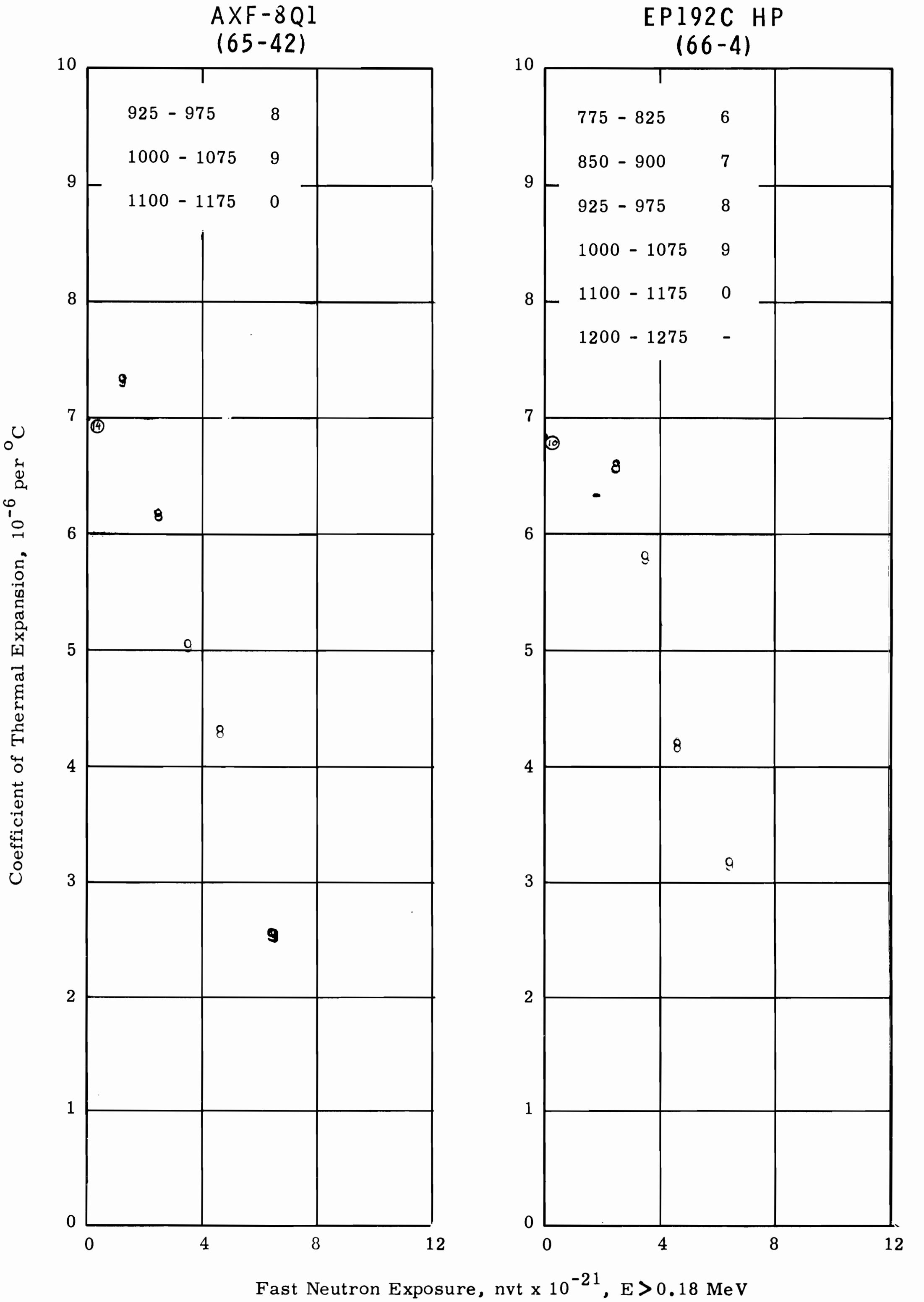

FIGURE 44. Coefficient of Thermal Expansion of Isotropic Graphites (Transverse).

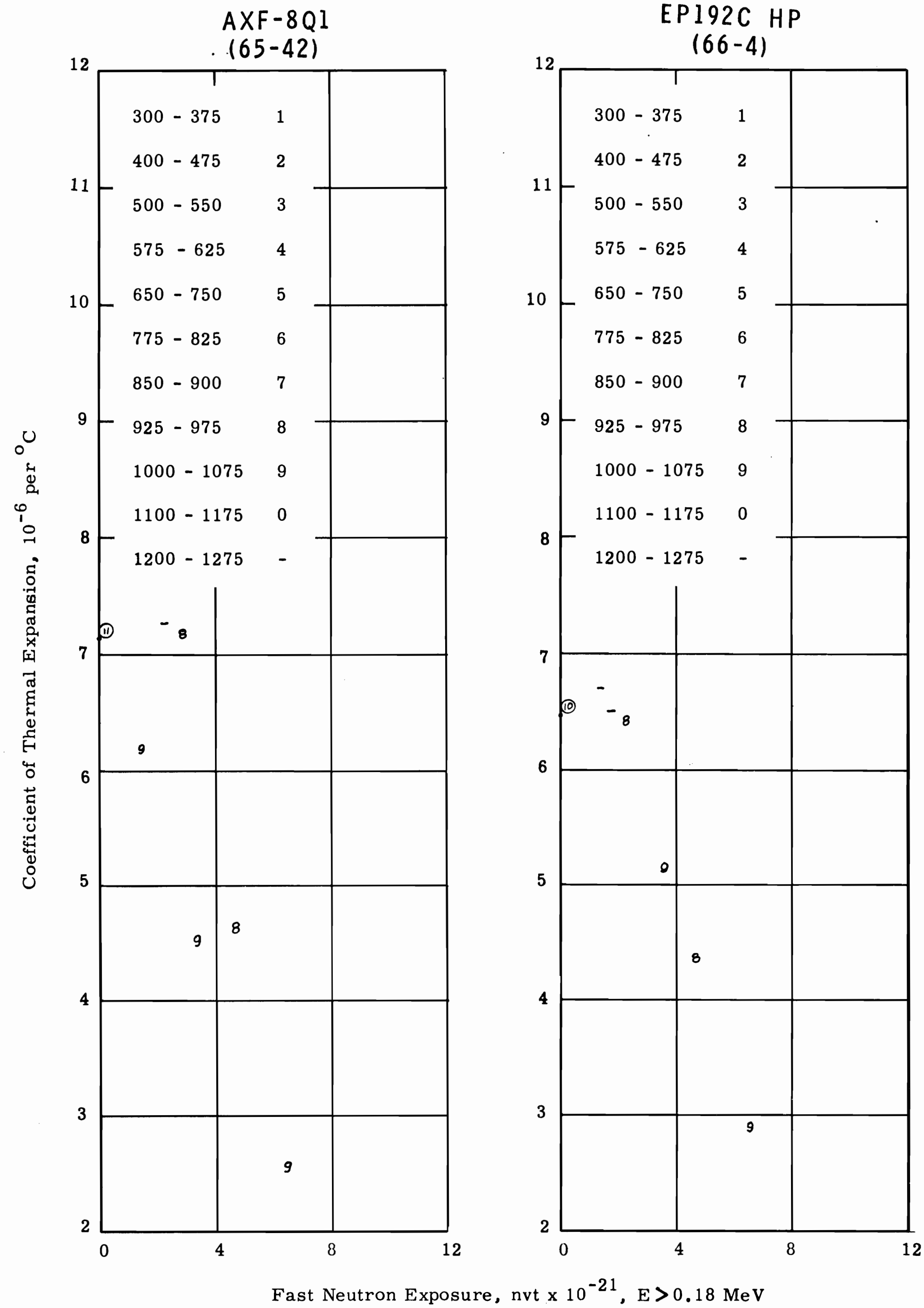

FIGURE 45. *Coefficient of Thermal Expansion of Isotropic Graphites (Parallel).*

an initial increase in CTE, apparently followed by a decrease back to near the unirradiated value.

The CTE data for NC8 graphite as shown in Figures 40 and 41 exhibit the same general behavior as for CSF, with a decrease followed by an increase in the transverse direction and little change in the parallel direction. This same behavior is observed for the other conventional graphites and the data are presented in Appendix E.

The changes in CTE for the raw-coke graphites 63-16 and 63-17 are shown in Figures 42 and 43. Both materials show large decreases in CTE with increasing fluence. This same decrease (Figures 44 and 45) occurs for the isotropic graphites AXF-8Q1 and EP192C HP, which showed the significantly different length-change behavior. This decrease in CTE with increasing fluence is observed for all raw-coke, isotropic, and specialty graphites, and the data are presented in BNWL-1056B, Figures E27 through E34.

There appears to be no logical explanation for the observed increase in CTE after turnaround for the conventional graphites, since the c-axis is expanding and cracks are being generated in the material. However, those changes would explain the decrease in CTE in the raw-coke and isotropic materials.

THERMAL CONDUCTIVITY

Thermal conductivity as a function of temperature was measured on some samples. Although some of the unirradiated data previously were plotted too high[5] by a factor of 10, all have been corrected and are presented in Figures 46 through 50. The unirradiated material shows a decrease in thermal conductivity as the temperature of measurement is increased. Upon irradiation, the thermal conductivity generally decreases to less than 0.12 cal/cm-sec-°C and is nearly constant with increasing measurement temperature.

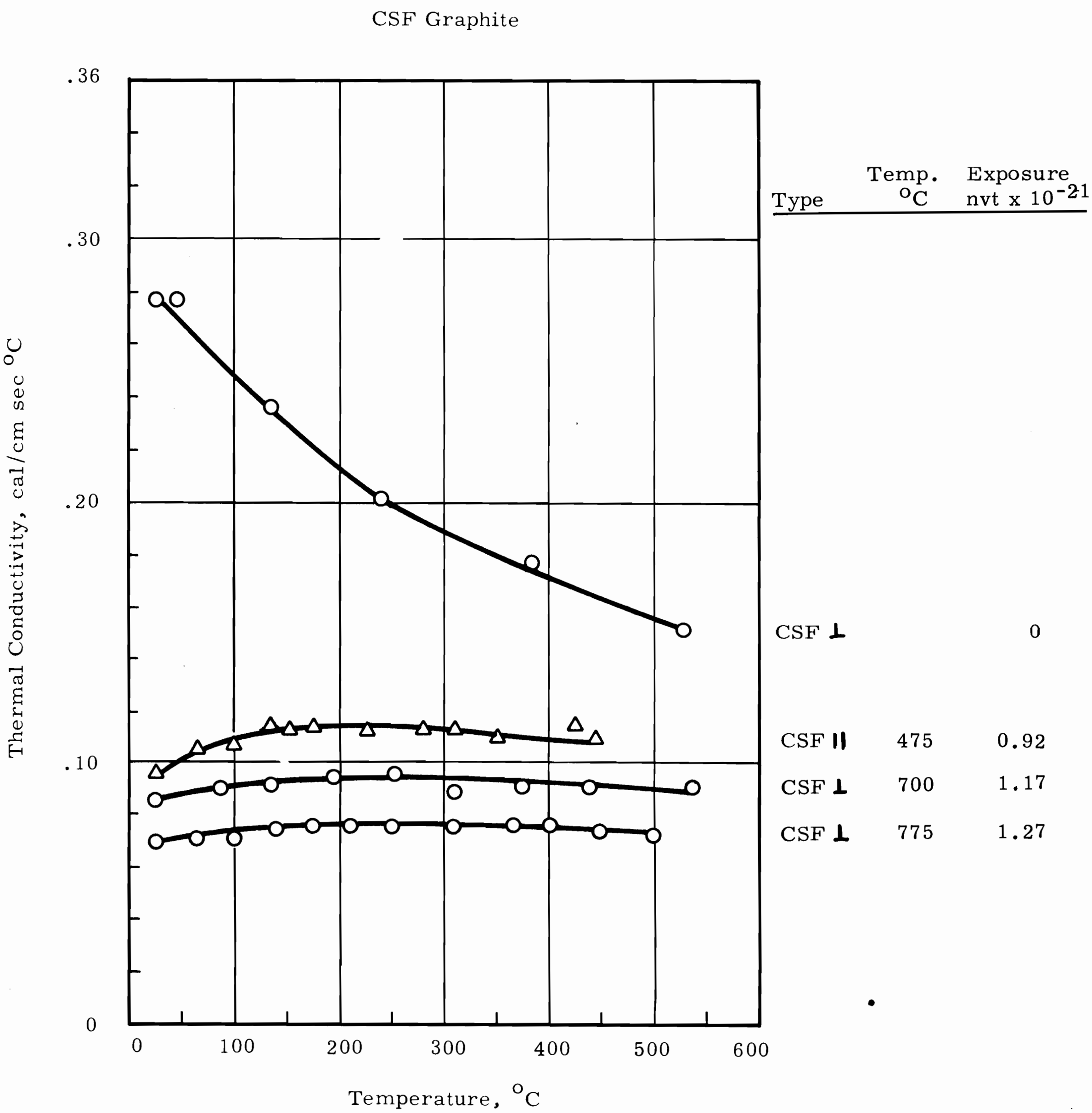

FIGURE 46. Thermal Conductivity of CSF Graphite.

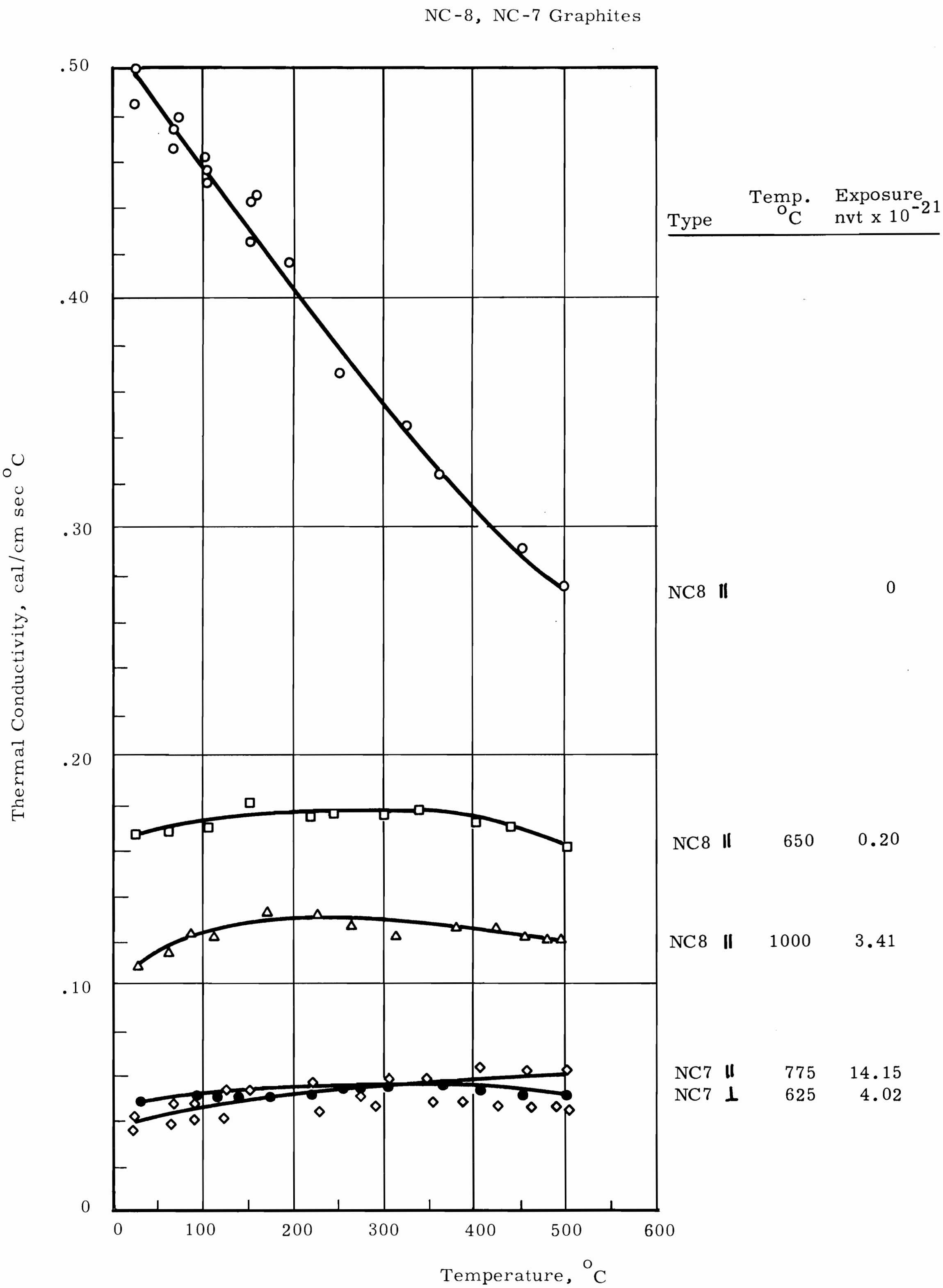

FIGURE 47. Thermal Conductivity of NC8 and NC7 Graphites.

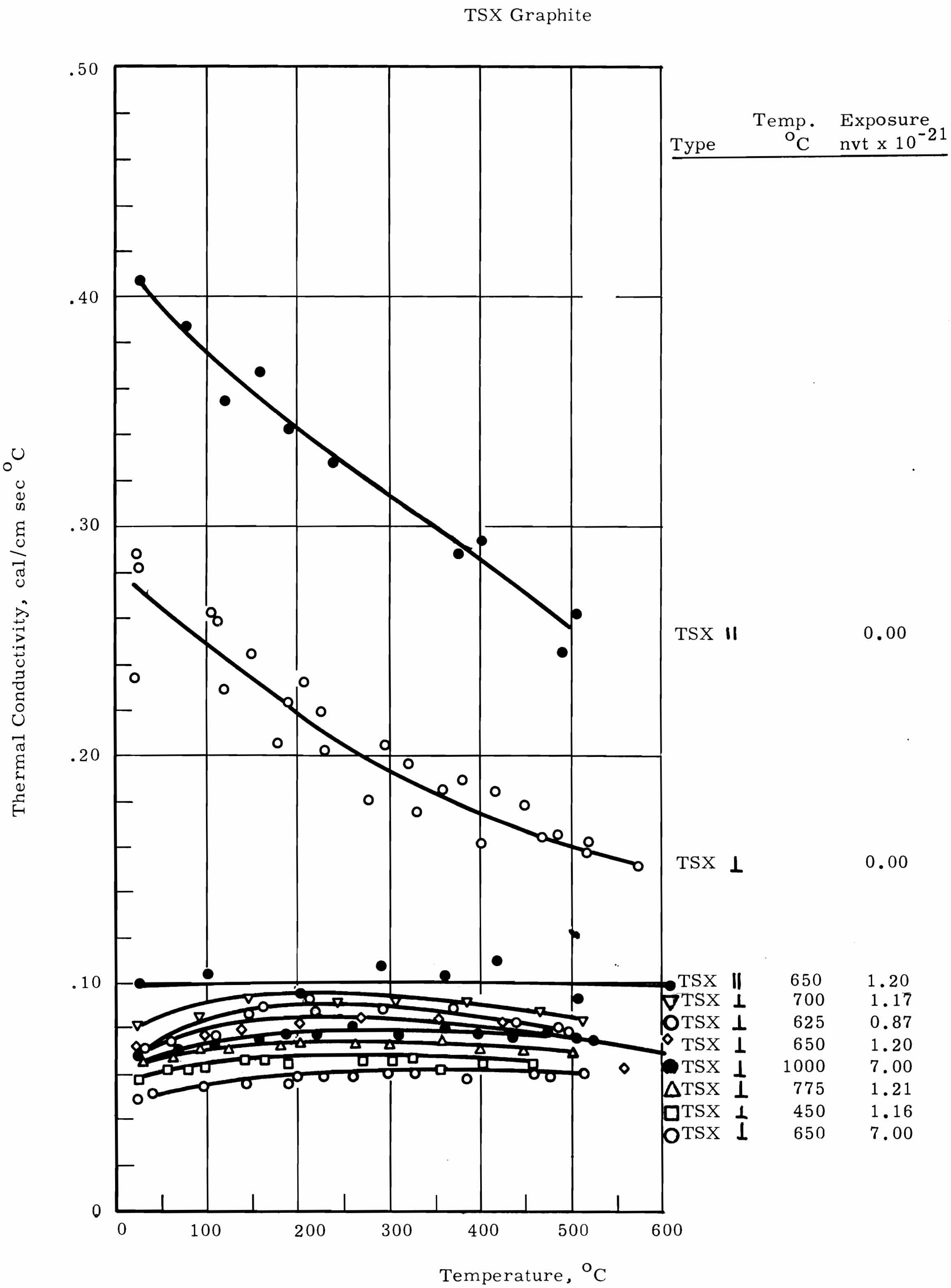

FIGURE 48. Thermal Conductivity of TSX Graphite.

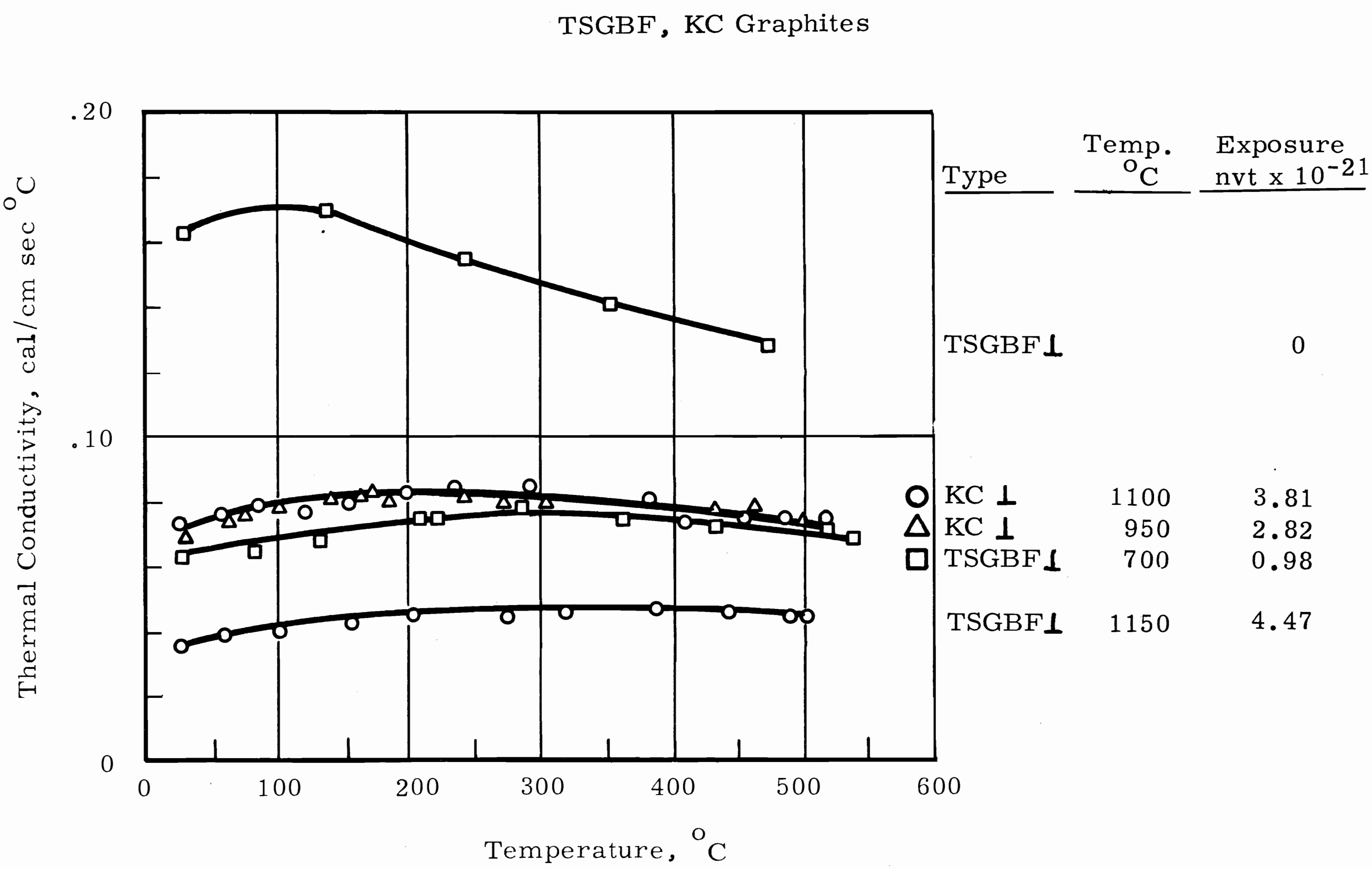

FIGURE 49. *Thermal Conductivity of TSGBF and KC Graphites.*

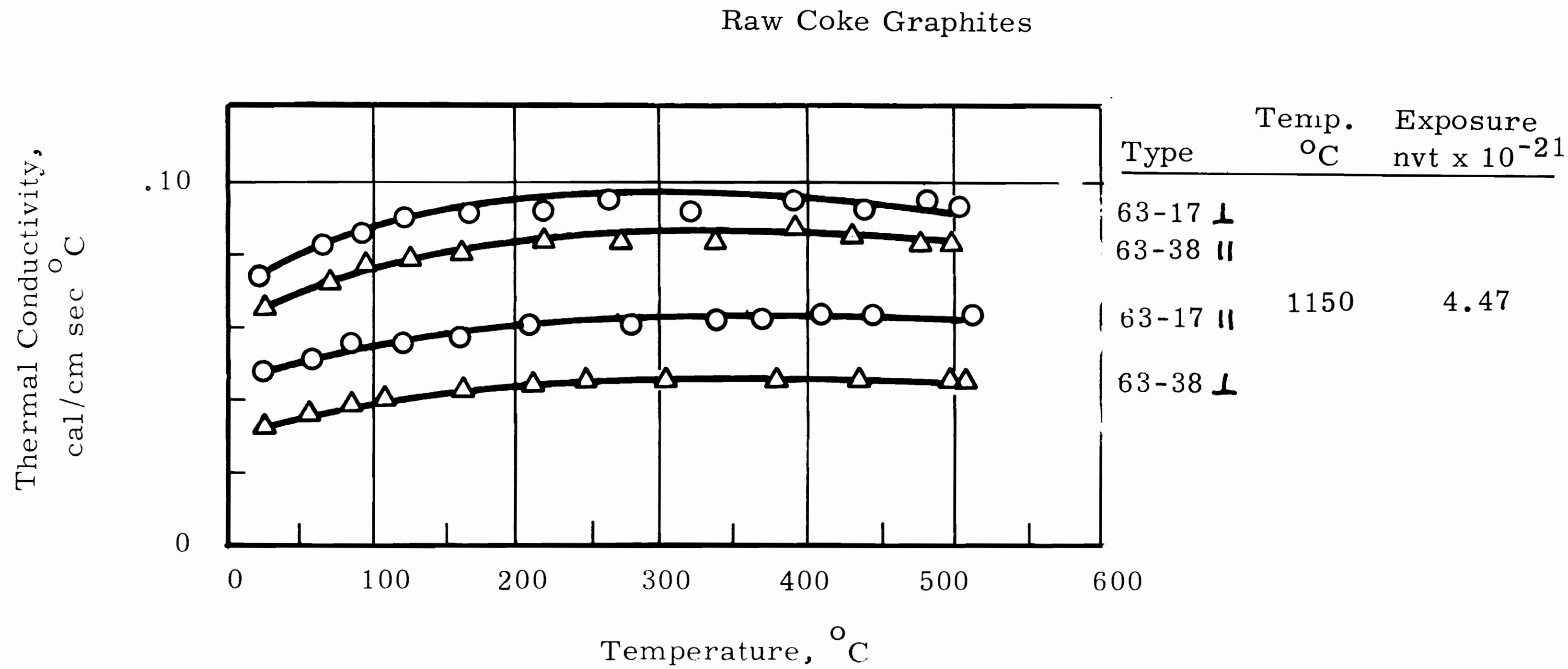

FIGURE 50. Thermal Conductivity of Raw Coke Graphites.

ELECTRICAL RESISTIVITY

Electrical resistivity shows a very rapid increase (between 100 and 200%) at very low neutron fluences. It then generally levels off at about 25 to 40 × 10^{-4} ohm-cm in the transverse direction and at 20 to 25 × 10^{-4} ohm-cm in the parallel direction and in a few cases decreases slightly until dimensional turnaround has been passed. At that point, the resistivity again increases with increasing fluence. With only a few exceptions, resistivity is less dependent on irradiation temperature than the other properties. The data for CSF graphite and for NC8 graphite are presented in Figures 51 through 54. All graphites, except for 63-38 parallel, DS13 parallel, and MSRE, show the same behavior and all the data are presented in BNWL-1056B, Appendix E.

YOUNG'S MODULUS OF ELASTICITY

The data on Young's modulus of elasticity as a function of neutron fluence are shown in Figures 55 and 56 for CSF graphite. Young's modulus increases between 50 and 100% at very low neutron fluences for most graphites. After the initial bulk expansion, the modulus shows only slight changes. The modulus in the parallel direction is about twice that in the transverse. That the modulus is somewhat dependent upon temperature is shown, for CSF irradiated graphite, by the largest increase in moduli at the lowest irradiation temperatures. The similar behavior of NC8 graphite is shown in Figures 57 and 58.

The Young's modulus for the raw-coke, isotropic, and specialty graphites is typified by the behavior of 63-16 and 65-18 graphites as shown in Figures 59 and 60. The changes up to about 4 × 10^{22} nvt are plus/minus 50% of the unirradiated value, and then as fluence increases the modulus tends to increase. Data for the other materials are presented in BNWL-1056B, Appendix E.

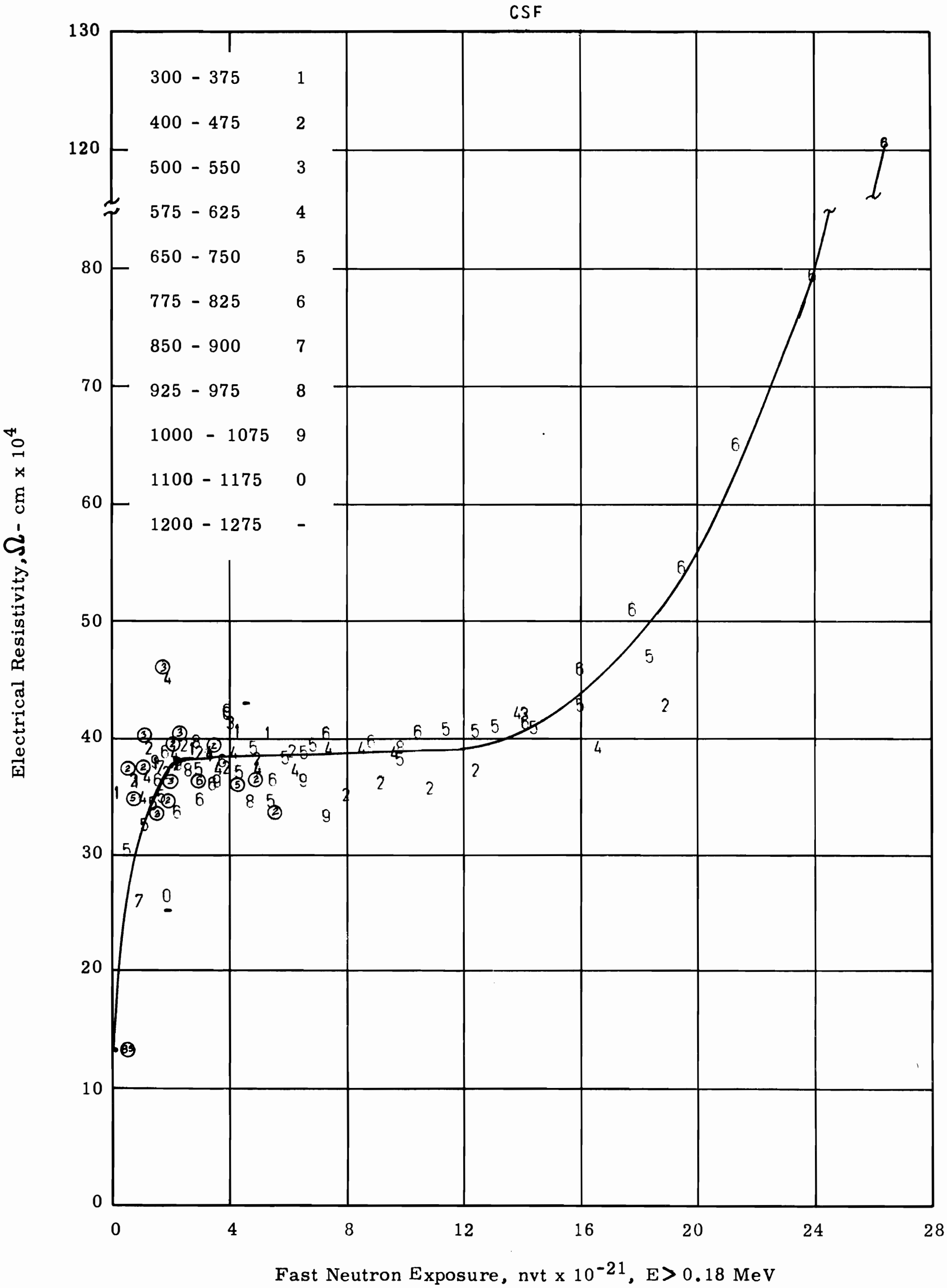

FIGURE 51. Electrical Resistivity of CSF Graphite (Transverse).

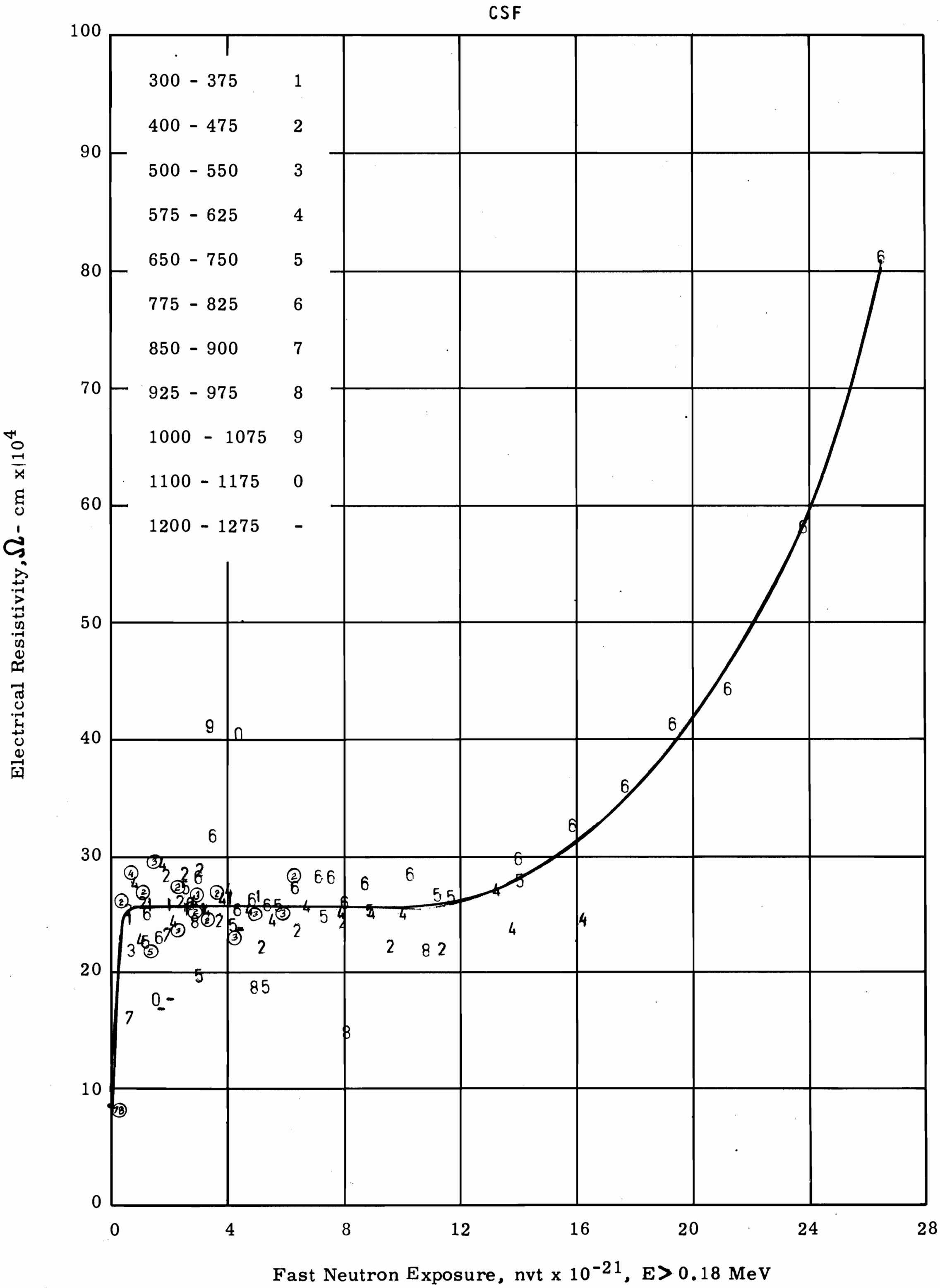

FIGURE 52. Electrical Resistivity of CSF Graphite (Parallel).

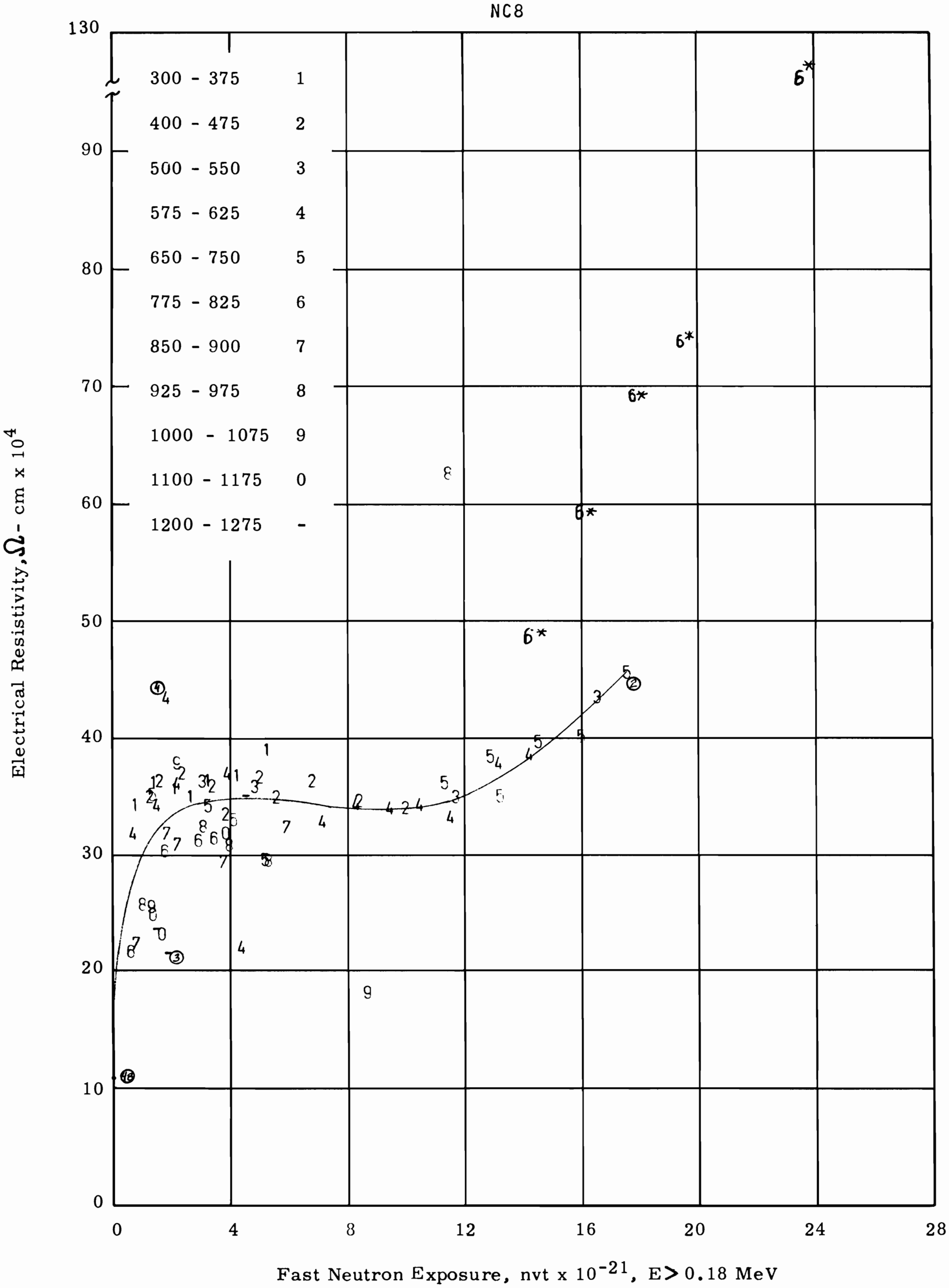

FIGURE 53. Electrical Resistivity of NC8 Graphite (Transverse).

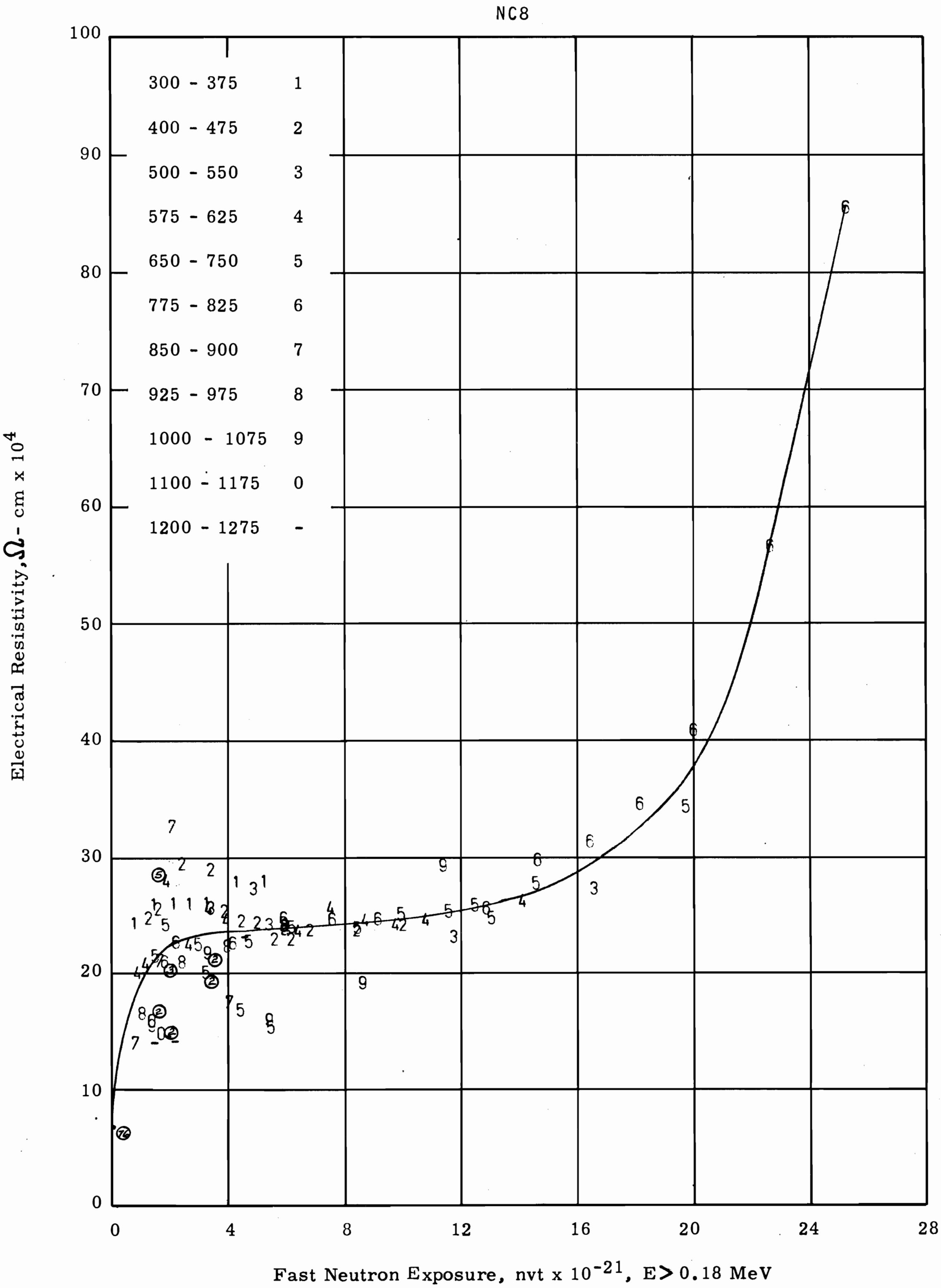

FIGURE 54. Electrical Resistivity of NC8 Graphite (Parallel).

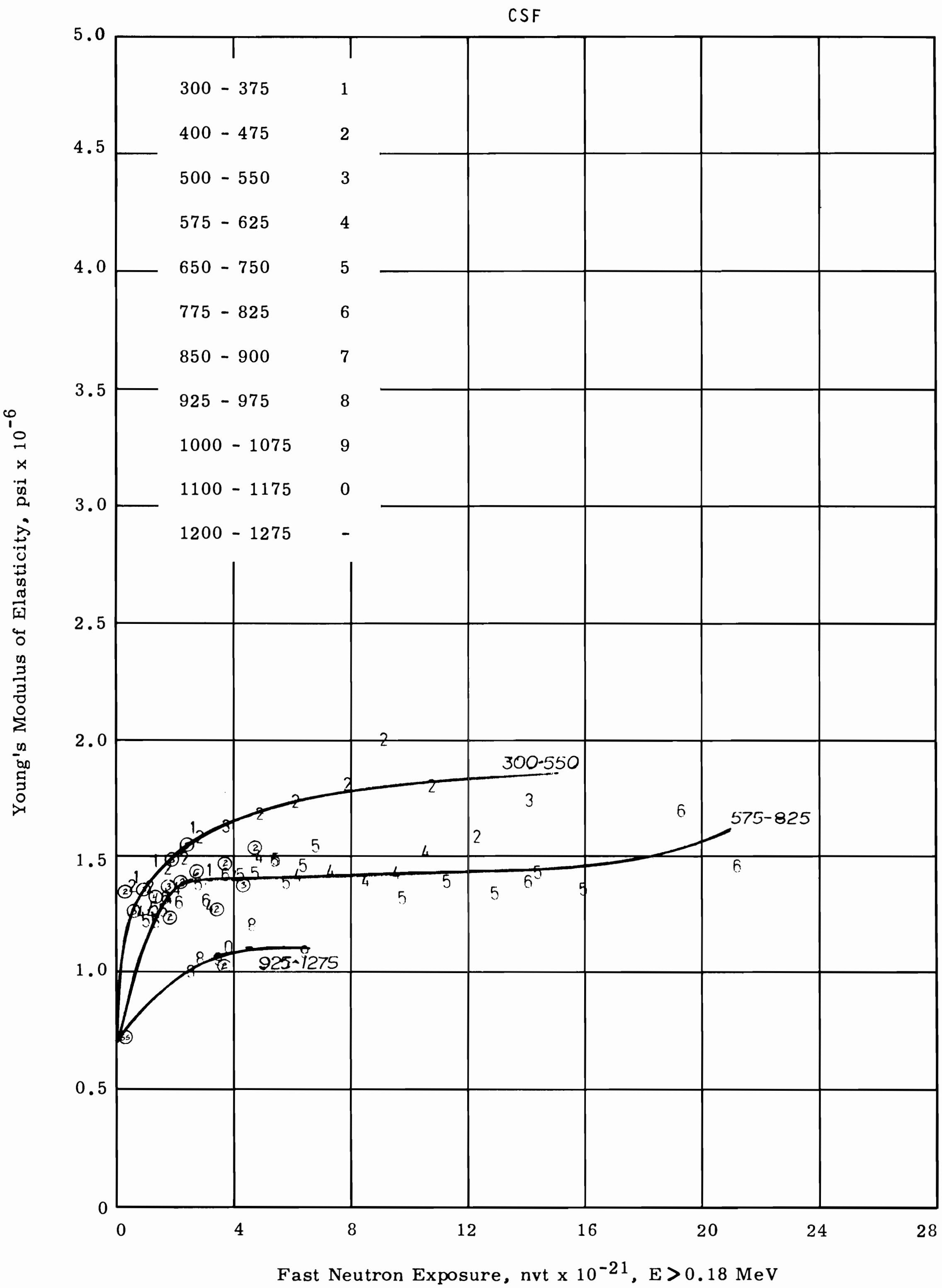

FIGURE 55. Young's Modulus of Elasticity of CSF Graphite (Transverse).

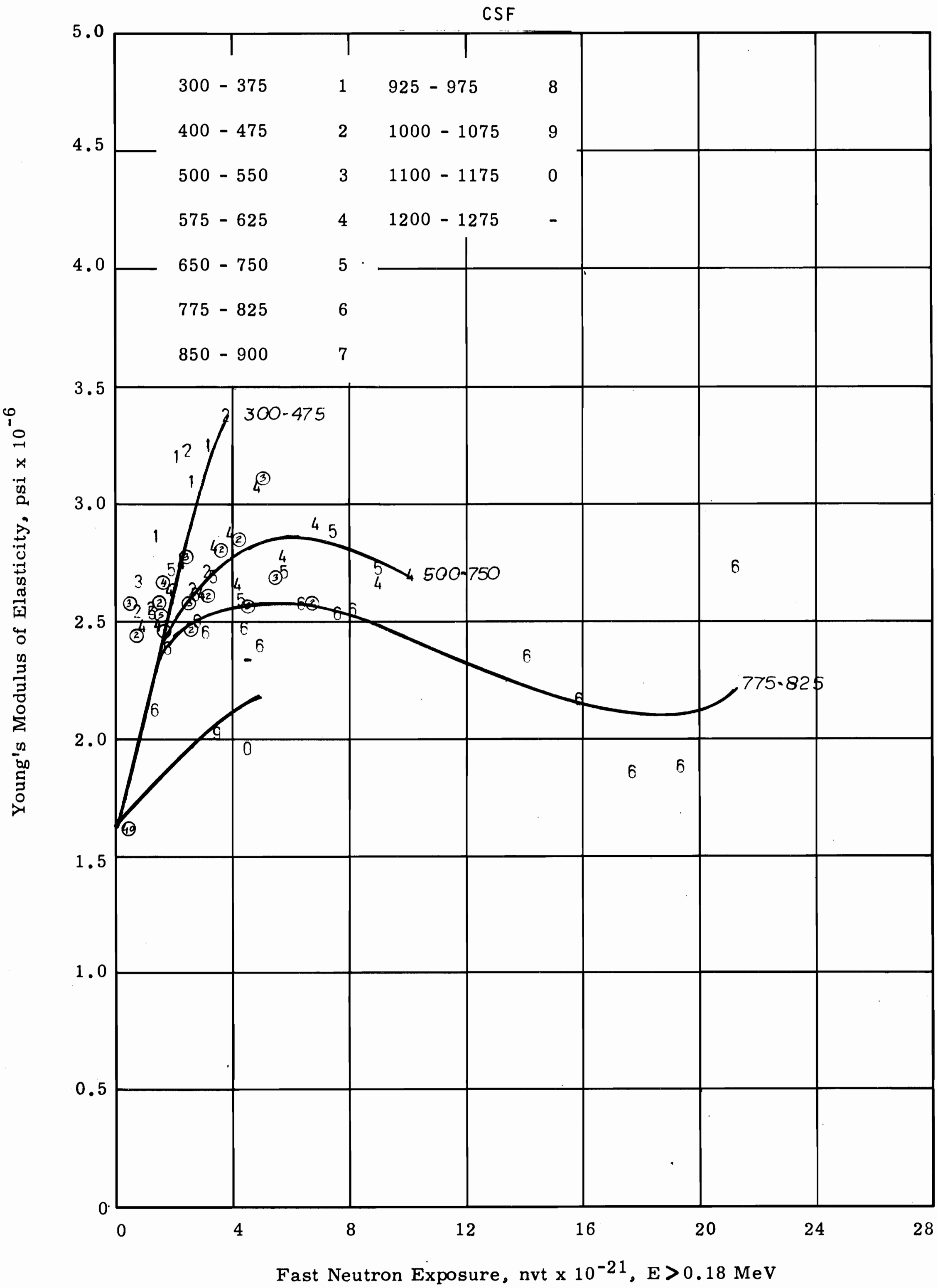

FIGURE 56. *Young's Modulus of Elasticity of CSF Graphite (Parallel).*

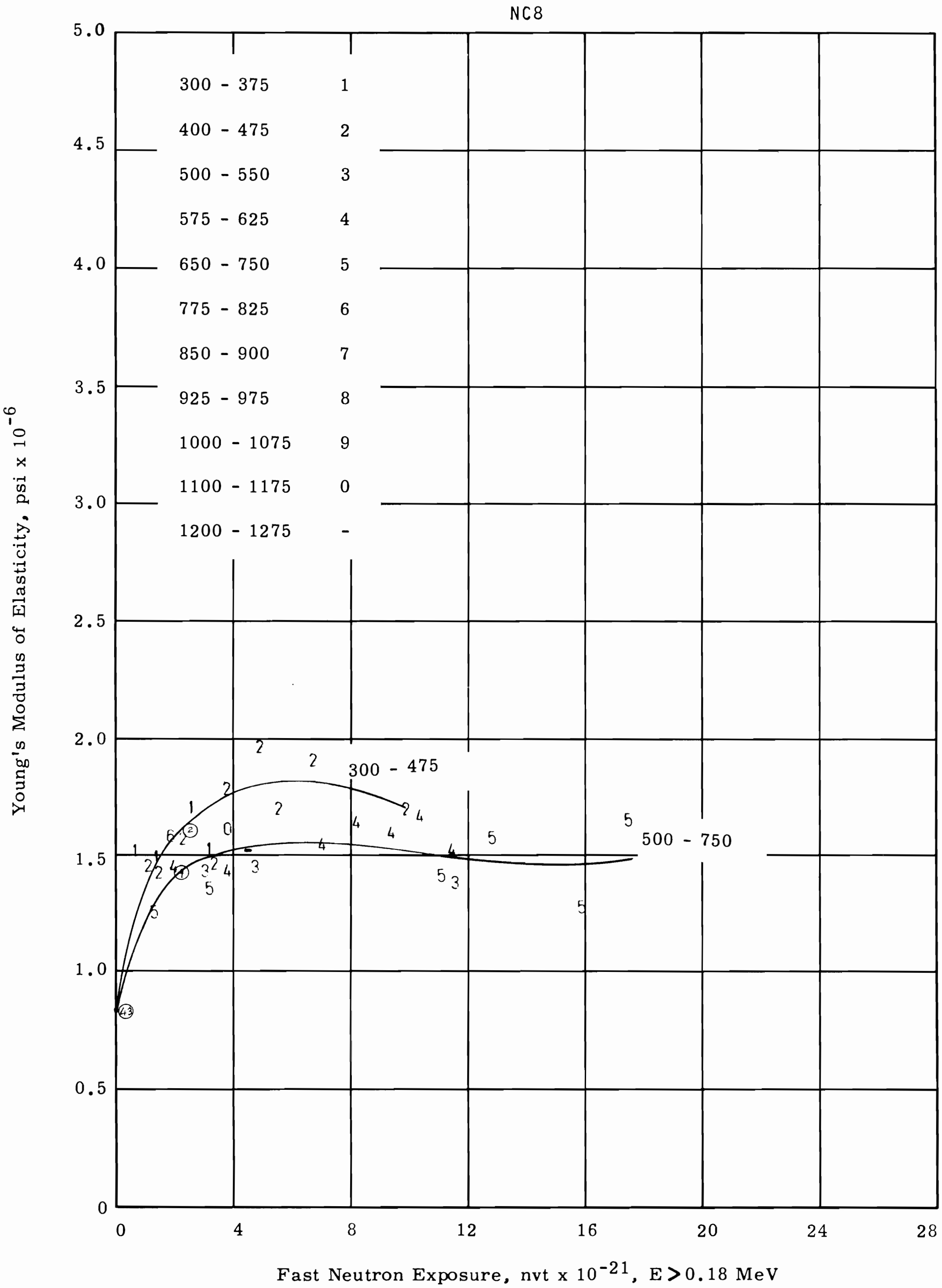

FIGURE 57. *Young's Modulus of Elasticity of NC8 Graphite (Transverse).*

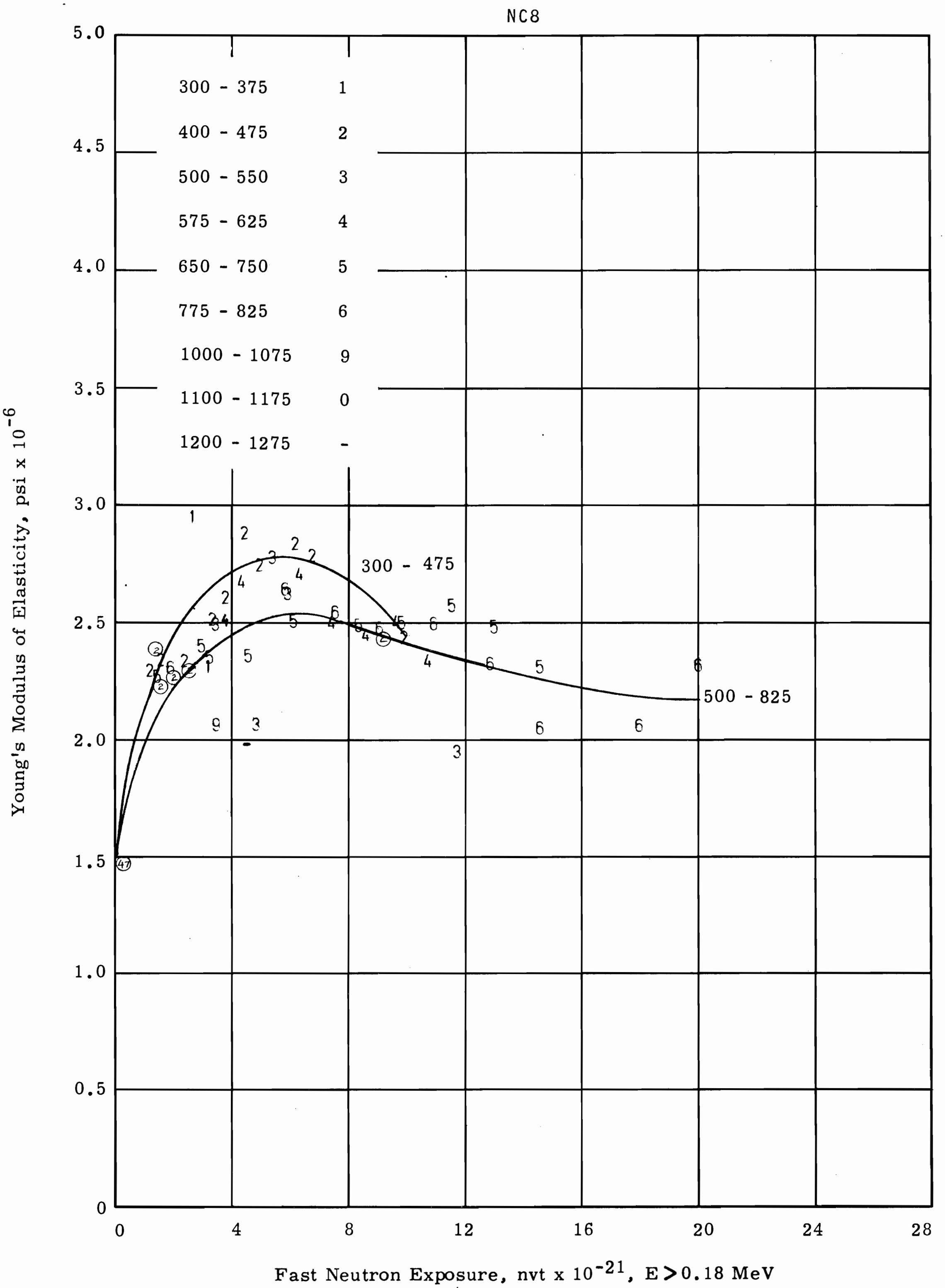

FIGURE 58. Young's Modulus of Elasticity of NC8 Graphite (Parallel).

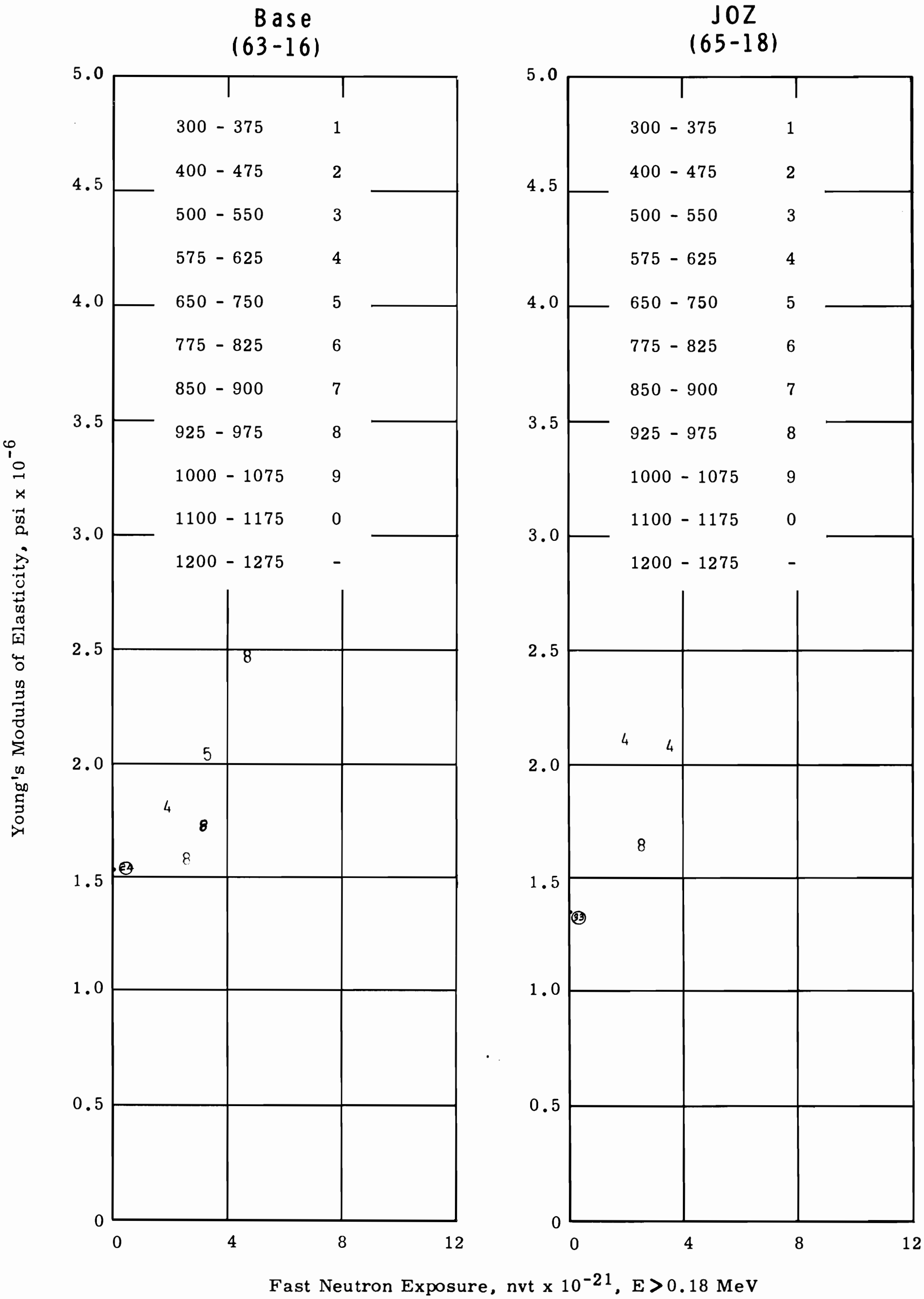

FIGURE 59. Young's Modulus of Elasticity of Raw Coke Graphites (Transverse).

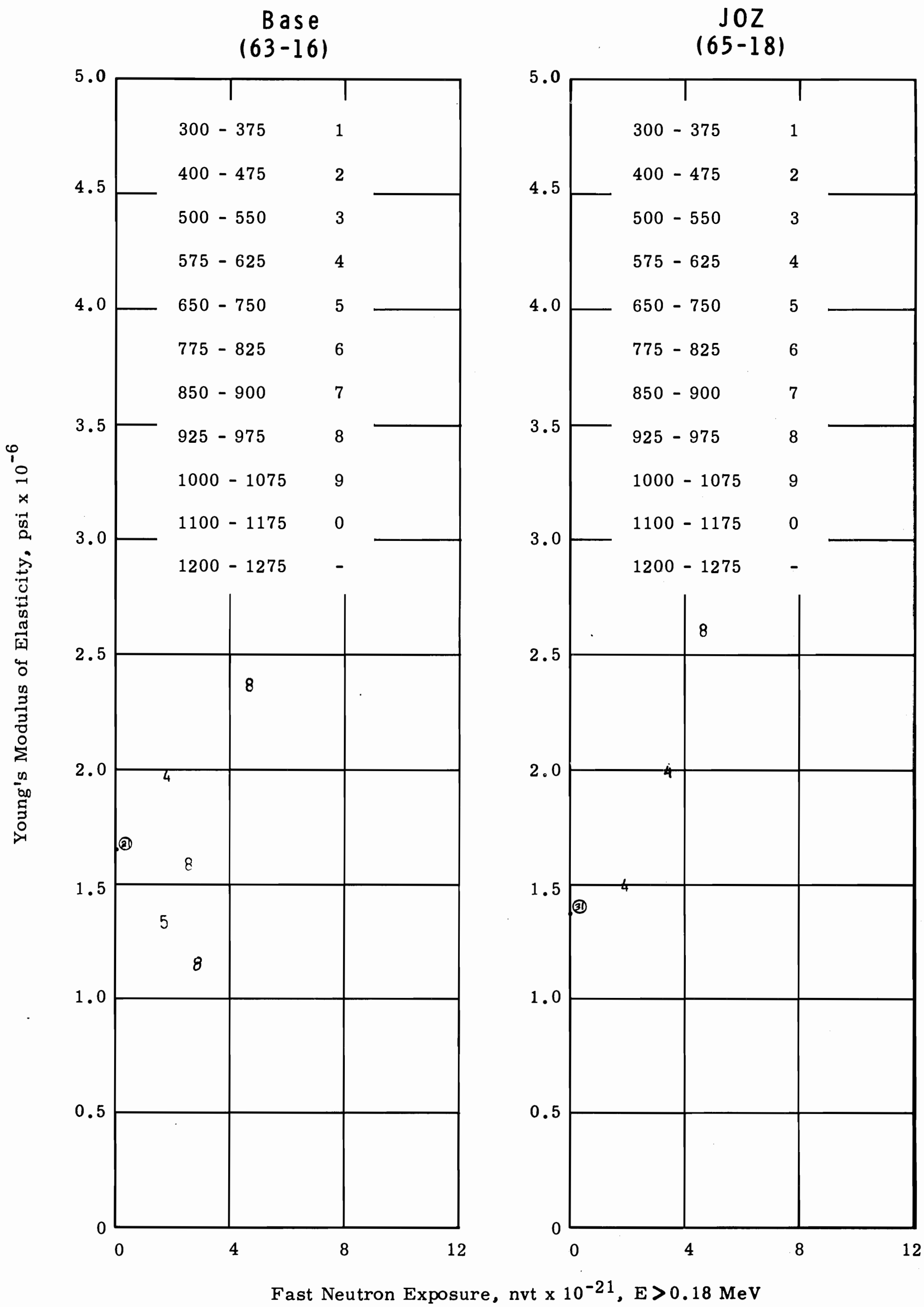

FIGURE 60. *Young's Modulus of Elasticity of Raw Coke Graphites (Parallel)*

CRYSTALLITE PARAMETERS

The effect of increasing neutron irradiation on the crystallite parameter, c (the distance between alternate layer planes), is shown in Figure 61 for CSF graphite. Although there is a wide scatter in the data, a general increase in c is suggested. The lower irradiation temperatures cause the largest increases.

Data for the apparent crystallite size in the c direction, L_c, are all about the same for the various reactor-grade graphites. All show regular decreases of about 75%, with the irradiations at lower temperatures generally showing a more rapid decrease to a value nearly constant for all irradiation temperatures. The data for CSF are shown in Figure 62.

The effects of increasing neutron fluence on a (the unit cell dimension in the layer plane) and L_a (the apparent crystallite size in the a direction) are less conclusive, with a general decrease suggested. The data for CSF graphite are presented in Figures 63 and 64.

The crystallite parameter data for the other graphites are all very similar to those for CSF graphite and are presented in BNWL-1056B, Appendix E.

STRENGTH

The only strength measurements obtained were reported previously[5] and are repeated in Table 2 for completeness.

TABLE 2. Strength of TSGBF Graphite.

	Strength, psi		
	Unirradiated	Irradiated[a]	Change, %
Tensile	1560	180	-88
Compressive	8540	3410	-60

a. *Irradiated at 1150 °C to 4.47 × 10^{21} nvt.*

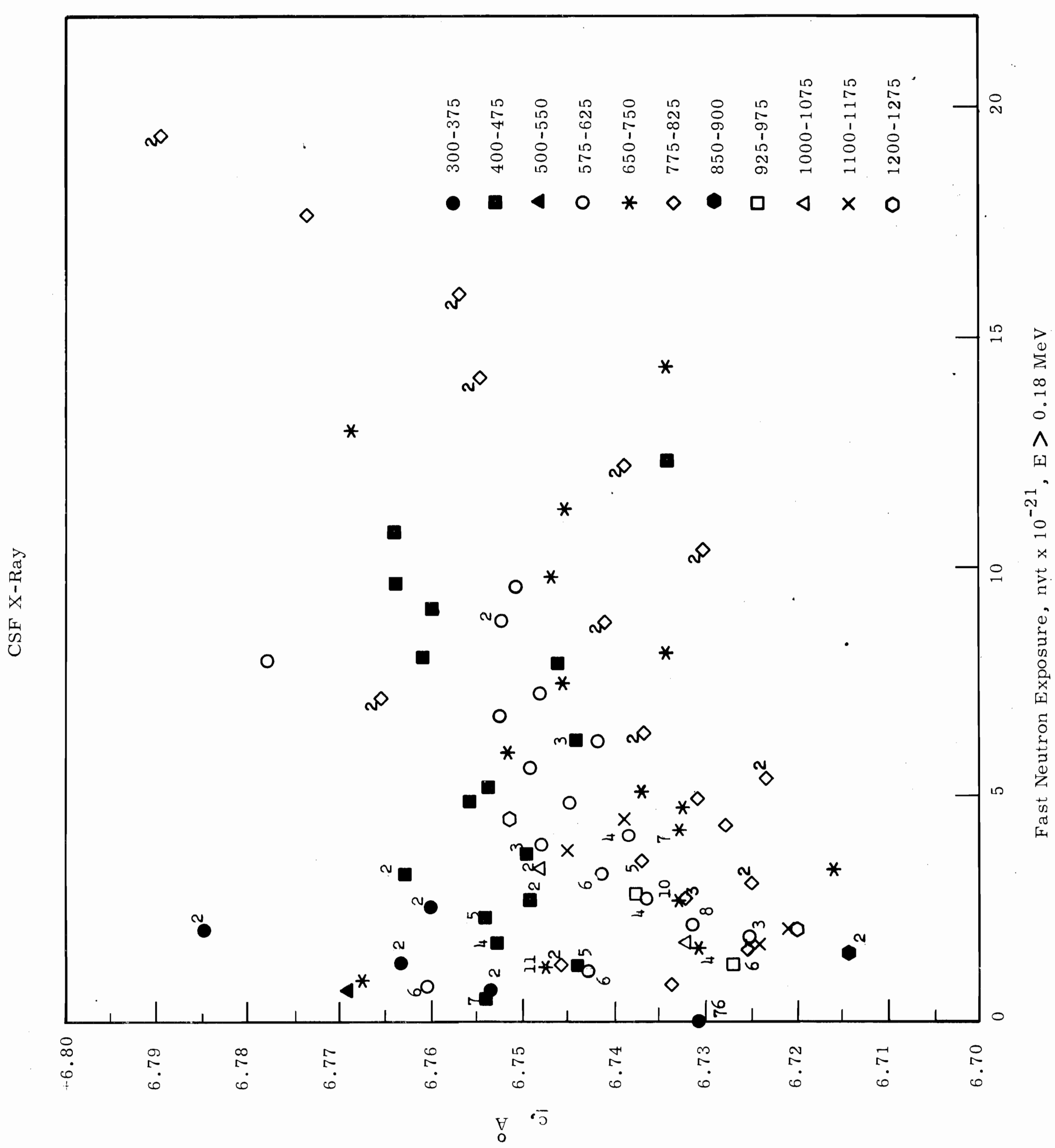

FIGURE 61. *Crystallite Layer Spacing (c) of CSF Graphite.*

CSF

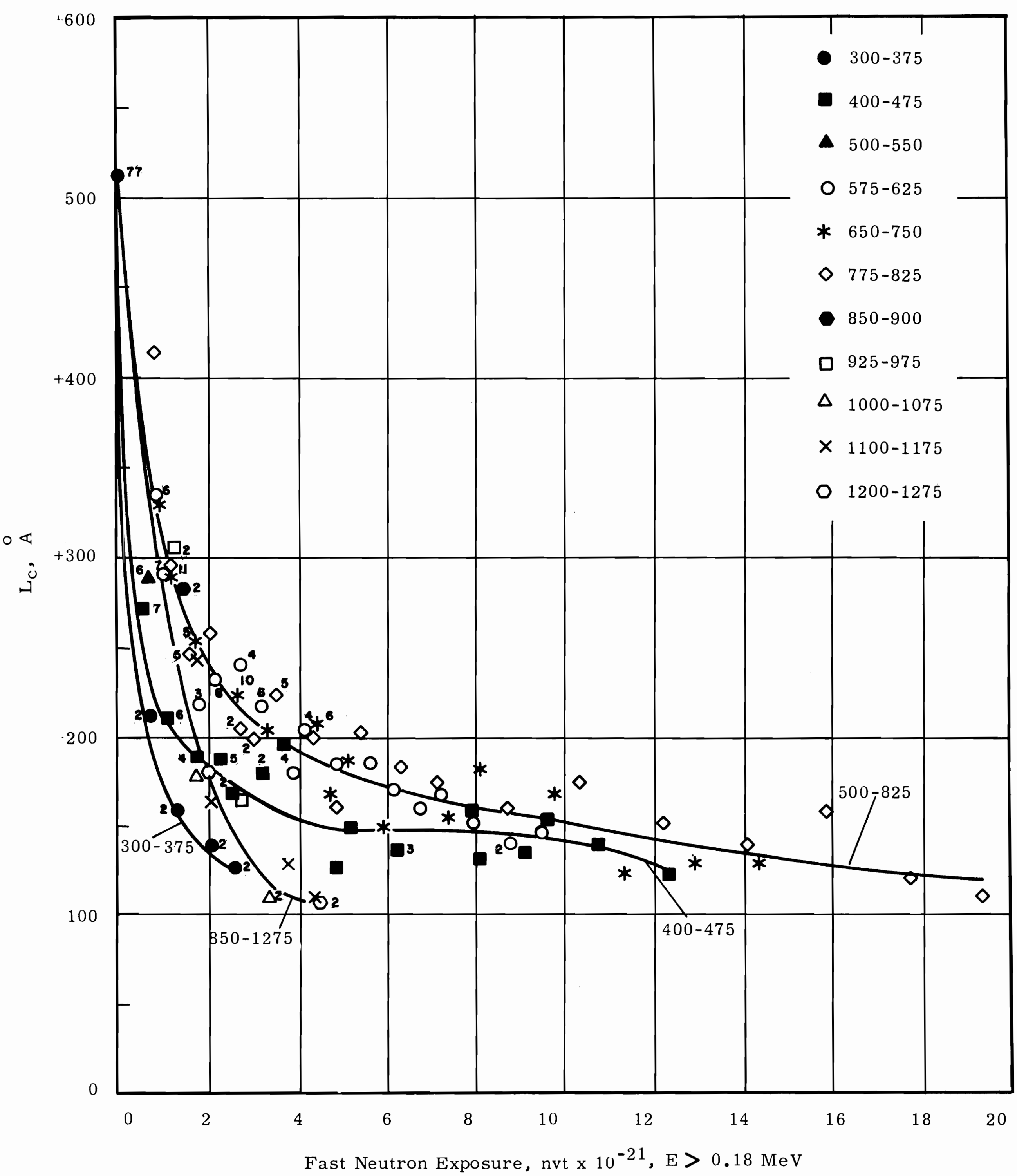

FIGURE 62. Apparent Crystallite Size (L_c) of CSF Graphite.

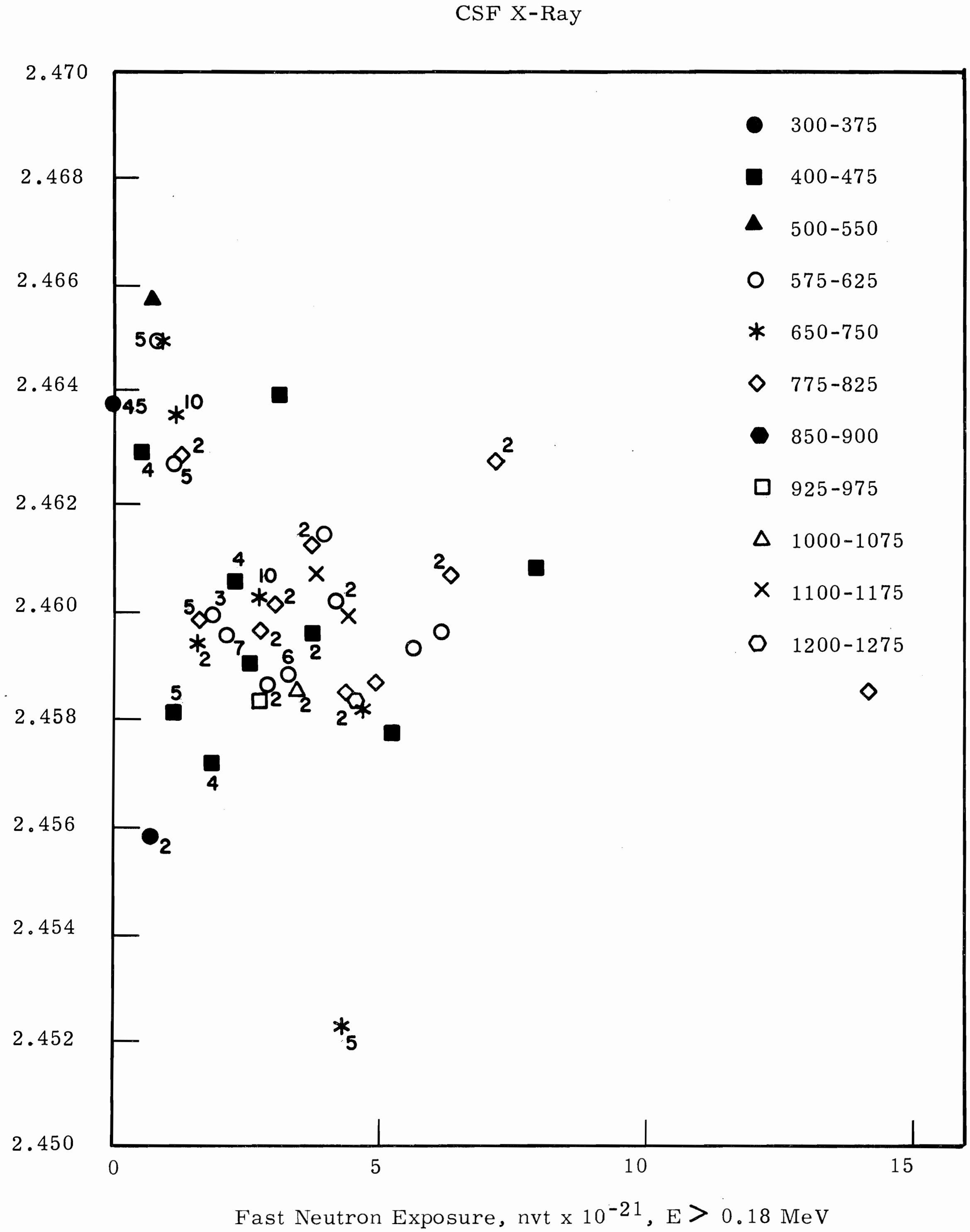

FIGURE 63. *Unit Cell Spacing (a) of CSF Graphite.*

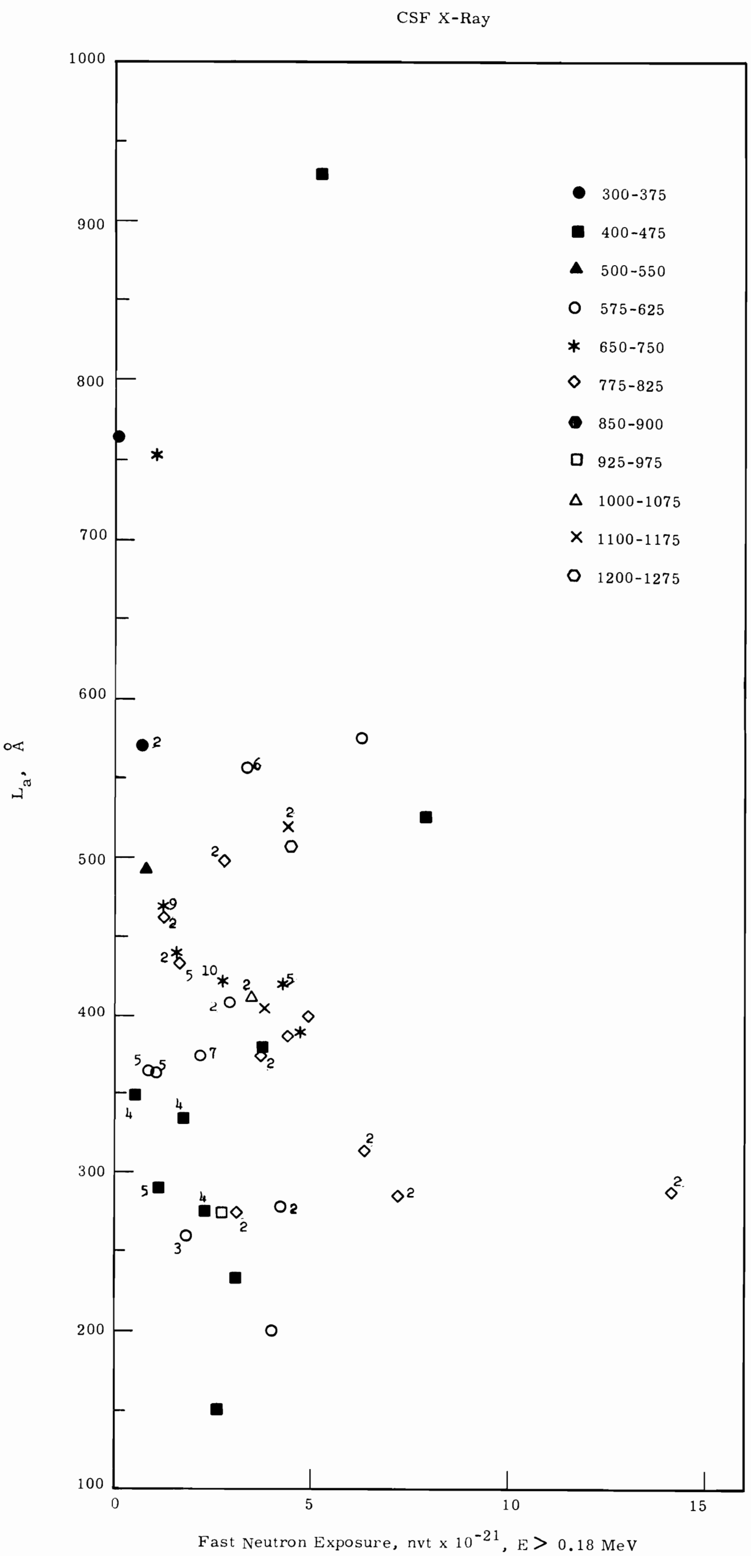

FIGURE 64. *Apparent Crystallite Size (L_a) of CSF Graphite.*

CONCLUSIONS

The dimensional behavior of the various irradiated graphites follows the general pattern reported earlier.[5,8,9] The material expands very slightly in the transverse direction, contracts, goes through a turnaround, and then expands very rapidly. In the parallel direction, the graphites generally contract at an increasing and then at a decreasing rate, pass through turnaround, and begin expanding.

Data for all graphites may be grouped in two temperature-dependent bands for each orientation. One is for the temperature range 300 to 800 °C and the other for the range 900 to 1200 °C. The data within each band are grouped closely. In the temperature range of 300 to 800 °C, the contraction rate decreases as the temperature increases. Turnaround is reached at about the same fluence for the different temperatures, but the net expansion after turnaround is greatest at 800 °C for a given fluence level. Graphites above 800 °C contract more rapidly, reach turnaround at lower fluences, and then expand very rapidly. The damage rate for the higher temperature band is appreciably higher. When the irradiation temperature of a sample is changed, the contraction rate changes to correspond to the rate at the new temperature. The total contraction is between that found for the old temperature and that for the new temperature.

Graphites which show the least contraction are well graphitized, highly crystalline, isotropic materials having a high CTE. However, these qualities, acting to minimize contraction by maximizing the c-axis crystallite growth, tend to aggravate the ultimate expansion which occurs. Because the contractions may delay ultimate expansion at higher fluences, well graphitized crystalline isotropic graphites with low CTE may be more desirable for long exposure high temperature use.

The observed changes are believed to be caused by the interrelated effects of c-axis expansion, a-axis contraction, crack closure (before turnaround), and creep. The observed results are from samples less than 1/2 in. in diameter and 4 in. long. Thus, the combined effects may possibly be different for large pieces. However, it is felt that expansion will ultimately also be the controlling behavior in the large sizes.

The large expansions observed are shown rather dramatically in Figure 65. The two CSF samples were originally the same length but after 2.7×10^{22} nvt at 800 °C, the transverse sample is nearly an inch longer than the parallel sample.

The bulk volume expansion resulting from the observed expansion in all directions results in a large decrease in density and nearly a total loss of strength. The effect of physical changes after turnaround is also exhibited by significant increase in electrical resistivity. Thermal conductivity decreases as a result of irradiation, while the coefficient of thermal expansion shows an increase for transverse samples of conventional graphites and significant decreases for both orientations of raw-coke and isotropic graphites. Young's modulus of elasticity increases at low neutron exposures, while the L_c decreases and the other X-ray crystallite parameters show considerable scatter.

ACKNOWLEDGEMENTS

Some of the high-temperature length change data (1100 to 1200 °C) were received from A. L. Pitner. The long arduous hours and the sincere concern shown by F. D. Hobbs and R. G. Henderson on capsule fabrication and data taking, and that shown by J. C. Knoll on data calculations and analyses, are sincerely appreciated.

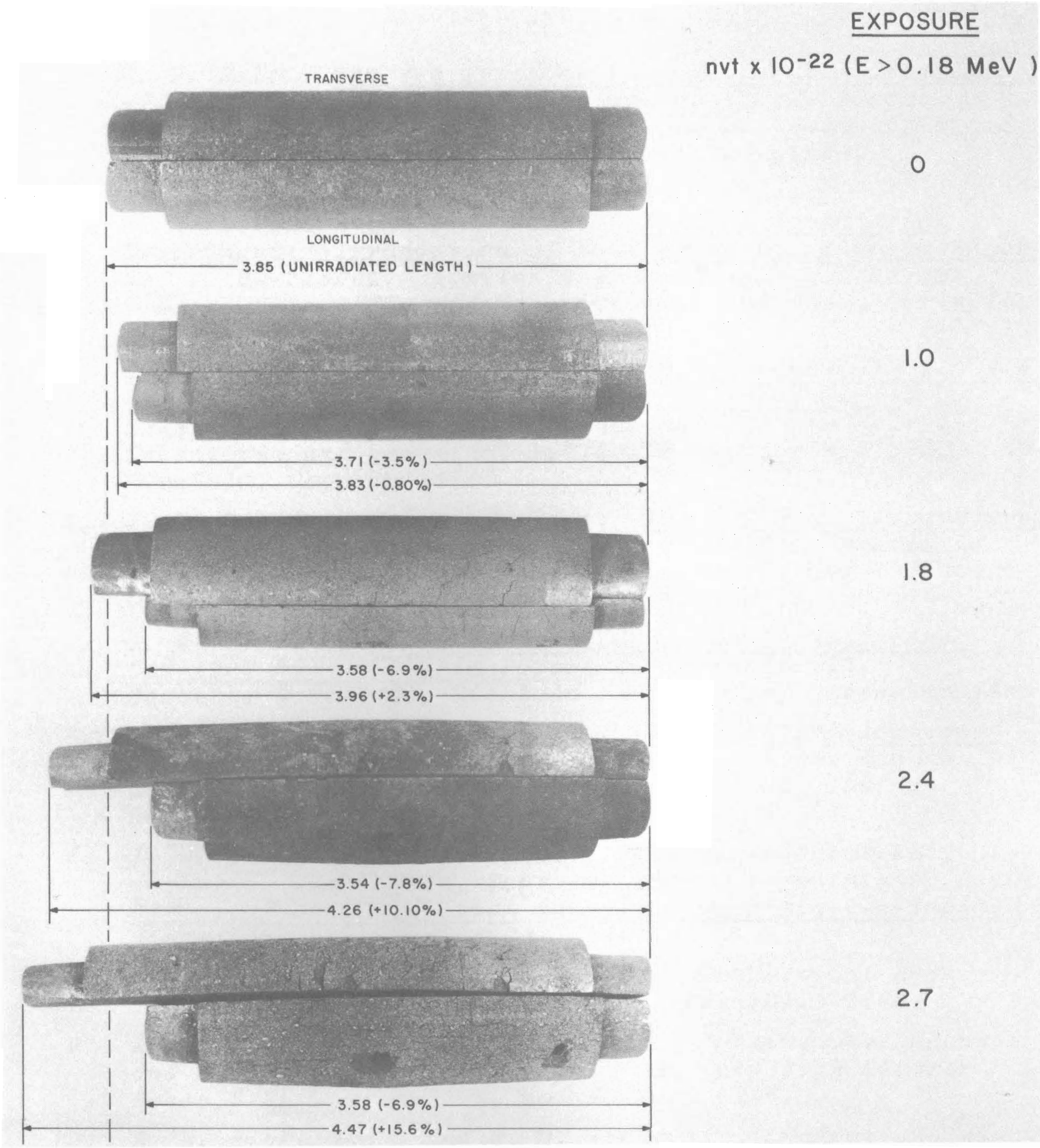

Neg 0672944

FIGURE 65. Radiation-Induced Dimensional Changes in CSF Graphite - 800 °C.

REFERENCES

1. J. W. Helm. The H-3 Irradiation Experiment: Irradiation of EGCR Graphite, Interim Report No. 2, HW-71500B. Available from Clearinghouse for Federal Scientific and Technical Publications, Springfield, Virginia, September 1964.

2. J. M. Davidson and J. W. Helm. The H-3 Irradiation Experiment: Irradiation of EGCR Graphite, Interim Report No. 1, HW-71500A. Available from Clearinghouse for Federal Scientific and Technical Publications, Springfield, Virginia, October 1961.

3. J. W. Helm. Irradiation of N-Reactor Graphite: The H-4, -5, -6 Irradiation Program, Interim Report No. 1, HW-81250A. Available from Clearinghouse for Federal Scientific and Technical Publications, Springfield, Virginia, October 1964.

4. J. M. Davidson and J. W. Helm. The H-1 High Temperature Graphite Irradiation Experiment, HW-64286. Available from Clearinghouse for Federal Scientific and Technical Publications, Springfield, Virginia, April 1961.

5. J. W. Helm. High-Temperature Graphite Irradiations: 800-1200 °C -- Interim Report No. 1, BNWL-112. Battelle-Northwest, Richland, Washington, September 1965.

6. J. H. Cox, Jr. and J. W. Helm. Graphite Irradiations 300-1200 °C, BNWL-SA-1847. Presented at the Eighth Biennial Conference on Carbon, June 19-23, 1967 at Buffalo, New York.

7. J. W. Helm. Unpublished Data. Battelle-Northwest, Richland, Washington, February 1966. (Preliminary Report: Effect of Preirradiation Annealing on Radiation-Induced Dimensional Changes of Graphite)

8. J. W. Helm. "Radiation Effects in Graphite at High Temperature," Carbon, vol. 3, pp. 493-501. 1966.

9. A. J. Perks and J. H. W. Simmons. "Dimensional Changes and Radiation Creep of Graphite at Very High Neutron Doses," Carbon, vol. 4, pp. 85-98. 1966.

10. R. E. Nightingale and E. M. Woodruff. "Radiation-Induced Dimensional Changes in Large Graphite Bars," Nucl. Sci. and Eng., vol. 19, pp. 390-392. 1969.

11. W. C. Morgan. "Effect of Low Compressive Stresses on Radiation-Induced Dimensional Changes in Graphite," Carbon, vol. 1, pp. 255-261. 1964.

12. J. W. Helm. Radiation-Induced Dimensional Changes of Graphite - Effect of Sample Sizes Less than One-Half Inch Diameter, BNWL-CC-399. Battelle-Northwest, Richland, Washington, December 1965.

13. J. H. Cox, Jr., R. W. Marek, and W. E. Parker. Effects of Some Process Temperatures on Radiation-Induced Contraction of Graphite, BNWL-489. Battelle-Northwest, Richland, Washington, August 1967.

14. J. W. Helm. "Irradiation Effects in Thermocouples," International Symposium on In-Pile Irradiation Equipment and Techniques at Harwell, England. May 1966.

15. G. B. Engle. Unpublished Data. General Atomics, San Diego, California, December 1966. (Personal Communication)

16. D. E. Baker. "Thermal Conductivity of Irradiated Graphite by a Rapid Thermal-Pulse Method," J. Nucl. Mater., vol. 12, no. 1, pp. 120-124. 1964.

DISTRIBUTION

No. of Copies	
OFFSITE	
1	AEC Chicago Patent Group G. H. Lee
4	AEC Division of Reactor Development and Technology J. E. Fox (2) R. E. Pahler J. M. Simmons
219	AEC Division of Technical Information Extension
1	Argonne National Laboratory R. M. Adams
3	Atomic Energy Research Establishment Metallurgy Division Harwell Didcot, Berkshire, ENGLAND W. N. Reynolds J. H. W. Simmons (2)
2	Atomics International K. W. Foster
1	Atomic Power Development Associates 1911 First Street, Detroit, Michigan W. E. McHugh
2	Basic Carbon Corporation Sanborn, New York H. M. Killmar
1	Berkeley Nuclear Lab. Berkeley, Glos., ENGLAND P. P. Jennings
1	Brookhaven National Laboratory D. H. Gurinsky

No. of
Copies

3 Centre d' Etudes Nucleaires de Saclay
Boite Postale No. 2
Gif-sur-Vvette (Seine-et-Oise), FRANCE

P. Leveque
J. Rappeneau (2)

3 Culcheth Laboratories
Reactor Materials Laboratory
UKAEA
Wigshaw Lane
Warrington, Lancashire, ENGLAND

B. T. Kelly (2)
P. T. Nettley

3 Dragon Project Office
Atomic Energy Establishment
Winfirth
Dorchester, Dorset, ENGLAND

R. A. U. Huddle
L. W. Graham (2)

1 Euratom C.C.R.
Petten, Netherlands

V. Lungagnani

1 General Electric Company
Pleasanton, California

G. E. Robinson

1 General Electric Company, Ltd.
Hirst Research Centre
Wembley, Middlesex, ENGLAND

Dr. H. H. W. Losty

1 Gmelin Institute Atomic Energy
Documentation Center
Postschliebfach 9088
Frankfurt, WEST GERMANY

Dr. Irmgard Wensel

No. of Copies	
4	Great Lakes Carbon Corporation Research and Development Department P. O. Box 637, Niagara Falls, New York B. L. Bailey L. H. Juel (3)
3	Gulf General Atomic Incorporated (AEC) G. B. Engle (2) R. Turner
1	Idaho Nuclear Corporation E. Fast
1	Los Alamos Scientific Laboratory W. S. Clouser
1	Marquardt Corporation D. W. Bareis
1	Nukem Nuclear 645 Hanan Postfach 869 West Germany G. Spener
3	Oak Ridge Operations Office W. J. Larkin D. F. Cope (2)
2	POCO Graphite, Inc. Garland, Texas R. K. Carlson
2	Pure Carbon Company St. Marys, Pennsylvania R. R. Paxton
1	Reactor Centrum Nederland Petten, Netherlands R. Blackstone
1	Rice University Houston, Texas J. L. Margrave

No. of
Copies

1 SIGRI ELEKTROGRAPHIT GmbH
8901 Meitingen Dei
Augsburg, WEST GERMANY

O. J. Vohler

2 Speer Carbon Products
Research & Development Laboratories
Packard Road & 47th Street
Niagara Falls, New York

W. E. Parker

2 Speer Carbon Products
Development Department
St. Marys, Pennsylvania

W. A. Bauer
M. B. Redmount

2 THTR Projektleitung
517 Julich
bei Aachen, WEST GERMANY

L. Valette

1 Union Carbide Corporation
Cleveland, Ohio

J. T. Meers

1 Union Carbide Corporation
270 Park Avenue, New York, N.Y.

P. J. Hastings

1 Union Carbide Corporation
Lawrenceburg, Tennessee

L. D. Stoughton

4 Union Carbide Corporation (ORNL Y-12)
W. P. Eatherly
B. L. Greenstreet
F. J. Witt (2)

2 Union Carbide Corporation (ORNL X-10)
R. Kennedy (2)

No. of Copies	
1	Wright Air Development Division Wright-Patterson AFB, Ohio R. H. Wilson (Major)

ONSITE-HANFORD

1	AEC Chicago Patent Group R. K. Sharp (Richland)
2	AEC RDT Site Representative P. G. Holsted
2	AEC Richland Operations Office R. L. Plum C. L. Robinson
3	Battelle Memorial Institute
4	Douglas United Nuclear, Inc. P. C. Carlson R. Cooperstein D. H. Curtiss A. Russell
25	Battelle-Northwest D. E. Baker J. H. Cox G. M. Dalen W. J. Gray J. W. Helm (3) R. G. Henderson F. D. Hobbs R. S. Hope A. J. Jervis J. C. Knoll R. E. Nightingale A. L. Pitner J. C. Tobin C. E. Vogel E. M. Woodruff H. H. Yoshikawa Technical Information Files (5) Technical Publications (2)